NFPA 204
Guide for Smoke and Heat Venting

1998 Edition

National Fire Protection Association, 1 Batterymarch Park, PO Box 9101, Quincy, MA 02269-9101
An International Codes and Standards Organization

Copyright ©
National Fire Protection Association, Inc.
One Batterymarch Park
Quincy, Massachusetts 02269

IMPORTANT NOTICE ABOUT THIS DOCUMENT

NFPA codes and standards, of which the document contained herein is one, are developed through a consensus standards development process approved by the American National Standards Institute. This process brings together volunteers representing varied viewpoints and interests to achieve consensus on fire and other safety issues. While the NFPA administers the process and establishes rules to promote fairness in the development of consensus, it does not independently test, evaluate, or verify the accuracy of any information or the soundness of any judgments contained in its codes and standards.

The NFPA disclaims liability for any personal injury, property or other damages of any nature whatsoever, whether special, indirect, consequential or compensatory, directly or indirectly resulting from the publication, use of, or reliance on this document. The NFPA also makes no guaranty or warranty as to the accuracy or completeness of any information published herein.

In issuing and making this document available, the NFPA is not undertaking to render professional or other services for or on behalf of any person or entity. Nor is the NFPA undertaking to perform any duty owed by any person or entity to someone else. Anyone using this document should rely on his or her own independent judgment or, as appropriate, seek the advice of a competent professional in determining the exercise of reasonable care in any given circumstances.

The NFPA has no power, nor does it undertake, to police or enforce compliance with the contents of this document. Nor does the NFPA list, certify, test or inspect products, designs, or installations for compliance with this document. Any certification or other statement of compliance with the requirements of this document shall not be attributable to the NFPA and is solely the responsibility of the certifier or maker of the statement.

NOTICES

All questions or other communications relating to this document and all requests for information on NFPA procedures governing its codes and standards development process, including information on the procedures for requesting Formal Interpretations, for proposing Tentative Interim Amendments, and for proposing revisions to NFPA documents during regular revision cycles, should be sent to NFPA headquarters, addressed to the attention of the Secretary, Standards Council, National Fire Protection Association, 1 Batterymarch Park, P.O. Box 9101, Quincy, MA 02269-9101.

Users of this document should be aware that this document may be amended from time to time through the issuance of Tentative Interim Amendments, and that an official NFPA document at any point in time consists of the current edition of the document together with any Tentative Interim Amendments then in effect. In order to determine whether this document is the current edition and whether it has been amended through the issuance of Tentative Interim Amendments, consult appropriate NFPA publications such as the *National Fire Codes*® Subscription Service, visit the NFPA website at www.nfpa.org, or contact the NFPA at the address listed above.

A statement, written or oral, that is not processed in accordance with Section 16 of the Regulations Governing Committee Projects shall not be considered the official position of NFPA or any of its Committees and shall not be considered to be, nor be relied upon as, a Formal Interpretation.

The NFPA does not take any position with respect to the validity of any patent rights asserted in connection with any items which are mentioned in or are the subject of this document, and the NFPA disclaims liability of the infringement of any patent resulting from the use of or reliance on this document. Users of this document are expressly advised that determination of the validity of any such patent rights, and the risk of infringement of such rights, is entirely their own responsibility.

Users of this document should consult applicable federal, state, and local laws and regulations. NFPA does not, by the publication of this document, intend to urge action that is not in compliance with applicable laws, and this document may not be construed as doing so.

Licensing Policy

This document is copyrighted by the National Fire Protection Association (NFPA). By making this document available for use and adoption by public authorities and others, the NFPA does not waive any rights in copyright to this document.

1. Adoption by Reference – Public authorities and others are urged to reference this document in laws, ordinances, regulations, administrative orders, or similar instruments. Any deletions, additions, and changes desired by the adopting authority must be noted separately. Those using this method are requested to notify the NFPA (Attention: Secretary, Standards Council) in writing of such use. The term "adoption by reference" means the citing of title and publishing information only.

2. Adoption by Transcription – A. Public authorities with lawmaking or rule-making powers only, upon written notice to the NFPA (Attention: Secretary, Standards Council), will be granted a royalty-free license to print and republish this document in whole or in part, with changes and additions, if any, noted separately, in laws, ordinances, regulations, administrative orders, or similar instruments having the force of law, provided that: (1) due notice of NFPA's copyright is contained in each law and in each copy thereof; and (2) that such printing and republication is limited to numbers sufficient to satisfy the jurisdiction's lawmaking or rule-making process. **B.** Once this NFPA Code or Standard has been adopted into law, all printings of this document by public authorities with lawmaking or rule-making powers or any other persons desiring to reproduce this document or its contents as adopted by the jurisdiction in whole or in part, in any form, upon written request to NFPA (Attention: Secretary, Standards Council), will be granted a nonexclusive license to print, republish, and vend this document in whole or in part, with changes and additions, if any, noted separately, provided that due notice of NFPA's copyright is contained in each copy. Such license shall be granted only upon agreement to pay NFPA a royalty. This royalty is required to provide funds for the research and development necessary to continue the work of NFPA and its volunteers in continually updating and revising NFPA standards. Under certain circumstances, public authorities with lawmaking or rule-making powers may apply for and may receive a special royalty where the public interest will be served thereby.

3. Scope of License Grant – The terms and conditions set forth above do not extend to the index of this document.

(For further explanation, see the Policy Concerning the Adoption, Printing, and Publication of NFPA Documents, which is available upon request from the NFPA.)

Copyright © 1998 NFPA, All Rights Reserved

NFPA 204

Guide for

Smoke and Heat Venting

1998 Edition

This edition of NFPA 204, *Guide for Smoke and Heat Venting*, was prepared by the Technical Committee on Smoke Management Systems and acted on by the National Fire Protection Association, Inc., at its Annual Meeting held May 18–21, 1998, in Cincinnati, OH. It was issued by the Standards Council on July 16, 1998, with an effective date of August 5, 1998, and supersedes all previous editions.

This edition of NFPA 204 was approved as an American National Standard on August 6, 1998.

Origin and Development of NFPA 204

This project was initiated in 1956 when the NFPA Board of Directors referred the subject to the Committee on Building Construction. A tentative guide was submitted to NFPA in 1958. Revised and tentatively adopted in 1959 and again in 1960, the guide was officially adopted in 1961. In 1968 a revised edition was adopted that included a new section, Inspection and Maintenance.

In 1975, a reconfirmation action failed as concerns over use of the guide in conjunction with automatic sprinklered buildings surfaced. Because of this controversy, work on a revision to the guide continued at a slow pace.

The Technical Committee and Subcommittee members agreed that the state of the art had progressed sufficiently to develop improved technology-based criteria for design of venting; therefore, the 1982 edition of the document represented a major advance in engineered smoke and heating venting, although reservations over vent and sprinkler applications still existed.

At the time this guide was formulated, the current venting theory was considered unwieldy for this format; consequently, the more adaptable theory as described herein was adopted. Appreciation must be extended to Dr. Gunnar Heskestad at the Factory Mutual Research Corporation for his major contribution to the theory applied in this guide, which is detailed in Appendix A.

The 1985 edition again revised Chapter 6 on the subject of venting in sprinklered buildings. Test data from work done at the Illinois Institute of Technology Research, which had been submitted to the Committee as part of a public proposal, did not permit consensus to be developed on whether sprinkler control was impaired or enhanced by the presence of automatic roof vents of typical spacing and area. The revised wording of Chapter 6 encouraged the designer to use the available tools and data referenced in the document while the use of automatic venting in sprinklered buildings was under review.

The 1991 edition made minor changes to Chapter 6 to acknowledge that a design basis existed for using sprinklers and automatic heat venting together but that such had not received wide recognition.

The 1998 edition represents a complete revision to the guide. The rewrite deletes the previous tables that listed vent areas and incorporates engineering equations and references computer models, such as LAVENT and DETACT, to provide the designer with the necessary tools to develop vent designs based on performance objectives. This rewrite is based extensively on state-of-the-art technology published in the references. In many cases, the authors of these references participated in the task group's rewrite efforts.

Technical Committee on Smoke Management Systems

James A. Milke, *Chair*
University of Maryland, MD [SE]

Daniel L. Arnold, Rolf Jensen & Assoc. Inc., GA [SE]

Donald W. Belles, Donald W. Belles & Assoc. Inc., TN [M]
Rep. American Architectural Mfrs. Assn.

James B. Buckley, Houston, TX [SE]

Paul J. Carrafa, Building Inspection Underwriters, Inc., PA [E]

Elmer F. Chapman, New York City Fire Dept., NY [E]

Michael Earl Dillon, Dillon Consulting Engr. Inc., CA [SE]

S. E. Egesdal, Honeywell Inc., MN [M]
Rep. Nat'l Electrical Mfrs. Assn.

Douglas H. Evans, Clark County Building Dept., NV [E]

Gunnar Heskestad, Factory Mutual Research Corp., MA [I]

Winfield T. Irwin, Irwin Services, PA [M]
Rep. North American Insulation Mfrs. Assn.

Daniel J. Kaiser, Underwriters Laboratories Inc., IL [RT]

John E. Kampmeyer, Maida Engr. Inc., PA [SE]
Rep. National Society of Professional Engrs.

Gary D. Lougheed, Nat'l Research Council of Canada, Canada [RT]

Francis J. McCabe, Prefco Products, PA [M]

Gregory R. Miller, Code Consultants Inc., MO [SE]

Harold E. Nelson, Hughes Associates Inc., MD [SE]

Erin A. M. Oneisom, U.S. Air Force, Civil Engr. Support Agency, FL [U]

Zenon A. Pihut, Texas Dept. of Health, TX [E]

Dale Rammien, Air Movement & Control Assn. Inc., IL [M]

James Edward Richardson, Colt International Ltd., England [M]

William A. Schmidt, Bowie, MD [SE]

Todd E. Schumann, Industrial Risk Insurers, IL [I]

J. Brooks Semple, Smoke/Fire Risk Mgmt. Inc., VA [SE]

Paul G. Turnbull, Landis & Gyr Powers Inc., IL [M]

Alternates

Craig Beyler, Hughes Assoc. Inc., MD [SE]
(Alt. to H. E. Nelson)

Richard J. Davis, Factory Mutual Research Corp., MA [I]
(Alt. to G. Heskestad)

Victor L. Dubrowski, Code Consultants Inc., MO [SE]
(Alt. to G. R. Miller)

Geraldine Massey, Dillon Consulting Engr. Inc., CA [SE]
(Alt. to M. E. Dillon)

Jayendra S. Parikh, Underwriters Laboratories Inc., IL [RT]
(Alt. to D. J. Kaiser)

James S. Slater, Pittway Systems Technology Group, IL [M]
(Alt. to S. E. Egesdal)

Randolph W. Tucker, Rolf Jensen & Assoc. Inc., TX [SE]
(Alt. to D. L. Arnold)

Peter J. Gore Willse, Industrial Risk Insurers, CT [I]
(Alt. to T. E. Schumann)

Michael L. Wolf, Greenheck, WI [M]
(Alt. to D. Rammien)

Nonvoting

Bent A. Borresen, Techno Consultant, Norway
(Alt. to C. N. Madsen)

E. G. Butcher, Fire Check Consultants, England
(Alt. to A. G. Parnell)

Gregory E. Harrington, NFPA Staff Liaison

Christian Norgaard Madsen, Techno Consultant, Norway

Alan G. Parnell, Fire Check Consultants, England

This list represents the membership at the time the Committee was balloted on the text of this edition. Since that time, changes in the membership may have occurred. A key to classifications is found at the back of this document.

NOTE: Membership on a committee shall not in and of itself constitute an endorsement of the Association or any document developed by the committee on which the member serves.

Committee Scope: This Committee shall have primary responsibility for documents on the design, installation, testing, operation, and maintenance of systems for the control, removal, or venting of heat or smoke from fires in buildings.

Contents

NFPA 204

Guide for

Smoke and Heat Venting

1998 Edition

NOTICE: An asterisk (*) following the number or letter designating a paragraph indicates that explanatory material on the paragraph can be found in Appendix A.

Information on referenced publications can be found in Chapter 10 and Appendix E. Detailed information on references cited in brackets throughout the document can be found in Section B-6, Section C-9, and Section E-1.

Chapter 1 General Information

1-1 Introduction.

1-1.1 Previous editions of this guide have included tables listing vent areas based on preselected design objectives. These tables were based on the hot upper layer at 20 percent of the ceiling height. Different layer depths were accommodated by using a multiplication factor. Curtain board and vent spacing rules were set. Minimum clear visibility times were related to fire growth rate, ceiling height, compartment size, curtain depth, and detector activation times using engineering equations and a set of assumptions that sometimes resulted in conservative solutions.

This edition has eliminated the previous tables listing vent areas. This edition incorporates engineering equations (hand calculations) or references models. The equations or models provide the designer with the necessary tools to develop vent designs based on selected performance objectives related to a specific building and a specific set of circumstances. Engineering equations are included for calculating vent flows, layer depths, and upper-layer temperatures based on a prescribed burning rate. An example using both hand calculations and the LAVENT (Link-Activated VENTs) computer model is presented in Appendix D.

The majority of the information provided in this guide applies to nonsprinklered buildings. A limited amount of guidance is provided in Chapter 8 for sprinklered buildings.

1-1.2 Some of the procedures in Chapter 6, "Sizing Vents," assume that the automatic activation of vents is initiated by a heat-responsive device with an established response time index (RTI) and known activation temperature. This assumption is not meant to preclude other means of vent initiation as long as the activation time of the alternative means is known or can be calculated using the procedures contained in this guide or otherwise established as acceptable by a specific listing, specific test data, or established engineering analysis. Other activation devices can include smoke detectors, thermoplastic drop-out vent panels, or other approved means of activation of vents.

1-1.3 The following list provides a general description of the significant phenomena that occur during a fire when a fire-venting strategy is implemented.

(a) Due to buoyancy, hot gases rise vertically from the combustion zone and then flow horizontally below the roof until blocked by a vertical barrier (a wall or curtain board), thus initiating a layer of hot gases below the roof.

(b) The volume and temperature of gases to be vented are a function of the fire's rate of heat release and the amount of air entrained into the buoyant plume produced.

(c) As the depth of the layer of hot gases increases, the layer temperature continues to rise and the vents open.

(d) The operation of vents within a curtained area enables some of the upper layer of hot gases to escape and thus slows the thickening rate of the layer of hot gases. With a sufficient venting area, the thickening rate of the layer can be arrested and even reversed. The rate of discharge through a vent of a given area is primarily determined by the depth of the layer of hot gases and the layer temperature. Adequate quantities of replacement inlet air from air inlets located below the hot upper layer are needed if the products of combustion-laden upper gases, are to be exhausted according to design. *[See Figures 1-1.3(a) and (b).]*

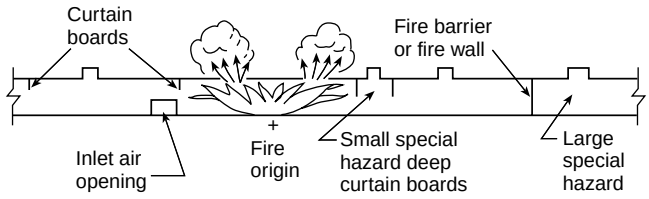

Figure 1-1.3(a) Behavior of combustion products under vented and curtained roof.

Figure 1-1.3(b) View of roof vents on building.

1-1.4* The equations and procedures for hand calculations in Section 6-1 provide two types of guidance. The first addresses the venting of limited-growth fires. These are fires that are not expected to grow beyond a predictable heat release rate. The second type of guidance is relevant to the venting of fires that, if unchecked, will continue to grow to an unpredictable size.

The engineering equations or models incorporated in this guide allow an estimate of how well smoke can be confined to a curtained area and how long the smoke interface can be maintained at a higher level than the design elevation of the curtained area. This minimum clear-visibility design time facilitates such activities as locating the fire, appraising the fire severity and its extent, evacuating the building, and making an informed decision on the deployment of personnel and equipment to be used for fire fighting.

1-2 Application and Scope.

1-2.1* The provisions of Chapters 2 through 7 of this guide are intended to offer guidance for the design of facilities for emergency venting of products of combustion from fires in

nonsprinklered, single-story buildings. Both manual and computer-modeled solution methods are provided in Chapter 6 to aid in design calculations. A limited amount of information regarding venting in sprinklered buildings is included in Chapter 8. These provisions do not attempt to specify under what conditions venting is to be provided; such conditions depend on an analysis of the individual situation and on local building code and fire code requirements.

1-2.2 This guide does not apply to ventilation designed for regulation of temperature within a building for personnel comfort or for cooling of production equipment or to venting provided for explosion pressure relief. *(See NFPA 68, Guide for Venting of Deflagrations.)*

1-2.3 This guide applies to building construction of all types.

1-2.4 The concepts set forth in this guide were developed for venting fires in large, undivided floor areas with ceiling heights sufficient to allow the design fire plume and smoke layer to develop (normally 4.6 m or greater). The application of these concepts to buildings of smaller area or lower ceiling heights necessitates careful engineering judgment.

1-3 Determination of Occupancy Hazard.

1-3.1 Tests and studies provide a basis for the division of occupancies into classes depending on the fuel available for contribution to fire. Wide variation is found in the quantities of combustible materials in the many kinds of buildings and areas of buildings. The evaluation should take into account the average or anticipated fuel loading and the rate of heat release anticipated from the combustible materials or flammable liquids contained therein.

1-3.2 Chapter 5 should be referenced to assist in quantifying types of fires in various occupancies. Characteristic heat release rates for both limited-growth and continuous-growth fires in various types of fuel arrays also are addressed in that chapter.

1-3.3 It should be recognized that many large facilities have buildings or areas subject to different fire hazards. Accordingly, venting facilities should be designed specifically for each space as discussed in this guide.

1-4 Nomenclature. The following symbols define the variables in the equations used throughout the main text of this guide. *(See Appendix B for an explanation of the unique nomenclature used in that appendix.)*

A = area (of burning surface)
A = area for fresh air, below design level
A_i = of smoke interface
A_v = actual total vent area
A_{va} = aerodynamic vent area
α = thermal diffusivity, $k/\rho c$
α_g = fire growth coefficient
c = specific heat
d = smoke layer depth
d_c = depth of curtain board
D = base diameter of the fire
g = acceleration of gravity
H = ceiling height above base of fire
h_c = heat of combustion
h_g = heat of gasification
K = fraction of adiabatic temperature rise
k = thermal conductivity
$k_e\beta$ = constant used in Eq. (5-3)
$k\rho c$ = thermal inertia
l = thickness
L = mean flame height
L_f = flame length, measured from leading edge of burning region
M = multiplier (vent size)
$\dot{m}$ = mass burning rate
$\dot{m}''$ = mass burning rate per unit area
$\dot{m}''_\infty$ = mass burning rate for an infinite diameter pool
$\dot{m}_v$ = mass flow rate through vent
$\dot{m}_p$ = mass flow rate in the plume
$\dot{m}_{pL}$ = $\dot{m}_p$ at mean flame height *(L)*
$\dot{q}''_i$ = incident heat flux per unit area
Q = total heat release rate
Q'' = total heat release rate per unit plan area
Q_c = convective heat release rate (approx. $0.7Q$)
r = radius from fire axis
RTI = response time index ($\tau^{1}/_{2}$, where τ is the time constant of the heat-responsive element for convective heating)
ρ = density
ρ_o = ambient density
t = time
t_d = time to detection (activation)
t_g = growth time
t_{ig} = time to ignition
t_r = design interval time
ΔT = gas temperature rise (from ambient) at detector site
ΔT_a = adiabatic temperature rise
ΔT_e = temperature rise (from ambient) of heat-responsive element
T_o = ambient air temperature
T_{ig} = ignition temperature
T_s = surface temperature
u = gas velocity at detector site
V = flame spread velocity
X_r = radiant fraction
y, y_{ceil}, y_{curt}, y_{fire} = elevation of smoke layer interface, ceiling, curtain, respectively, and fire above floor
z = height above base of fire
z_o = height of "virtual origin" above base of fire (below base of fire, if negative)

Chapter 2 Basic Phenomena

2-1 Principles of Venting.

2-1.1 Venting Objectives. Venting of a building is provided to slow or stop the descent of a smoke layer for purposes such as the following:

(a) To provide occupants with the opportunity to travel to a safe area
(b) To facilitate manual fire fighting by enabling fire fighters to reach the origin or seat of the fire
(c) To reduce damage to buildings and contents due to smoke and hot gases

2-1.2 Vent Designs and Smoke Generation. The heat release rate of a fire, the fuel geometry, the height of the clear layer above the base of the fire, and the design depth of the smoke layer are major factors affecting the production of smoke. Given such knowledge about a fire, venting designs can be developed in accordance with this guide in which the vent area is calculated to achieve a mass rate of flow through vents that matches the mass rate of production of smoke. Such a design prevents descent of the smoke layer below the design height of the clear layer. Alternative designs are possible where the vent flow is less than the rate of smoke production in which the descent of the smoke layer is slowed sufficiently to meet design objectives. Smoke includes the quantity of air that is entrained or otherwise mixed into the mass.

2-1.3 Vent Mass Flow. Vent design criteria in this guide assume that the mass flow rate through a vent is determined primarily by buoyancy pressure. Mass flow through a vent, therefore, is governed mainly by the free vent area and the depth of the hot layer and its temperature.

(a) Venting becomes more effective with smoke temperature differentials between ambient temperature and an upper layer of approximately 110°C or higher. Where temperature differentials of less than 110°C are expected, vent flows might be reduced significantly; therefore, consideration should be given to using powered exhaust. NFPA 92B, *Guide for Smoke Management Systems in Malls, Atria, and Large Areas,* should be consulted for guidance for power venting at these lower temperatures.

(b) The vent design criteria in this guide also allow the fire to reach a size such that the flame plume enters the upper hot layer. Flame height may be estimated using Eq. (6-1).

2-2 Smoke Production.

2-2.1 Entrainment at the Plume Boundary. The rate of smoke production depends on the rate of air entrainment into a column of hot gases produced by and located above a fire. Entrainment is affected by the fire diameter and rate of heat release, and it is strongly affected by the distance between the base of the fire and the point at which the smoke plume enters the hot upper layer.

2-2.2 Base of the Fire. The location of the base of the fire is that level at which significant entrainment begins to occur. For the purposes of the equations in this guide, the base of the fire is at the bottom of the burning zone.

2-2.3 Fire Size. Since smoke production is related to the size of a fire, it logically follows that, all factors being equal, larger fires produce more smoke. Entrainment, however, is strongly affected by the distance between the base of a fire and the bottom of the hot layer. Therefore, the base of the fire (where combustion and entrainment begin) should be selected carefully. It is possible for a smaller fire having a base near the floor to produce more smoke than a larger fire with a base at a higher elevation. Each possible fire scenario should be considered carefully before establishing the conditions of the design fire.

2-2.4 Entrainment and Clear Height. Entrainment is assumed to be limited to the clear height between the base of the fire and the bottom of the hot layer. The buoyant plume associated with a fire produces a flow into the hot upper layer. As the plume impinges on the ceiling, the plume turns and forms a ceiling jet. The ceiling jet flows radially outward along the ceiling.

2-2.5 Smoke Production as a Function of Shape of Fire. The entrainment formulas specified in this guide assume a single fire in predicting smoke production. Where the possibility of multiple fires and, therefore, multiple plumes exists, smoke production rates increase beyond the rate predicted for a single plume for a fire of equivalent output. It also should be understood that smoke entrainment relationships are developed primarily for the case of axisymmetric plumes. For linelike fires where a long, narrow plume is created by a fuel or storage array, the smoke production relationships in this guide might not be valid. However, if the height of the smoke layer interface above the base of the fire $(H - d)$ is large compared to the largest horizontal dimension of the fire (e.g., greater than approximately 3 times), the empirically derived relationships in this guide can be used to predict smoke production.

2-2.6 Virtual Origin. Plume mass flow above the flame level is based on the concept that, except for absolute scales, the shapes of velocity and temperature profiles at the mean flame height are invariable. This concept leads to an expression for mass flow above the flames that involves the so-called "virtual origin," a point source from which the plume above the flames appears to originate. The virtual origin might be above or below the base of the fire.

2-3 Vent Flows.

2-3.1 Buoyancy and Vent Flow. Flow through a vent in this guide is calculated on the basis of buoyancy pressure. It is assumed that openings exist to the outside and, therefore, no pressure results from the expansion of gases. Wind effects are not taken into account, as wind might assist or interfere with vent flows, depending on specific circumstances. It is also assumed that the fire environment in a building space is divided into two zones — a hot upper layer and a relatively cool, clear (comparatively free of smoke) lower region. When a fire grows to a size approaching ventilation-limited burning, the building might no longer maintain a clear lower region, and this guide would no longer be applicable. Finally, caution needs to be exercised where using this guide for conditions under which the upper-gas-layer temperature approaches 600°C, since flashover might occur within the compartment. When a fire develops to flashover or ventilation-limited burning, the relationships provided in this guide are not applicable.

2-3.2 Buoyancy Pressure. Buoyancy pressure is related to the depth of the hot layer, the absolute temperature of the hot layer, the temperature rise above ambient of the hot layer, and the density of the ambient air.

2-3.3 Vent Mass Flow. The mass rate of flow of hot gases through a vent is a function of vent area, layer depth, and hot layer temperature.

2-3.4 Temperature and Vent Flow. The temperature of the hot layer above ambient affects mass flow through a vent. Maximum flow occurs at temperature differentials of approximately 300°C above ambient. Flows at other temperature differentials are diminished, as shown in Figure 2-3.4.

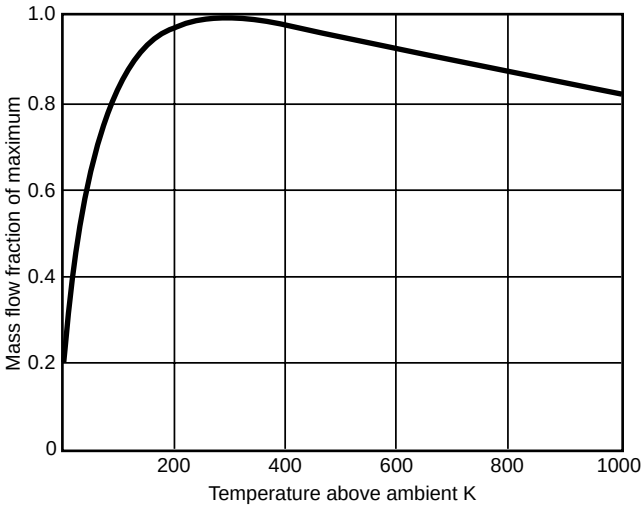

Figure 2-3.4 Effect of temperature on mass flow through a vent.

2-3.5 Inlet Air.

2-3.5.1 To function as intended, a building venting system needs sufficiently large fresh air openings at low levels. The effect of inlet air on vent flow is addressed in 6-1.3.1. For example, where high upper-layer temperatures of 400 K above ambient are anticipated, 80 percent of the predicted vent flow is expected to be achieved with an inlet area/vent area ratio of 1, whereas it is expected that 90 percent of the vent flow will result from a ratio of 2. Where relatively low upper-layer temperatures, such as 200 K above ambient, are expected, a ratio of inlet air/vent area of 1 would result in about 70 percent of the desired vent flow, whereas a ratio of 2 would be expected to produce about 90 percent of the vent flow.

2-3.5.2 If doors and windows below the design smoke layer do not meet the total recommended inlet air opening area, special air inlet provisions are necessary.

2-3.5.3 It is essential that a dependable means for admitting or supplying inlet air be provided promptly after the first vent opens.

2-3.5.4 Makeup Air System. The simplest method of introducing makeup air into the space is through direct openings to the outside, such as through doors and louvers, that can be opened on system activation. Such openings can be coordinated with the architectural design and can be located as necessary below the design smoke layer. For spaces where such openings are not practicable, a powered air supply system might be considered. This might be an adaptation of the building's HVAC system, provided that capacities, outlet grille locations, and velocities are suitable. For such systems, means should be provided to prevent supply systems from operating until exhaust flow has been established to avoid pressurization of the fire area.

Chapter 3 Vents

3-1 Types of Vents.

3-1.1 Experience has shown that any roof opening over a fire relieves some heat and smoke. However, building designers and fire protection engineers cannot rely on casual inclusion of skylights, windows, or monitors as adequate venting means. Standards exist (UL 793, *Automatically Operated Roof Vents for Smoke and Heat;* UBC Standard 15-7, *Automatic Smoke and Heat Vents*) that include design criteria and test procedures for unit vents requiring simulated fire tests as well as engineering analysis.

3-1.2 Guidelines for the inspection and maintenance of vents are contained in Chapter 9.

3-2 Vent Design Constraints.

3-2.1 Materials of construction and methods of installation need to be used appropriately to resist expected extremes of temperature, wind, building movement, rain, hail, snow, ice, sunlight, corrosive environment, internal and external dust, dirt, and debris. Compatibility between the vent-mounting elements (e.g., holding power, electrochemical interaction, wind lift, building movement) and the building structure to which they are attached needs to be ensured.

3-2.2 Vents designed for multiple functions (e.g., the entrance of day-lighting, roof access, comfort ventilation) need maintenance of the fire protection function that might be impaired by the other uses. These impairments can include loss of spring tension, racking or wear of moving parts, adverse exterior cooling effects on the fire protection release mechanism, adverse changes in performance sequence such as premature heat actuation leading to opening of the vent, or reduced sensitivity to heat.

3-2.3 To avoid inadvertent operation, it is important that the actuating means be selected with regard to the full range of expected ambient conditions.

3-2.4 The venting system might consist of a single unit (entire unit opens fully with a single sensor) or multiple units in rows, clusters, groups, or other arrays that satisfy the venting recommendations for the specific hazard.

3-2.5 If the hazard is localized (e.g., dip tank or solvent storage), it is recommended that the vents be located directly above such hazard.

3-2.6 It is essential that the specific vent mechanism and structure be arranged to be inspected easily.

3-3 Methods of Operation.

3-3.1 An automatic mechanism for opening the roof vents is recommended for effective release of heat, smoke, and gaseous by-products. If excessive smoke is likely to be generated prior to the release of heat sufficient to open vents, smoke detectors with appropriate linkages to open vents should be used.

3-3.2 If failure of a vent-operating component occurs, it should lead to an open vent condition. Gravity should be used as the opening force, with ensurance that the opening mechanism cannot be blocked easily by snow, roof debris, or internal projections. Alternative opening mechanisms should be reliable.

3-3.3 All mechanically opened vents also should be designed to open by manual means.

3-3.4 To be effective, latching mechanisms should be jamproof, corrosion-resistant, and resistant to pressure differentials arising from windstorms, process operations, overhead doors, or traffic vibrations.

3-4 Dimensions and Spacing of Vents. The dimensions and spacing of vents can be considered effective where the following criteria are met:

(a) Either (1) the area of a unit vent or cluster does not exceed $2d_c^2$ or $2d^2$, where d_c is the depth of the curtain board and d is the design depth of the smoke layer, or (2) the width of the monitor does not exceed the depth of the curtain board, d_c, or the design depth of the smoke layer, d, where curtains are not provided. These depths are measured from the centerline of the vent. *[See Figures 4-3(a) through (d).]*

(b) The vent spacing is such that, in plan view, the roof and the nearest vent, all within the curtained area, does not exceed $2.8H$ (the diagonal of a square whose side is $2H$), where H is the ceiling height. *[See Figures 4-3(a) through (d).]*

(c) The total vent area per curtained compartment under the ceiling depends on the severity of the expected fire, which is discussed in Chapter 5.

3-5 Mechanical Vents. Where mechanical vents are considered, see Chapter 7.

Chapter 4 Curtain Boards

4-1 General. In large, open areas, curtain boards enhance prompt activation of the vents and venting effectiveness by containing the smoke in the curtained area.

4-2 Construction. Curtain boards should be made of substantial, noncombustible materials and should be constructed to resist the passage of smoke.

4-3 Location and Depth. To ensure smoke containment, curtain boards, where provided, should extend down from the ceiling for a sufficient distance to ensure that the value of d_c, as shown in Figure 4-3, is a minimum of 20 percent of the ceiling height, H, measured as follows:

(a) For flat roofs, from the ceiling to the floor
(b) For sloped roofs, from the center of the vent to the floor

Where there are differing vent heights, H, each vent should be calculated individually.

NOTE: If d_c exceeds 20 percent of H, $H - d_c$ should be not less than 3 m. For Figure 4-3, this concept is valid where $\Delta d / d_c$ is much less than 1.

4-4 Spacing.

4-4.1 The distance between curtain boards (or between walls without intervening curtain boards) should not exceed 8 times the ceiling height to ensure that vents remote from the fire within the curtained compartment are effective.

4-4.2 Smaller curtained areas should be used where occupancies are particularly vulnerable to damage. The distance between these curtain boards should be not less than twice the ceiling height. This spacing guidance can be disregarded for curtain boards that extend down to a depth of at least 40 percent of the ceiling height.

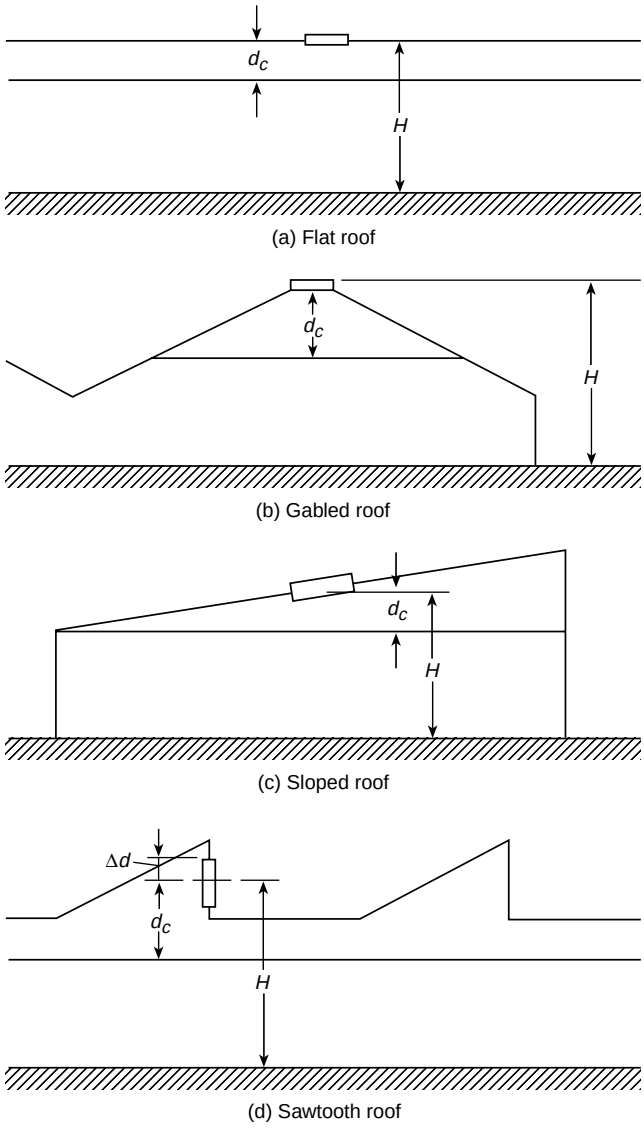

Figure 4-3 Measurement of ceiling height *(H)* and curtain board depth *(d_c)*.

Chapter 5 Predicting the Rate of Heat Release of Fires

5-1 Introduction. This chapter presents techniques for estimating the heat release rate of various fuel arrays likely to be present in buildings where smoke and heat venting is a potential fire safety provision. It primarily addresses the estimation of fuel concentrations found in storage and manufacturing locations. NFPA 92B, *Guide for Smoke Management Systems in Malls, Atria, and Large Areas,* addresses the types of fuel arrays more common to the types of building situations covered by that standard.

This guide is applicable to situations in which the hot layer does not enhance the burning rate. The methods provided in this chapter for estimating the rate of heat release, therefore, are based on "free burning" conditions in which no ceiling or hot gas layer effects are involved. It is assumed, therefore, that the burning rate is relatively unaffected by the hot layer.

5-2 Sources of Data. The following sources of data appear in their approximate order of priority, given equal quality of data acquisition:

(a) Actual tests of the array involved
(b) Actual tests of similar arrays
(c) Algorithms derived from tests of arrays having similar fuels and dimensional characteristics
(d) Calculations based on tested properties and materials and expected flame flux
(e) Mathematical models of fire spread and development

5-3 Actual Tests of the Array Involved. Where an actual calorific test of the specific array under consideration has been conducted and the data are in a form that can be expressed as rate of heat release, the data can then be used as input for the methods in this guide. Since actual test data seldom produce the steady state assumed for a limited-growth fire or the square-of-time growth assumed for a continuous-growth fire, engineering judgment is usually needed to derive the actual input necessary if either of these approaches is used. If LAVENT or another computer model capable of responding to a rate of heat release versus time curve is used, the data can be used directly. Currently there is no established catalog of tests of specific arrays. Some test data can be found in technical reports. Alternatively, individual tests can be conducted.

Many fire tests do not include a direct measurement of rate of heat release. In some cases, that measure can be derived based on measurement of mass loss rate using the following equation:

$$Q = \dot{m}(h_c) \tag{5-1}$$

where Q is in kW, $\dot{m}$ is in kg/sec, and h_c is in kJ/kg.

In other cases, a direct measurement can be derived based on measurement of flame height as follows:

$$Q = 37(L + 1.02D)^{5/2} \tag{5-2}$$

where Q is in kW, L is in m, and D is in m.

5-4 Actual Tests of Arrays Similar to That Involved. Where an actual calorific test of the specific array under consideration cannot be found, it might be possible to find data on one or more tests that are similar to the fuel of concern in important matters such as type of fuel, arrangement, or ignition scenario. The more the actual tests are similar to the fuel of concern, the higher the confidence that can be placed in the derived rate of heat release. Added engineering judgment, however, might be needed to adjust the test data to that approximating the fuel of concern. If the rate of heat release has not been directly measured, it can be estimated using the methods provided in Section 5-3.

5-5 Algorithms Derived from Tests of Arrays Having Similar Fuels and Dimensional Characteristics.

5-5.1 Pool Fires. In many cases, the rate of heat release of a tested array has been divided by a common dimension, such as occupied floor area, to derive a normalized rate of heat release per unit area. The rate of heat release of pool fires is the best documented and accepted algorithm in this class.

An equation for the mass release rate from a pool fire is as follows [Babrauskas 1995]:

$$\dot{m}'' = \dot{m}''_\infty(1 - e^{-(k_e\beta)D}) \tag{5-3}$$

The variables $\dot{m}''_\infty$ and $k_e\beta$ for Eq. (5-3) are as shown in Table 5-5.1.

Table 5-5.1 Data for Large Pool Burning Rate Estimates

Material	Density (kg/m^3)	h_c (MJ/kg)	$\dot{m}''_\infty$ (kg/m^{2}sec)	$k_e\beta$ (m^{-1})
Cryogenics[a]				
Liquid H_2	70	120.0	0.017	6.1
LNG (mostly CH_4)	415	50.0	0.078	1.1
LPG (mostly C_3H_8)	585	46.0	0.099	1.4
Alcohols				
Methanol (CH_3OH)	796	20.0	0.017	∞[c]
Ethanol (C_2H_5OH)	794	26.8	0.015	∞[c]
Simple organic fuels				
Butane (C_4H_{10})	573	45.7	0.078	2.7
Benzene (C_5H_6)	874	40.1	0.085	2.7
Hexane (C_6H_{14})	650	44.7	0.074	1.9
Heptane (C_7H_{16})	675	44.6	0.101	1.1
Xylene (C_8H_{10})	870	40.8	0.090	1.4
Acetone (C_3H_6O)	791	25.8	0.041	1.9
Dioxane ($C_4H_8O_2$)	1035	26.2	0.018[b]	5.4[b]
Diethyl ether ($C_4H_{10}O$)	714	34.2	0.085	0.7
Petroleum products				
Benzine	740	44.7	0.048	3.6
Gasoline	740	43.7	0.055	2.1
Kerosene	820	43.2	0.039	3.5
JP-4	760	43.5	0.051	3.6
JP-5	810	43.0	0.054	1.6

Table 5-5.1 Data for Large Pool Burning Rate Estimates *(Continued)*

Material	Density (kg/m^3)	h_c (MJ/kg)	$\dot{m}''_\infty$ (kg/m^2sec)	$k_e\beta$ (m^{-1})
Transformer oil, hydrocarbon	760	46.4	0.039[b]	0.7[b]
Fuel oil, heavy	940–1000	39.7	0.035	1.7
Crude oil	830–880	42.5–42.7	0.022–0.045	2.8
Solids				
Polymethylmethacrylate $(C_5H_8O_2)_n$	1184	24.9	0.020	3.3
Polypropylene $(C_3H_6)_n$	905	43.2	0.018	
Polystyrene $(C_8H_8)_n$	1050	39.7	0.034	

[a]For pools on dry land, not over water.
[b]Estimate is uncertain, since only two data points are available.
[c]Value is independent of the diameter in a turbulent regimen.

The mass rates derived from Eq. (5-3) are converted to rates of heat release using Eq. (5-1) and the heat of combustion, h_c, from the Table 5-5.1. The rate of heat release per unit area times the area of the pool yields heat release data for the anticipated fire.

5-5.2 Other Normalized Data. Other data based on burning rate per unit area in tests have been developed. Tables 5-5.2(a) and (b) list these data.

Table 5-5.2(a) Unit Heat Release Rates for Fuels Burning in the Open

Commodity	Heat Release Rate (kW)
Wood or PMMA* (vertical)	
0.61 m height	100/m of width
1.83 m height	240/m of width
2.44 m height	620/m of width
3.66 m height	1000/m of width
Wood or PMMA	
Top of horizontal surface	$720/m^2$ of surface
Solid polystyrene (vertical)	
0.61 m height	220/m of width
1.83 m height	450/m of width
2.44 m height	1400/m of width
3.66 m height	2400/m of width
Solid polystyrene (horizontal)	$1400/m^2$ of surface
Solid polypropylene (vertical)	
0.61 m height	220/m of width
1.83 m height	350/m of width
2.44 m height	970/m of width
3.66 m height	1600/m of width
Solid polypropylene (horizontal)	$800/m^2$ of surface

*PMMA = polymethyl methacrylate (plexiglass, lucite, acrylic).

Table 5-5.2(b) Unit Heat Release Rate for Commodities

Commodity	Heat Release Rate (kW per m^2 of floor area)*
Wood pallets, stacked 0.46 m high (6–12% moisture)	1,420
Wood pallets, stacked 1.52 m high (6–12% moisture)	4,000
Wood pallets, stacked 3.05 m high (6–12% moisture)	6,800
Wood pallets, stacked 4.88 m high (6–12% moisture)	10,200
Mail bags, filled, stored 1.52 m high	400
Cartons, compartmented, stacked 4.5 m high	1,700
PE letter trays, filled, stacked 1.5 m high on cart	8,500
PE trash barrels in cartons, stacked 4.5 m high	2,000
PE fiberglass shower stalls in cartons, stacked 4.6 m high	1,400
PE bottles packed in cartons	6,200
PE bottles in cartons, stacked 4.5 m high	2,000
PU insulation board, rigid foam, stacked 4.6 m high	1,900
PS jars packed in cartons	14,200
PS tubs nested in cartons, stacked 4.2 m high	5,400
PS toy parts in cartons, stacked 4.5 m high	2,000
PS insulation board, rigid foam, stacked 4.2 m high	3,300
PVC bottles packed in cartons	3,400
PP tubs packed in cartons	4,400
PP and PE film in rolls, stacked 4.1 m high	6,200
Methyl alcohol	740
Gasoline	2,500
Kerosene	1,700
Fuel oil, no. 2	1,700

*Heat release rate per unit floor area of fully involved combustibles, based on negligible radiative feedback from the surroundings and 100 percent combustion efficiency.
Note:
PE = polyethylene PU = polyurethane
PP = polypropylene PV = polyvinyl chloride
PS = polystyrene

5-5.3 Other Useful Data. Examples of other data that are not normalized but that might be useful in developing the rate of heat release curve are included in Tables 5-5.3(a) through (d).

Table 5-5.3(a) Characteristics of Ignition Sources

Fuel	Typical Heat Output (W)	Burn Time[a] (sec)	Maximum Flame Height (mm)	Flame Width (mm)	Maximum Heat Flux (kW/m^2)
Cigarette 1.1 g (not puffed, laid on solid surface)			—	—	
Bone dry	5	1,200			42
Conditioned to 50% R.H.	5	1,200	—	—	35
Methenamine pill, 0.15 g	45	90	—	—	4
Match, wooden (laid on solid surface)	80	20–30	30	14	18–20
Wood cribs, BS 5852 Part 2					
No. 4 crib, 8.5 g	1,000	190			15[d]
No. 5 crib, 17 g	1,900	200			17[d]
No. 6 crib, 60 g	2,600	190			20[d]
No. 7 crib, 126 g	6,400	350			25[d]
Crumpled brown lunch bag, 6 g	1,200	80			
Crumpled wax paper, 4.5 g (tight)	1,800	25			
Crumpled wax paper, 4.5 g (loose)	5,300	20			
Folded double-sheet newspaper, 22 g (bottom ignition)	4,000	100			
Crumpled double-sheet newspaper, 22 g (top ignition)	7,400	40			
Crumpled double-sheet newspaper, 22 g (bottom ignition)	17,000	20			
Polyethylene wastebasket, 285 g, filled with 12 milk cartons (390 g)	50,000	200[b]	550	200	35[c]
Plastic trash bags, filled with cellulosic trash (1.2–14 kg)[e]	120,000 to 50,000	200[b]			

[a]Time duration of significant flaming.
[b]Total burn time in excess of 1800 seconds.
[c]As measured on simulation burner.
[d]Measured from 25 mm away.
[e]Results vary greatly with packing density.

Table 5-5.3(b) Characteristics of Typical Furnishings as Ignition Sources

Fuel	Total Mass (kg)	Total Heat Content (MJ)	Maximum Rate of Heat Release (kW)	Maximum Thermal Radiation to Center of Floor* (kW/m^2)
Wastepaper basket	0.73–1.04	0.7–7.3	4–18	0.1
Curtains, velvet/cotton	1.9	24	160–240	1.3–3.4
Curtains, acrylic/cotton	1.4	15–16	130–150	0.9–1.2
TV set	27–33	145–150	120–290	0.3–2.6
Chair mockup	1.36	21–22	63–66	0.4–0.5
Sofa mockup	2.8	42	130	0.9
Arm chair	26	18	160	1.2
Christmas tree, dry	6.5–7.4	11–41	500–650	3.4–14

*Measured at approximately 2 m from the burning object.

Table 5-5.3(c) Maximum Heat Release Rates from Fire Detection Institute Analysis

Fuel	Approximate Value (kW)
Medium wastebasket with milk cartons	100
Large barrel with milk cartons	140
Upholstered chair with polyurethane foam	350
Latex foam mattress (heat at room door)	1200
Furnished living room (heat at open door)	4000–8000

Table 5-5.3(d) Mass Loss and Heat Release Rates of Chairs

Specimen	(kg)	Mass Combustible (kg)	Style	Frame	Padding	Fabric	Interliner	Peak, m (g/sec)	Peak, Q (kW)
C12	17.9	17.0	Traditional easy chair	Wood	Cotton	Nylon		19.0	290[a]
F22	31.9		Traditional easy chair	Wood	Cotton (FR)	Cotton		25.0	370[a]
F23	31.2		Traditional easy chair	Wood	Cotton (FR)	Olefin		42.0	700[b]
F27	29.0		Traditional easy chair	Wood	Mixed	Cotton		58.0	920[b]
F28	29.2		Traditional easy chair	Wood	Mixed	Cotton		42.0	730[b]
CO2	13.1	12.2	Traditional easy chair	Wood	Cotton, PU	Olefin		13.2	800[b]
CO3	13.6	12.7	Traditional easy chair	Wood	Cotton, PU	Cotton		17.5	460[a]
CO1	12.6	11.7	Traditional easy chair	Wood	Cotton, PU	Cotton		17.5	260[a]
CO4	12.2	11.3	Traditional easy chair	Wood	PU	Nylon		75.7	1350[b]
C16	19.1	18.2	Traditional easy chair	Wood	PU	Nylon	Neoprene	NA	180[b]
F25	27.8		Traditional easy chair	Wood	PU	Olefin		80.0	1990
T66	23.0		Traditional easy chair	Wood	PU, polyester	Cotton		27.7	640
F21	28.3		Traditional easy chair	Wood	PU (FR)	Olefin		83.0	1970
F24	28.3		Traditional easy chair	Wood	PU (FR)	Cotton		46.0	700
C13	19.1	18.2	Traditional easy chair	Wood	PU	Nylon	Neoprene	15.0	230[a]
C14	21.8	20.9	Traditional easy chair	Wood	PU	Olefin	Neoprene	13.7	220[a]
C15	21.8	20.9	Traditional easy chair	Wood	PU	Olefin	Neoprene	13.1	210[b]
T49	15.7		Easy chair	Wood	PU	Cotton		14.3	210
F26	19.2		Thinner easy chair	Wood	PU (FR)	Olefin		61.0	810
F33	39.2		Traditional loveseat	Wood	Mixed	Cotton		75.0	940
F31	40.0		Traditional loveseat	Wood	PU (FR)	Olefin		130.0	2890
F32	51.5		Traditional sofa	Wood	PU (FR)	Olefin		145.0	3120
T57	54.6		Loveseat	Wood	PU, cotton	PVC		61.9	1100
T56	11.2		Office chair	Wood	Latex	PVC		3.1	80
CO9/T64	16.6	16.2	Foam block chair	Wood (part)	PU, polyester	PU		19.9	460
CO7/T48	11.4	11.2	Modern easy chair	PS foam	PU	PU		38.0	960
C10	12.1	8.6	Pedestal chair	Rigid PU foam	PU	PU		15.2	240[a]
C11	14.3	14.3	Foam block chair		PU	Nylon		NA	810[b]
F29	14.0		Traditional easy chair	PP foam	PU	Olefin		72.0	1950
F30	25.2		Traditional easy chair	Rigid PU foam	PU	Olefin		41.0	1060
CO8	16.3	15.4	Pedestal swivel chair	Molded PE	PU	PVC		112.0	830[b]
CO5	7.3	7.3	Bean bag chair		Polystyrene	PVC		22.2	370[a]
CO6	20.4	20.4	Frameless foam back chair		PU	Acrylic		151.0	2480[b]
T50	16.5		Waiting room chair	Metal	Cotton	PVC		NA	<10
T53	15.5	1.9	Waiting room chair	Metal	PU	PVC		13.1	270
T54	27.3	5.8	Metal frame loveseat	Metal	PU	PVC		19.9	370
T75/F20	7.5(×4)	2.6	Stacking chairs (4)	Metal	PU	PVC		7.2	160

[a]Estimated from mass loss records and assumed Wh_c.
[b]Estimated from doorway gas concentrations.

5-6 Calculated Fire Description Based on Tested Properties.

5-6.1 Background. It is possible to make general estimates of the rate of heat release of burning materials based on the fire properties of that material. The fire properties involved are determined by small-scale tests. The most important of these tests are the calorimeter tests involving both oxygen depletion calorimetry and the application of external heat flux to the sample while determining time to ignition, rate of mass release, and rate of heat release for the specific applied flux. Most prominent of the current test apparatus are the cone calorimeter (ASTM E 1354, *Standard Test Method for Heat and Visible Smoke Release Rates for Materials and Products Using an Oxygen Consumption Calorimeter*) and the Factory Mutual calorimeter [Tewarson 1995].

In addition to the directly measured properties, it is possible to derive ignition temperature, critical ignition flux, effective thermal inertia ($k\rho c$), heat of combustion, and heat of gasification based on results from these calorimeters. Properties not derivable from these calorimeters and essential to determining flame spread in directions not concurrent with the flow of the flame can be obtained from the LIFT (lateral ignition and flame travel) apparatus (ASTM E 1321, *Standard Test Method for Determining Material Ignition and Flame Spread Properties*).

This section presents a concept of the use of fire property test data as the basis of an analytical evaluation of the rate of heat release involved in the use of a tested material. The approach outlined in this section is based on that presented by Nelson and Forssell [1994].

5-6.2 Discussion of Measured Properties. Table 5-6.2 lists the type of fire properties obtainable from the cone or Factory Mutual calorimeters and similar instruments.

Table 5-6.2 Relation of Calorimeter-Measured Properties to Fire Analysis

Property	Ignition	Flame Spread	Fire Size (energy)
Rate of heat release[1]		X	X
Mass loss[1]			X
Time to ignition[1]	X	X	
Effective thermal properties[2]	X	X	
Heat of combustion[2]		X	X
Heat of gasification[2]			X
Critical ignition flux[2]	X	X	
Ignition temperature[2]	X	X	

[1]Property is a function of the externally applied incident flux.
[2]Derived properties from calorimeter measurements.

In Table 5-6.2, the rate of heat release, mass loss, and time to ignition are functions of the externally applied incident radiant heat flux imposed on the tested sample. The purpose of the externally applied flux is to simulate the fire environment surrounding a burning item.

In general, it can be estimated that a free-burning fuel package (i.e., one that burns in the open and is not affected by energy feedback from a hot gas layer of a heat source other than its own flame) is impacted by a flux in the range of 25 kW/m^2 to 50 kW/m^2. If the fire is in a space and conditions are approaching flashover, the flux can increase to the range of 50 kW/m^2 to 75 kW/m^2. In a fully developed, post-flashover fire, a range of 75 kW/m^2 to greater than 100 kW/m^2 can be expected. The following is a discussion of the individual properties measured or derived and the usual form used to report the property.

(a) *Rate of Heat Release.* The rate of heat release is determined by oxygen depletion calorimetry. Each test is run at a user-specific incident flux, either for a predetermined period of time or until the sample is consumed. The complete results are presented in the form of a plot of heat release rate versus time, with the level of applied flux noted. In some cases, the rate of heat release for several tests of the same material at different levels of applied flux is plotted on a single curve for comparison. Figure 5-6.2(a) is an example of such a plotting.

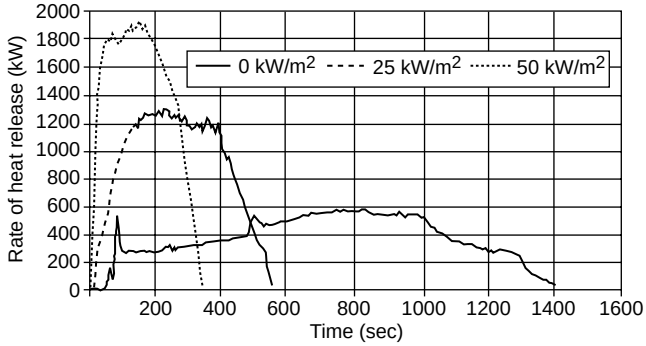

Figure 5-6.2(a) Typical graphic output of cone calorimeter test.

Often only the peak rate of heat release at a specific flux is reported. Table 5-6.2(a) is an example.

Table 5-6.2(a) Average Maximum Heat Release Rates (kW/m^2)

Material	Orientation	25 kW/m^2 Exposing Flux	50 kW/m^2 Exposing Flux	75 kW/m^2 Exposing Flux
PMMA	Horizontal	650	900	1300
	Vertical	560	720	1300
Pine	Horizontal	140	240	265
	Vertical	130	170	240
Sample A	Horizontal	125	200	250
	Vertical	90	130	220
Sample B	Horizontal	140	175	240
	Vertical	60	200	330
Sample C	Horizontal	—	215	250
	Vertical	—	165	170
Sample D	Horizontal	70	145	145
	Vertical	—	125	125

(b) *Mass Loss Rate.* Mass loss rate is determined by a load cell. The method of reporting is identical to that for rate of heat release. In the typical situation in which the material has a consistent heat of combustion, the curves for mass loss rate and rate of heat release are similar in shape.

(c) *Time to Ignition.* Time to ignition is reported for each individual test and applied flux level conducted.

(d) *Effective Thermal Inertia ($k\rho c$).* Effective thermal inertia is a measurement of the heat rise response of the tested material to the heat flux imposed on the sample. It is derived at the

time of ignition and is based on the ratio of the actual incident flux to the critical ignition flux and the time to ignition. A series of tests at different levels of applied flux is necessary to derive the effective thermal inertia. Effective thermal inertia derived in this manner can differ from, and be preferable to, handbook data for the values of k, ρ, and c that are derived without a fire.

(e) *Heat of Combustion.* Heat of combustion is derived by dividing the measured rate of heat release by the measured mass loss rate. It is normally reported as a single value, unless the sample is a composite material and the rates of heat release and mass loss vary significantly with time and exposure.

(f) *Heat of Gasification.* Heat of gasification is the flux needed to pyrolyze a unit mass of fuel. It is derived as a heat balance and is usually reported as a single value in terms of the amount of energy per unit mass of material released (e.g., kJ/g).

(g) *Critical Ignition Flux.* Critical ignition flux is the minimum level of incident flux on the sample needed to ignite the sample given an unlimited time of application. At incident flux levels less than the critical ignition flux, ignition does not take place.

(h) *Ignition Temperature.* Ignition temperature of a sample is the surface temperature at which flame occurs. This sample material value is independent of the incident flux and is derivable from the calorimeter tests, the LIFT apparatus test, and other tests. It is derived from the time to ignite in a given test, the applied flux in that test, and the effective thermal inertia of the sample. It is reported at a single temperature. If the test includes a pilot flame or spark, the reported temperature is for piloted ignition; if there is no pilot present, the temperature is for auto-ignition. Most available data are for piloted ignition.

5-6.3 Ignition. Equations for time to ignition, t_{ig}, are given for both thermally thin and thermally thick materials, as defined in 5-6.3(a) and (b). For materials of intermediate depth, estimates for t_{ig} necessitate considerations beyond the scope of this presentation [Drysdale 1985, Carslaw and Jaeger 1959].

(a) *Thermally Thin Materials.* Relative to ignition from a constant incident heat flux, $\dot{q}''_i$, at the exposed surface and with relatively small heat transfer losses at the unexposed surface, a thermally thin material is one whose temperature is relatively uniform throughout its entire thickness, l, at $t = t_{ig}$. For example, at $t = t_{ig}$,

$$T_{exposed} - T_{unexposed} = T_{ig} - T_{unexposed} < 0.1(T_{ig} - T_o) \tag{5-4}$$

Equation (5-4) can be used to show that a material is thermally thin [Carslaw and Jaeger 1959] if

$$l < 0.6(t_{ig}\alpha)^{1/2} \tag{5-5}$$

For example, for sheets of maple or oak wood (where the thermal diffusivity $\alpha = 1.28 \times 10^{-7}$ m^2/sec [DiNenno et al. 1995]), if $t_{ig} = 35$ sec is measured in a piloted ignition test, then, according to Eq. (5-5), if the sample thickness is less than approximately 0.0013 m, the unexposed surface of the sample can be expected to be relatively close to T_{ig} at the time of ignition, and the sample is considered to be thermally thin.

The time to ignition of a thermally thin material subjected to incident flux above a critical incident flux is

$$t_{ig} = \rho c l \frac{(T_{ig} - T_o)}{\dot{q}''_i} \tag{5-6}$$

(b) *Thermally Thick Materials.* Relative to the type of ignition test described in 5-6.3(a), a sample of a material of a thickness, l, is considered to be thermally thick if the increase in temperature of the unexposed surface is relatively small compared to that of the exposed surface at $t = t_{ig}$. For example, at $t = t_{ig}$,

$$T_{unexposed} - T_o < 0.1(T_{exposed} - T_o) = 0.1(T_{ig} - T_o) \tag{5-7}$$

Equation (5-7) can be used to show that a material is thermally thick [Carslaw and Jaeger 1959] if

$$1 > 2(t_{ig}\alpha)^{1/2} \tag{5-8}$$

For example, according to Eq. (5-8), in the case of an ignition test on a sheet of maple or oak wood, if $t_{ig} = 35$ sec is measured in a piloted ignition test, then, if the sample thickness is greater than approximately 0.0042 m, the unexposed surface of the sample can be expected to be relatively close to T_o at the time of ignition, and the sample is considered to be thermally thick.

Time to ignition of a thermally thick material subjected to incident flux above a critical incident flux is

$$t_{ig} = \frac{\pi}{4} k\rho c \left(\frac{T_{ig} - T_o}{\dot{q}''_i} \right)^2 \tag{5-9}$$

It should be noted that a particular material is not intrinsically thermally thin or thick (i.e., the characteristic of being thermally thin or thick is not a material characteristic or property) but rather depends on the thickness of the particular sample (i.e., a particular material can be implemented in either a thermally thick or a thermally thin configuration).

(c) *Propagation Between Separate Fuel Packages.* Where the concern is for propagation between individual, separated fuel packages, incident flux can be calculated using traditional radiation heat transfer procedures [Tien et al. 1995].

The rate of radiation heat transfer from a flaming fuel package of total energy release rate, Q, to a facing surface element of an exposed fuel package can be estimated from the following equation:

$$\dot{q}''_i = \frac{X_r Q}{4\pi r^2} \tag{5-10}$$

5-6.4 *Estimating Rate of Heat Release.* As discussed in 5-6.2, tests have demonstrated that the energy feedback from a burning fuel package ranges from approximately 25 kW/m^2 to 50 kW/m^2. For a reasonably conservative analysis, it is recommended that test data developed with an incident flux of 50 kW/m^2 be used. For a first-order approximation, it should be assumed that all of the surfaces that can be simultaneously involved in burning are releasing energy at a rate equal to that determined by testing the material in a fire properties calorimeter with an incident flux of 50 kW/m^2 for a free-burning material and 75 kW/m^2 to 100 kW/m^2 for post-flashover conditions.

In making this estimate, it is necessary to assume that all surfaces that can "see" an exposing flame (or superheated gas, in the post-flashover condition) are burning and releasing energy and mass at the tested rate. If sufficient air is present, the rate of heat release estimate is then calculated as the product of the exposed area and the rate of heat release per unit area as determined in the test calorimeter. Where there are test data taken at

the incident flux of the exposing flame, the tested rate of heat release should be used. Where the test data are for a different incident flux, the burning rate should be estimated using the heat of gasification as expressed in Eq. (5-11) to calculate the mass burning rate per unit area.

$$\dot{m}'' = \frac{\dot{q}_i''}{h_g} \tag{5-11}$$

The resulting mass loss rate is then multiplied by the derived effective heat of combustion and the burning area exposed to the incident flux to produce the estimated rate of heat release.

$$Q = \dot{m}'' h_c A \tag{5-12}$$

5-6.5 Flame Spread. If it is desired to predict the growth of fire as it propagates over combustible surfaces, it is necessary to estimate flame spread. The computation of flame spread rates is an emerging technology still in an embryonic stage. Predictions should be considered as order of magnitude estimates.

Flame spread is the movement of the flame front across the surface of a material that is burning (or exposed to an ignition flame) but whose exposed surface is not yet fully involved. Physically, flame spread can be treated as a succession of ignitions resulting from the heat energy produced by the burning portion of a material, its flame, and any other incident heat energy imposed on the unburned surface. Other sources of incident energy include another burning object, high-temperature gases that can accumulate in the upper portion of an enclosed space, and the radiant heat sources used in a test apparatus such as the cone calorimeter or the LIFT mechanism.

For analysis purposes, flame spread can be divided into the following two categories:

(a) Concurrent, or wind-aided, flame spread, which moves in the same direction as the flame
(b) Lateral, or opposed, flame spread, which moves in any other direction

Concurrent flame spread is assisted by the incident heat flux from the flame to unignited portions of the burning material. Lateral flame spread is not so assisted and tends to be much slower in progression unless an external source of heat flux is present. Concurrent flame spread for thermally thick materials can be expressed as follows:

$$V = \frac{(\dot{q}_i'')^2 L_f}{k\rho c (T_{ig} - T_s)^2} \tag{5-13}$$

The values for $k\rho c$ and ignition temperature are calculated from the cone calorimeter as discussed. For this equation, the flame length, L_f, is measured from the leading edge of the burning region, and T_s is the initial temperature of the solid material.

5-6.6 Classification of Fires for Engineering Equations. The engineering equations in Section 6-1 are appropriate for steady fires, limited growth fires, and t-squared forms of continuous growth fires.

Chapter 6 Sizing Vents

6-1 Hand Calculations.

6-1.1 Elements of Problem.

6-1.1.1 In Figure 6-1.1.1, H is the distance between the base of the fire and the ceiling; d_c is the depth of the curtain boards and d is the design depth of the smoke layer; $\dot{m}_p$ is the mass flow rate of hot gas from the fire plume into the smoke layer; $\dot{m}_v$ is the mass flow rate of hot gas out of the vent (or vents); and A_v is the vent area (total vent area in curtained compartment, if more than one vent exists).

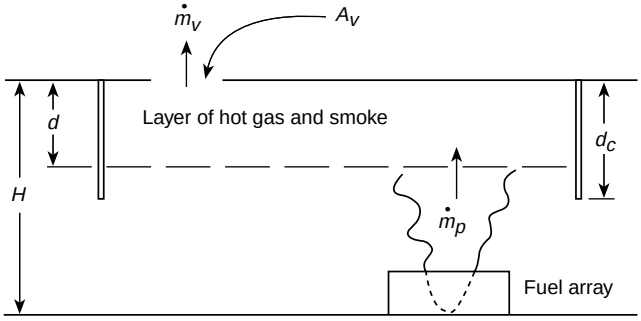

Figure 6-1.1.1 Schematic of venting system.

6-1.1.2 First, equilibrium conditions are assumed, with the layer already having formed. The smoke interface is level with the bottom of the curtain boards. At equilibrium, the mass flow rate into the smoke layer, $\dot{m}_p$, equals the mass flow rate out of the vent, $\dot{m}_v$.

6-1.1.3 The vent area calculated for equilibrium conditions corresponds to the area needed for a long-term steady fire or to the area needed at the end of a design interval for a very slow growing fire. For shorter-term steady fires and for faster-growing fires, the calculated equilibrium vent area will prevent the smoke interface from descending completely to the bottom of the curtain boards. Therefore, equilibrium calculations represent a safety factor in the design.

6-1.2 Mass Flow Rate in Plume, $\dot{m}_p$.

6-1.2.1 The mass flow rate in the plume depends on whether locations above or below the mean flame height are considered (i.e., whether the flames are below the smoke interface or reach into the smoke layer). The mean flame height is calculated from Eq. (6-1) [Heskestad 1995] as follows:

$$L = -1.02D + 0.235 Q^{2/5} \tag{6-1}$$

where:
L = mean flame height (m)
D = base diameter of fire (m)
Q = total heat release rate (kW)

6-1.2.2 When the mean flame height, L, is below the interface and z is at or above the flame height but at or below the interface height, the mass flow rate in the fire plume is calculated as follows *(see 6-1.4.2 for application):*

$$\dot{m}_p = [0.071 Q_c^{1/3} (z - z_o)^{5/3}][1 + 0.027 Q_c^{2/3} (z - z_o)^{-5/3}] \tag{6-2}$$

where:

$\dot{m}_p$ = mass flowrate in the plume (kg/sec)
Q_c = convective heat release rate (approx. $0.7Q$) (kW)
z = height above the base of the fire (m)
z_o = height of "virtual origin" above the base of the fire (below the base of the fire, if negative) (m)

6-1.2.3 When z is at or below the flame height and at or below the interface, the mass flow rate can be expressed as follows [Heskestad 1995] *(see 6-1.4.2 for application):*

$$\dot{m}_p = (0.0056 Q_c)\frac{z}{L} \tag{6-3}$$

It should be noted that, at the mean flame height, the mass flow rate is

$$\dot{m}_{pL} = 0.0056 Q_c \tag{6-4}$$

6-1.2.4 The virtual origin, z_o, is the effective point source of the fire plume [Heskestad 1995]:

$$z_o = 0.083 Q^{2/5} - 1.02 D \tag{6-5}$$

where Q is in kW and D is in m.

6-1.2.5 For combustibles that extend in depth, such as storages, the base of the fire is selected in a horizontal plane containing the worst-case ignition location (i.e., the lowest point of the combustible array). Consequently, the base of the design fire is often selected on the floor of the building.

6-1.3 Mass Flow Rate Through Vents, $\dot{m}_p$.

6-1.3.1 The inlet area for fresh air in the building below the design level of the smoke interface, A_i, can throttle the inlet flow if it is not sufficiently large. The effective vent area with throttled inlet area is smaller than the unthrottled area, and the calculated vent area, A_v, should be increased by the following multiplier, M [Hinkley 1995]:

$$M = \left[1 + \left(\frac{A_v}{A_i}\right)^2 \frac{T_o}{T}\right]^{1/2} \tag{6-6}$$

where:

T_o = the ambient temperature

T = the smoke layer temperature

When $T = 440$ K, $T_o = 293$ K, and the vent area and inlet area are the same ($A_v/A_i = 1$), the multiplier is 1.29. Increasing the inlet area to twice the vent area, so that $A_v/A_i = 0.5$, the multiplier is 1.08. Reducing the inlet area to $^1/_2$ the vent area, so that $A_v/A_i = 2$, the multiplier is 1.90. The required vent areas, A_v, determined by 6-1.4, should be adjusted using the appropriate multiplier from Eq. (6-6), including the effects of the temperature ratio, T_o/T.

6-1.3.2 Equating the buoyancy head across the vent to the dynamic head in the vent, from Bernoulli's equation, provides the following:

$$\frac{1}{2}\rho u^2 = \Delta\rho\, gd \tag{6-7}$$

where:

ρ = the smoke layer density

$\Delta\rho = \rho_o - \rho$

ρ_o = the ambient density

u = the gas velocity in the vent

g = the acceleration of gravity

d = smoke layer depth

The mass flow through the vent is the product of gas density, velocity, and aerodynamic area (A_{va}), which, with the aid of Eq. (6-7) and the ideal gas law, becomes

$$\dot{m}_v = (2\rho_o^2 g)^{1/2}\left(\frac{T_o \Delta T}{T^2}\right)^{1/2} A_{va} d^{1/2} \tag{6-8}$$

In this case, T is the smoke layer temperature and $\Delta T = T - T_o$.

6-1.3.3 It should be noted that the factor $[(T_o\Delta T)/T^2]^{1/2}$ is quite insensitive to temperature as long as the smoke layer temperature rise, ΔT, is not small. For example, assuming $T_o =$ 294 K, the factor varies through 0.47, 0.50, and 0.47 as the smoke layer temperature rise varies through 150 K, 320 K, and 570 K. At a temperature rise of 60 K the factor is 0.38, and at a temperature rise of 20 K it is 0.24, or about one-half its maximum value. Consequently, roof venting by natural ventilation becomes increasingly less effective as the smoke layer temperature decreases. For low smoke layer temperatures, powered ventilation as covered in NFPA 92B, *Guide for Smoke Management Systems in Malls, Atria, and Large Areas,* should be considered.

6-1.3.4 A representative smoke layer temperature rise, ΔT, can be estimated as a fraction, K, of the adiabatic temperature rise, ΔT_a, as follows:

$$\Delta T = K\Delta T_a = \frac{KQ_c}{c_p \dot{m}_p} \tag{6-9}$$

where c_p is the specific heat of air at constant pressure. The plume mass flow, $\dot{m}_p$, is evaluated from Eq. (6-2) or (6-3), with $z = H - d$ (where H is the ceiling height above the base of the fire). Equation (6-2) is used if the flame height, L, of Eq. (6-1) is smaller than $(H - d)$, and Eq. (6-3) is used if the flame height, L, is larger than $(H - d)$. From experimentation [Hinkley et al. 1992], it is evident that the fraction, K, decreases with the distance from the fire, but a representative value, $K =$ 0.5, can be used. Adopted values of temperature rise should be limited to 1000°C.

6-1.4 Required Vent Area.

6-1.4.1 The required actual vent area is the minimum total area, A_v, of all the open vents in a curtained compartment needed to prevent the smoke from underspilling the curtain boards or from descending below the design level of the smoke interface.

6-1.4.2 The required aerodynamic vent area, A_{va}, is calculated with the aid of Eqs. (6-1), (6-2), (6-3), (6-5), (6-8), and (6-9), setting $z = H - d$, where H is the ceiling height above the base of the fire (usually the floor).

6-1.4.3 The area, A_{va}, calculated according to the procedures in 6-1.4.2, is the aerodynamic vent area, which is always smaller than the geometric vent area, A_v. For simple apertures, A_{va} can be taken as 0.61 times the geometric throughflow area. In other words, the calculated vent areas, A_{va}, should be increased by a factor of 1/0.61 to establish the geometric vent area. If the discharge coefficient is different from 0.61, the calculated vent areas should be multiplied by the ratio of 0.61 to the actual discharge coefficient.

6-1.4.4 The calculated vent areas also should be increased by the multiplier, M, in Eq. (6-6) to account for limited inlet area for fresh air. The resulting vent area is distributed among individual vents within the curtained compartment.

6-1.4.5 Steady Fires (Limited-Growth Fires).

6-1.4.5.1 For steady fires, or fires that do not develop beyond a maximum size, the required vent area per curtained compartment is calculated based on the maximum anticipated heat release rate, Q and Q_c, the associated distance from the fire base to the bottom of the curtain boards or to the design elevation of the smoke interface, $H - d$, and the estimated fire diameter, D.

6-1.4.5.2 These fires include special-hazard fires and fires in occupancies with concentrations of combustibles separated by sufficiently wide aisles. The minimum aisle width to prevent lateral spread by radiation, W_{min} [Alpert and Ward 1984], can be estimated from Eq. (6-10) for radiant heat flux from a fire and a conservatively low value for the ignition flux of most materials (20.4 kW/m^2):

$$W_{min} = 0.042\,Q^{1/2} \tag{6-10}$$

where Q is in kW and W_{min} is in m.

The values produced by Eq. (6-10) can be produced from Eq. (5-10) if X_r is assumed to be 0.5.

6-1.4.5.3 The fire diameter, D, is taken as the diameter of a circle having the same area as the floor area of the fuel concentration.

6-1.4.5.4 The heat release rate is taken as the heat release rate per unit area times the floor area of the fuel concentration. The maximum foreseeable storage height (above the fire base) and associated heat release rate should be considered.

6-1.4.5.5 The heat release rate per unit area might be available from listings for a given storage height, such as Table 5-5.2(b). To establish estimates for other than specified heights, it can be assumed that the heat release rate per unit area is proportional to the storage height, based on tests [Yu and Stavrianidis 1991] and the data in Table 5-5.2(b) for wood pallets. For fuel configurations that have not been tested, the procedures of Chapter 5 should be used.

6-1.4.5.6 There is a distinct possibility that a combustible storage array could collapse before the end of the design interval of the venting system. (The design interval might end, for example, when manual fire fighting is expected to begin.) The fire diameter increases, contributing to increased smoke production (via a lower flame height and virtual origin). However, the heat release rate and fire growth rate after collapse are likely to be smaller than with no collapse. Consequently, it is reasonable to assume that the net effect of collapse is not significant for the calculation procedure.

6-1.4.6 Growing Fires (Continuous-Growth Fires).

6-1.4.6.1* A t-squared fire growth is assumed:

$$Q = 1000(t/t_g)^2 \tag{6-11}$$

where Q is in kW and t and t_g are in seconds.

Here, t is the time from effective ignition (*see Figure 6-1.4.6.1*) following an incubation period and t_g is the time, t, at which the fire exceeds an intermediate size of 1000 kW. The growth time, t_g, is a measure of the fire growth rate; the smaller the growth time, the faster the fire grows.

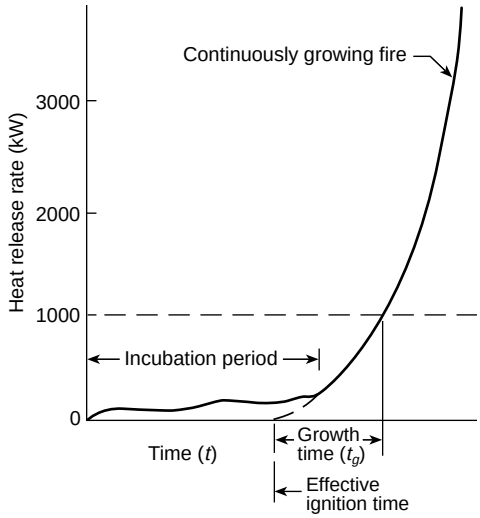

Figure 6-1.4.6.1 Conceptual illustration of continuous-growth fire.

6-1.4.6.2 Instead of growth time, t_g, t-squared fire growth can be expressed in terms of a fire growth coefficient, α_g, as follows:

$$Q = \alpha_g t^2 \tag{6-11a}$$

where Q is in kW, t is in sec, and α_g is in kW sec^{-2} = kW sec^{2}.

Comparing Eq. (6-11a) and Eq. (6-11), the following relation exists:

$$\alpha_g = \frac{1000}{t_g^2} \tag{6-11b}$$

6-1.4.6.3 Growth times for a number of combustible arrays have been obtained (see Table 6-1.4.6.3). These are specified for certain storage heights. Actual tests [Yu and Stavrianidis 1991] have demonstrated that it is reasonable to assume that the instantaneous heat release rate per unit height of the storage array is insensitive to the storage height. Such behavior corresponds to the growth time, t_g, being inversely proportional to the square root of the storage height. Alternatively, it corresponds to the fire growth coefficient, α_g, being directly proportional to the storage height. For example, if the storage height is $^1/_3$ the tested height, the growth time is $[1/(^1/_3)]^{1/2} = 1.73$ times the growth time from the test. If the storage height is three times the tested height, the growth time is $(^1/_3)^{1/2} = 0.58$ times the growth time from the test. For fuel configurations that have not been tested, the procedures discussed in Chapter 5 might be applicable

6-1.4.6.4 A venting system must be able to maintain the smoke layer above the design level from the time of ignition until the end of the design interval, t_r, where t_r is measured from the time of detection, t_d.

At the end of the design interval, the heat release rate is

$$Q = 1000\left(\frac{t_r + t_d}{t_g}\right)^2 \tag{6-12}$$

where Q is in kW and t_r, t_d, and t_g are in seconds.

The end of the design interval, t_r, may be selected to correspond to various critical events:

(a) Arrival of the emergency response team
(b) Arrival of fire fighters from the public fire department
(c) Completion of evacuation
(d) Other critical events

Table 6-1.4.6.3 Continuous-Growth Fires

Fuel	Growth Time* (sec)
Wood pallets, stacked 0.46 m high (6–12% moisture)	160–320
Wood pallets, stacked 1.52 m high (6–12% moisture)	90–190
Wood pallets, stacked 3.05 m high (6–12% moisture)	80-120
Wood pallets, stacked 4.88 m high (6–12% moisture)	75–120
Mail bags, filled, stored 1.52 m high	190
Cartons, compartmented, stacked 4.57 m high	60
Paper, vertical rolls, stacked 6.10 m high	17–28
Cotton (also PE, PE/cot acrylic/nylon/PE), garments in 3.66-m high rack	22–43
"Ordinary combustibles" rack storage, 4.57–9.14 m high	40–270
Paper products, densely packed in cartons, rack storage, 6.10 m high	470
PE letter trays, filled, stacked 1.52 m high on cart	180
PE trash barrels in cartons, stacked 4.57 m high	55
FRP shower stalls in cartons, stacked 4.57 m high	85
PE bottles packed in compartmented cartons, stacked 4.57 m high	85
PE bottles in cartons, stacked 4.57 m high	75
PE pallets, stacked 0.91 m high	150
PE pallets, stacked 1.83–2.44 m high	32–57
PU mattress, single, horizontal	120
PU insulation board, rigid foam, stacked 4.57 m high	8
PS jars packed in compartmented cartons, stacked 4.57 m high	55
PS tubs nested in cartons, stacked 4.27 m high	110
PS toy parts in cartons, stacked 4.57 m high	120
PS insulation board, rigid foam, stacked 4.27 m high	7
PVC bottles packed in compartmented cartons, stacked 4.57 m high	9
PP tubs packed in compartmented cartons, stacked 4.57 m high	10
PP and PE film in rolls, stacked 4.27 m high	40
Distilled spirits in barrels, stacked 6.10 m high	25–40

Note: FRP = fiberglass-reinforced polyester
PE = polyethylene
PP = polypropylene
PS = polystyrene
PU = polyurethane
PVC = polyvinyl chloride
*Growth times of developing fires in various combustibles, assuming 100 percent combustion efficiency.

6-1.4.6.5 The instantaneous diameter of the fire needed for calculation of L and z_o can be calculated from the instantaneous heat release rate, Q, and data on the heat release rate per unit floor area, Q'' (according to listings such as in Table 5-5.2(b) and assuming Q'' is proportional to storage height):

$$D = \left(\frac{4Q}{\pi Q''}\right)^{1/2} \tag{6-13}$$

6-1.4.7 Detection (Activation).

6-1.4.7.1 Detection (activation) for the purpose of actuating vents should be either by heat or smoke at the vent location or by heat or smoke detectors installed on a regular matrix.

6-1.4.7.2 The earlier the fire is detected, the earlier evacuation of the building can begin. Furthermore, for continuous-growth fires, the earlier the fire is detected and vents actuated, the smaller the fire size at the end of the design interval, and the smaller the required vent area. In the case of limited-growth fires, the earlier the fire is detected and the vents actuated, the less likely to occur are an initial underspill of smoke at the curtain boards and smoke layer excursion to low heights.

6-1.4.7.2.1 For calculating both the detection time, t_d, of the first detector projected to operate and the detection time of the detector controlling the actuation of the last projected vent to operate in a curtained area prior to the end of the design interval, the design fire should be assumed to be farthest possible from both detectors within the curtained area.

6-1.4.7.2.1.1 Detection times for heat detectors and fusible links, with the latter serving as common actuators for commercial heat and smoke vents, can be determined with the aid of NFPA 72, *National Fire Alarm Code®*, provided the spacing between detectors does not exceed 15 m.

6-1.4.7.2.1.2 If the spacing between heat detectors (or fusible links) exceeds 15 m, the detection time can be determined from the following response differential equation [Heskestad and Bill 1989(A)]:

$$\frac{d(\Delta T_e)}{dt} = \frac{u^{1/2}}{RTI}(\Delta T - \Delta T_e) \tag{6-14}$$

The detection time is the time, $t = t_d$, when T_e reaches the value associated with the rated temperature of the heat-responsive element.

6-1.4.7.2.1.3 In the case of continuous-growth, t-squared fires, gas temperatures for the calculation in Eq. (6-14) can be determined from the following [Heskestad and Delichatsios 1989(B)]:

$$\Delta T = 3575\left[\frac{t/(t_g^{2/5}H^{4/5}) - 0.442(1 + r/H)}{\dfrac{1 + 1.65r/H}{[t_g^{4/5}H^{3/5}]}}\right]^{-4/3} \tag{6-15}$$

where:

ΔT = 0, the interpretation, is applied when the numerator of the first bracket is zero or negative and

H = ceiling height above the fire base

r = radius from fire axis

and where T is in °C, t_g is in seconds, and H is in m.

6-1.4.7.2.1.4 Gas velocities for the calculation in Eq. (6-14) can be evaluated from a relation between gas velocity and temperature as follows [Heskestad and Delichatsios 1989(B)]:

$$\left(\frac{1}{(\Delta T/T_o g)H}\right)^{1/2} = 0.59\left(\frac{r}{H}\right)^{-0.63} \quad (6\text{-}16)$$

where:

T_o = ambient air temperature

g = acceleration of gravity

6-1.4.7.2.2 Detection times for smoke detectors can be determined with the aid of Eq. (6-15) as the time to reach a certain temperature rise, ΔT, at response, which is also the foundation for smoke detector spacing curves in NFPA 72, *National Fire Alarm Code*. This temperature rise should be determined in dedicated tests, or the equivalent, for the combustible of the occupancy and the detector model to be installed. A temperature rise of 10°C or less at detection is considered representative of a reasonably sensitive detector for a specific combustible.

6-1.4.7.2.3 The response data in NFPA 72, *National Fire Alarm Code*, as well as the temperature and velocity relations in Eqs. (6-15) and (6-16), assume extensive, flat, horizontal ceilings. This assumption might appear optimistic for installations involving beamed ceilings. However, any delay in operation due to beams is at least partially offset by the opposite effects of the following:

(a) Heat banking up under the ceiling because of curtain boards or walls

(b) The nearest vent or detector usually being closer to the fire than the assumed, greatest possible distance

6-1.4.7.3 Detection Computer Programs.

6-1.4.7.3.1 A computer program, known as DETACT-T2 [Evans and Stroup 1985], is available for calculating detection times of heat detectors in continuous growth, *t*-squared fires. It is equivalent to solving Eq. (6-14) with the aid of Eq. (6-16) and is effectively a predecessor of Eq. (6-15). The program calculates detection times for smoke detectors *(see 6-1.4.7.2.2)* based on the effective predecessor. The effective predecessor assumes complete combustion of the test fuel used in the experiments leading to the equation, whereas Eq. (6-15) is based on the actual heat of combustion. However, DETACT-T2 can still be used, provided that the projected fire growth coefficient, α_g, is multiplied by the factor 1.67. In addition, when using DETACT-T2, the outputs of heat release rate at detector response from the program calculations are to be divided by 1.67 in order to establish actual heat release rates at detector response.

6-1.4.7.3.2 Another computer program, known as DETACT-QS [Evans and Stroup 1985], is available for calculating detection times of heat detectors and smoke detectors in fires of arbitrary fire growth. Quasi-steady gas temperatures and velocities are assumed (i.e., instantaneously, gas temperatures and velocities under the ceiling are assumed to be related to the heat release rate as in a steady-state fire). For *t*-squared fires, this program would be less accurate than DETACT-T2 (if the projected fire growth coefficient is increased as described in 6-1.4.7.3.1), especially for fast-growing fires, but DETACT-QS does provide a means of handling fires that cannot be approximated as *t*-squared fires.

6-1.4.8 Selection of Design Basis. The vent area in a curtained compartment should not be required to exceed the vent area calculated for the largest limited-growth fire predicted for the combustibles beneath the curtained area. Using sufficiently small concentrations of combustibles and aisle widths at least as large as calculated from Eq. (6-10), it might be possible to satisfy the venting needs using smaller vent areas than required by a continuous growth vent design.

6-1.5 Limitations.

6-1.5.1 A design for a given building and its combustible contents and their distribution would comprise selecting a design basis (limited-growth versus continuous-growth fire) and establishing the following parameters:

(a) Layout of curtained areas
(b) A curtain depth
(c) Type detector and specific characteristics
(d) Detector spacing
(e) An appropriate design interval, t_r, following detection for maintaining a clear layer (for continuous-growth fires)
(f) Total vent area per curtained compartment
(g) Distribution of individual vents
(h) An air inlet area

Certain limitations of venting designs should be observed.

6-1.5.1.1 The distance from the fire base to the smoke interface, $H - d$, is a dominant variable. Some design situations can result in smoke layer temperatures as expressed in Eq. (6-9) (with $K = 0.5$) that exceed 600°C. Since fire can flash over to all the combustibles under the curtained area at this temperature, it clearly represents an unacceptable design situation.

Temperature limits exist for structural members. For example, structural steel has lost approximately half of its strength at a temperature of 540°C. Initiation of charring of wood members is typically assumed to occur at 280°C. The temperature of unprotected steel and surfaces of wood will closely follow the exposing smoke temperature. Practical options include enforcing limits on areas of fuel concentrations or heights of the combustible, or both, to limit the heat release rate to levels low enough to prevent the occurrence of unacceptable design temperatures.

6-1.5.1.2 Danger to unprotected steel directly over the fire depends on local temperatures in the smoke layer over the fire. These temperatures reach the 540°C limit earlier than the average smoke layer temperature calculated using $K = 0.5$ in Eq. (6-9). In Eq. (6-9), $K = 1$ should be used to assess this limitation, which necessitates further restricting the storage height of the combustible.

6-1.5.2 The feasibility of roof venting should be questioned when the heat release rate approaches values associated with ventilation control of the burning process (i.e., where the fire becomes controlled by the makeup air replacing the vented hot gas and smoke). Ventilation-controlled fires might be unable to support a clear layer. This limiting heat release rate is termed $Q_{feasible}$ and can be estimated from the following [Heskestad 1991]:

$$Q_{feasible} = 23,200(H - d)^{5/2} \quad (6\text{-}17)$$

where $Q_{feasible}$ is in kW and H and d are in m.

Venting at heat release rates greater than $Q_{feasible}$ to maintain a clear layer necessitates larger vent areas than those indicated by the calculation scheme provided.

6-2 Models. For consistency with Appendix B and with referenced documents on the fire model LAVENT, the nomenclature for this section differs from other sections. The definitions for the variables used in this section are provided in Section B-7, Nomenclature, of Appendix B.

6-2.1 Mathematical Models to Simulate Fire-Generated Environments and the Action of Vents. A ceiling vent design is successful to the extent that it controls a fire-generated environment developing in a space of fire origin according to any of a variety of possible specified criteria. For example, if the likely growth rate of a fire in a particular burning commodity is known, a vent system with a large enough vent area, designed to provide for timely opening of the vents, can be expected to lead to rates of smoke removal that are so large that fire fighters, arriving at the fire at a specified time subsequent to fire detection, are able to attack the fire successfully and protect commodities in adjacent spaces from being damaged.

To evaluate the success of a particular design, it is necessary to predict the development of the fire environment as a function of any of a number of physical characteristics that define and might have a significant effect on the fire scenario. Examples of such characteristics include the following:

(a) The floor-to-ceiling height and area of the space and the thermal properties of its ceiling, walls, and floor
(b) The type of barriers that separate the space of fire origin and adjacent spaces (e.g., full walls with vertical doorlike vents or ceiling-mounted curtain boards)
(c) The material type and arrangement of the burning commodities (e.g., wood pallets in plan-area arrays of 3 m × 3 m and stacked 2 m high)
(d) The type, location, and method of deployment of devices that detect the fire and actuate the opening of the vents (e.g., fusible links of specified RTI and distributed at a specified spacing distance below the ceiling)
(e) The size of the open area of the vents themselves

The best way to predict the fire environment and evaluate the likely effectiveness of a vent design is to use a reliable mathematical model that simulates the various relevant physical phenomena that come into play during the fire scenario. Such an analytical tool should be designed to solve well-formulated mathematical problems, based on basic relevant principles of physics and fundamentally sound, well-established, empirical relationships.

Even in the case of a particular class of problem, such as an engineering problem associated with successful vent design, there is a good deal of variation among applicable mathematical models that could be developed to carry out the task. Such models might differ from one another in the number and detail of the individual physical phenomena taken into account. Therefore, the list of physical characteristics that define and could have a significant effect on the fire scenario does not include outside wind conditions, which could have an important influence on the fire-generated environment.

A model might or might not include the effect of wind. A model that does include the effect of wind is more difficult to develop and validate and is more complicated to use. Note that the effect of wind is not taken into account in the LAVENT model discussed in 6-2.2. However, by using reasonably well accepted mathematical modeling concepts, LAVENT could be developed to the point that it could be used to simulate this effect.

Subsection 6-2.2 describes a group of phenomena that represent a physical basis for estimating the fire-generated environment and the response of heat-responsive elements in well-ventilated compartment fires with curtain boards and ceiling vents activated by fusible links, thermoplastic drop-out panels, or other alternative means of activation, or smoke detectors. The phenomena include the following:

(a) Growth of the smoke layer in the curtained compartment
(b) The flow dynamics of the buoyant fire plume
(c) The flow of smoke through open ceiling vents
(d) The flow of smoke below curtain boards
(e) Continuation of the fire plume in the upper layer
(f) Heat transfer to the ceiling surface and the thermal response of the ceiling
(g) The velocity and temperature distribution of plume-driven, near-ceiling flows
(h) The response of near-ceiling–deployed heat-responsive elements and smoke detectors

All the phenomena in items (a) through (h) are taken into account in the LAVENT model, which was developed to simulate the well-ventilated compartment fires with curtain boards and fusible link-actuated or smoke detector–actuated ceiling vents. Other models that could be developed for a similar purpose typically would also be expected to simulate these basic phenomena.

6-2.2 The Physical Basis for the Fire Model LAVENT.

6-2.2.1 The Basic Fire Scenario. The space to be considered is defined by ceiling-mounted curtain boards with a fire and with near-ceiling fusible link-actuated ceiling vents and sprinklers. The curtained area should be considered as one of several such spaces in a large building compartment. Also, by specifying that the curtains be deep enough, they can be thought of as simulating the walls of a single uncurtained compartment.

This subsection discusses critical physical phenomena that determine the overall environment in the curtained space up to the time of sprinkler actuation. The objective is to identify and describe the phenomena in a manner that captures the essential features of this generic class of fire scenario and allows for a complete and general, but concise and relatively simple, mathematical/computer simulation.

The overall building compartment is assumed to have near-floor intake air openings that are large enough to maintain the inside environment, below any near-ceiling smoke layers that might form, at outside-ambient conditions. Figure 6-2.2.1 depicts the generic fire scenario considered. It is assumed that a two-layer zone-type model adequately describes the phenomena under investigation. The lower layer is identical to the outside ambient. The upper smoke layer thickness and properties change with time, but the layer is assumed to be uniform in space at any time. Conservation of energy and mass along with the perfect gas law is applied to the upper layer. This leads to equations that necessitate estimates of the net rate of enthalpy flow plus heat transfer and the net rate of mass flow to the upper layer. Qualitative features of the phenomena that contribute to these flows and heat transfer are described briefly.

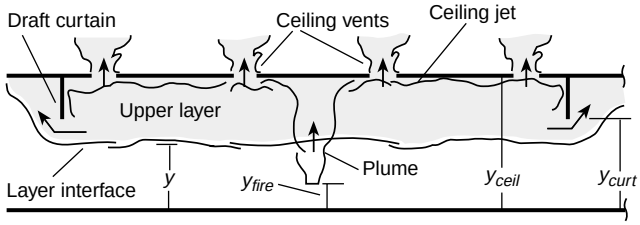

Figure 6-2.2.1 LAVENT model: fire in a building space with curtain boards and ceiling vents.

6-2.2.2 Flow Through the Ceiling Vents. Flow is driven through ceiling vents by cross-vent hydrostatic pressure differences. The traditional calculation uses orifice-type flow calculations. Bernoulli's equation is applied across a vent, and it is assumed that, away from and on either side of the vent, the environment is relatively quiescent. Figure 6-2.2.2 depicts the known, instantaneous, hydrostatic pressure distribution in the outside environment and throughout the depth of the curtained space. These are used to calculate the resulting cross-vent pressure difference, then the actual instantaneous mass and enthalpy flow rates through a vent.

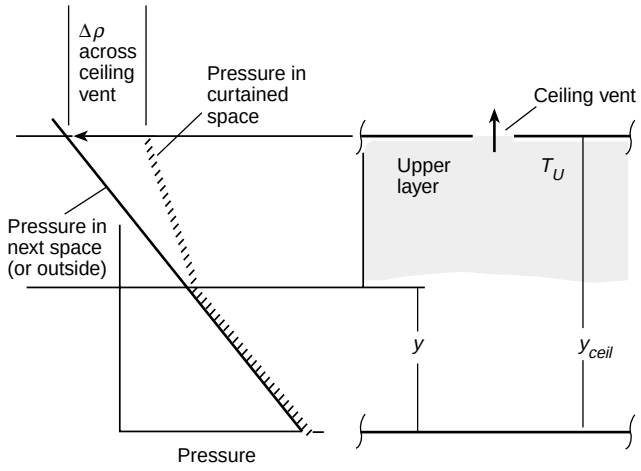

Figure 6-2.2.2 Flow through a ceiling vent.

6-2.2.3 Flow Below the Curtain Boards. If and when the layer interface drops below the bottom of the curtain boards, the smoke starts to flow out of the curtained space. As with the ceiling vents, this flow rate is determined by the cross-vent hydrostatic pressure difference. As depicted in Figure 6-2.2.3, however, the pressure difference in this case is not constant across the flow. Nonetheless, even in this configuration, the instantaneous flow rates are easily determined with well-known vertical-vent flow equations used traditionally in zone-type fire models.

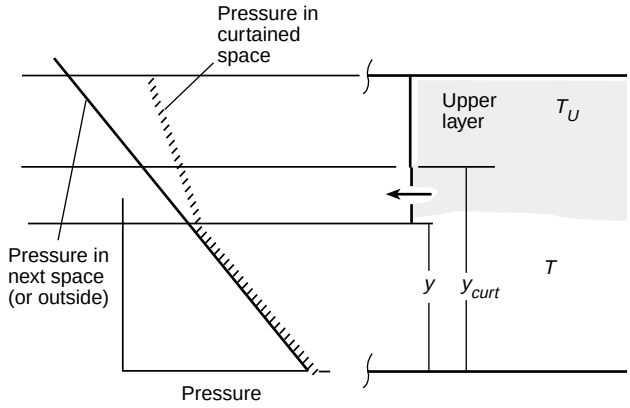

Figure 6-2.2.3 Flow below a curtain board.

6-2.2.4 The Fire, the Fire Plume, and Radiation Heat Transfer. The major contributors to the upper-layer flow and surface heat transfer are the fire and its plume. These properties are depicted in Figure 6-2.2.4. It is assumed that the rate of energy release of the fire's combustion zone does not vary significantly from known free-burn values that are available and assumed to be specified *(see Chapter 5)*. A known, fixed fraction of this energy is assumed to be radiated isotropically, as in the case of a point source, from the combustion zone. The smoke layer is assumed to be relatively transparent (i.e., all radiation from the fire is incident on the bounding surfaces of the compartment).

A plume model, selected from the several available in the literature, is used to determine the rate of mass and enthalpy flow in the plume at the elevation of the layer interface. It is assumed that all of this flow penetrates the layer interface and enters the upper layer.

As the plume flow enters the upper layer, the forces of buoyancy that act to drive the plume toward the ceiling are reduced immediately because of the temperature increase of the upper-layer environment over that of the lower ambient. As a result, the continued ascent of the plume gases is less vigorous (i.e., is at a reduced velocity) than it would be in the absence of the layer. Also, as the plume gases continue their ascent, the temperature becomes higher than it would be without the upper layer. Such higher temperatures are a result of the modified plume entrainment, which is now occurring in the relatively high temperature upper layer rather than in the ambient temperature lower layer. Methods of predicting the characteristics of the modified upper-plume flow are available.

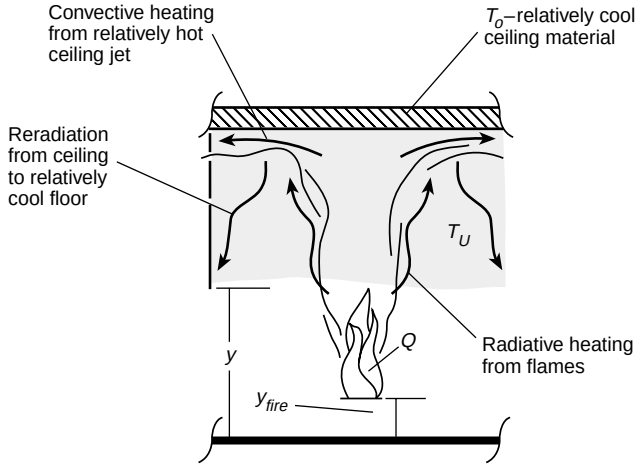

Figure 6-2.2.4 The fire, the fire plume, and heat transfer to the ceiling.

6-2.2.5 Convective Heat Transfer to the Ceiling. Having penetrated the interface, the plume continues to rise toward the ceiling of the curtained compartment. As it impinges on the ceiling surface, the plume flow turns and forms a relatively high temperature, high velocity, turbulent ceiling jet that flows radially outward along the ceiling and transfers heat to the relatively cool ceiling surface. The ceiling jet is cooled by convection, and the ceiling material is heated by conduction. Eventually, the now-cooled ceiling jet reaches the extremities of the curtained space and is deposited into and mixed with the upper layer. The convective heat transfer rate and the ceiling surface temperature on which it depends are both strong functions of the radial distance from the point of plume–ceiling impingement, and both decrease rapidly with increasing radius.

6-2.2.6 Thermal Response of the Ceiling. The thermal response of the ceiling is driven by transient heat conduction. For the time period typically considered, radial gradients in ceiling surface conditions are small enough so that

the conduction heat transfer is quasi–one dimensional in space. Therefore, the thermal response of the ceiling can be obtained from the solution to a set of one-dimensional conduction problems at a few discrete radial positions. These can be solved subject to net convection and radiation heat flux boundary conditions.

Interpolation in the radial direction between the solutions leads to a sufficiently smooth representation of the distributions of ceiling surface temperature and convective heat transfer rate. The latter is integrated over the ceiling surface to obtain the net instantaneous rate of convective heat transfer losses from the ceiling jet.

6-2.2.7 The Ceiling Jet and the Response of Heat-Responsive Elements. Convective heating and the thermal response of a near-ceiling heat-responsive element such as a fusible link or thermoplastic "drop-out" panel are determined from the local ceiling jet velocity and temperature. Velocity and temperature depend on vertical distance below the ceiling and radial distance from the fire plume axis. If and when its fusion (activation) temperature is reached, the device(s) operated by the link or other heat-responsive element is actuated.

For specific radial distances that are relatively near the plume, the ceiling jet is an inertially dominated flow. Its velocity distribution, depicted in Figure 6-2.2.7(a), can be estimated from the characteristics of the plume, upstream of ceiling impingement. The ceiling jet temperature distribution, depicted in Figure 6-2.2.7(b) for a relative "hot" or "cool" ceiling surface, is then estimated from the velocity (which is now known), upper-layer temperature, and ceiling-surface temperature, and heat flux distributions.

$$\Delta T_{CJ} = T_{CJ} - T_u = \begin{matrix}\text{ceiling jet} \\ \text{temperature}\end{matrix} - \begin{matrix}\text{upper-layer} \\ \text{temperature}\end{matrix}$$

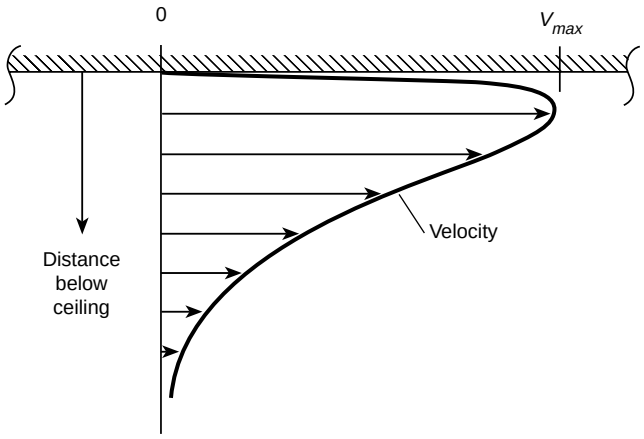

Figure 6-2.2.7(a) Ceiling jet velocity.

6-2.3 The LAVENT Model Equations and Computer Code.

6-2.3.1 The Model Equations: Guidelines, Assumptions, and Limitations. Appendix B provides details of all equations of the LAVENT mathematical fire model and its associated computer program developed to simulate all the phenomena described in 6-2.2. LAVENT can be used to simulate and study parametrically a wide range of relevant fire scenarios involving these phenomena.

Included in B-5.5 is a summary of guidelines, assumptions, and limitations to LAVENT. For example, as specified in that

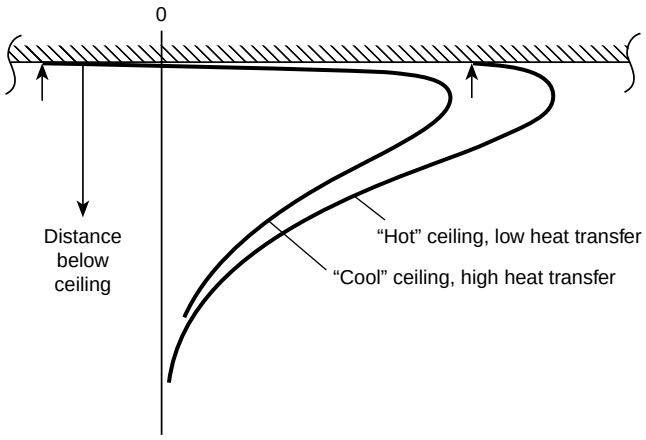

Figure 6-2.2.7(b) Ceiling jet temperature.

paragraph, LAVENT assumes that, at all times during a simulated fire, the overall building space containing the curtained area of fire origin is vented to the outside (e.g., through open doorways). It is assumed, furthermore, that the area of the outside vents is large relative to the area of the open ceiling vents in the curtained compartment.

Therefore, if the total area of the outside vents is A_{out}, then $(A_{out}/A_V)^2$ is significantly larger than 1 (e.g., $A_{out}/A_V > 2$). If the outside vents are in the bounding walls of the curtained space, not in adjacent spaces, they should be located entirely below the layer interface. Paragraph B-5.5 should be referenced for the details of other guidelines, assumptions, and limitations.

If the actual size of the outside vents is not significantly larger than the vent area, consideration should be given to increasing the vent area to account for the restrictions in inlet air using the multiplier provided in 6-1.3.1.

6-2.3.2 A User Guide for the Computer Code. Appendix C is a user guide for the LAVENT computer code. The appendix includes a comprehensive discussion of the inputs and calculated results of a default simulation involving a fire growing in a large pile of wood pallets (*t*-squared growth to a steady 33 MW) in a 9.1-m high curtained warehouse-type space with multiple fusible-link–actuated vents and near-ceiling–deployed fusible sprinkler links. Vents actuated by alternate means such as thermoplastic "drop-out" panels with equivalent performance characteristics can also be modeled using LAVENT. *(Refer to 1-1.2.)* Inputs to LAVENT include the following.

(a) *Dimensions of the Curtained Compartment of Fire Origin.* Length, width, and height of the curtained compartment of fire origin.

(b) *Dimensions of the Curtain Board.* Floor to bottom of the curtain separation distance and length of the curtain (a portion of the perimeter of the curtained space can include floor-to-ceiling walls).

(c) *Properties of the Ceiling.* Thickness, density, thermal conductivity, and heat capacity of the ceiling material.

(d) *Characteristics of the Fire.* Elevation of the base of the fire above the floor (*see 6-1.2);* total energy release rate of the fire, Q, at different times during the course of the simulated fire scenario (the computer code uses linear interpolation to approximate Q between these times); and the plan area of the fire, or the total energy release rate per unit area of the fire (in cases where the user supplies the latter input, the computer code estimates the changing area of the fire at any moment by using the current total energy release rate).

(e)* *Characteristics of the Ceiling Vent-Actuating Fusible Links or Vent-Actuating Smoke Detectors and of the Corresponding Ceiling Vents.* Horizontal distance from the fire, vertical distance below the ceiling surface, response time index (RTI), and fuse temperature of the ceiling vent-actuating fusible links; also, the clear open area, A_t, of their associated ceiling vents.

(f)* *Characteristics of Fusible Sprinkler Links.* Horizontal distance from the fire; vertical distance below the ceiling surface; RTI; and fuse temperature of fusible sprinkler links.

6-2.3.3 Computer Requirements. LAVENT is written in Fortran 77. The executable code operates on IBM PC-compatible computers and necessitates a minimum of 300 kilobytes of memory.

6-2.4 Experimental Validation of LAVENT. LAVENT has had some limited experimental validation in experiments with 3.34-m^2 pool fires in a 37 m × 40 m × 14 m high aircraft hangar [Walton and Notarianni, 1993; Notarianni, 1992]. The hangar was equipped with near-ceiling mounted brass disks of known RTI, which were used to simulate sprinkler links or heat detector elements. The experiments did not involve ceiling vents. Experimental validation of the various mathematical submodel equation sets that comprise the generalized LAVENT simulation is also implicit. This is the case, since the mathematical submodels of LAVENT, presented in Appendix B, are based on and carefully reproduced correlations of data acquired in appropriate experimental studies of the isolated physical phenomena that, taken together, make up the combined effects of a LAVENT-simulated fire scenario. To learn of the experimental basis and validation of the LAVENT submodels, the reader is referred to B-6, References, for Appendix B.

Chapter 7 Mechanical Exhaust Systems

7-1 General. For mechanical venting systems capable of functioning under the expected fire exposure, exhaust rates per curtained compartment are calculated from Eq. (6-2) or (6-3), with the aid of Eqs. (6-1) and (6-5). Gas temperatures are calculated from Eq. (6-9).

7-2 System Conversion. If a gravity venting system has been designed and the projected gas temperature rise in the smoke layer exceeds 150°C, conversion to an equivalent mechanical system can be done using Table 7-2.

Table 7-2 Conversion Factors for Equivalent Mechanical System

Design Depth of Smoke Layer (m)	Mechanical Exhaust Capacity per Unit Area of Gravity Vent ($kg/sec \cdot m^2$)
1.8	2.15
2.4	2.47
3.0	2.76
3.6	3.03
4.8	3.49
6.0	3.91
7.2	4.28

7-3 Intake Air. Adequate intake air should be provided to make up air for mechanical exhaust systems. Such intake might be powered or nonpowered.

Chapter 8 Venting in Sprinklered Buildings

8-1 Introduction. The previous chapters represent the state of technology of vent and curtain board design in the absence of sprinklers. A broadly accepted equivalent design basis for using sprinklers, vents, and curtain boards together for hazard control (e.g., property protection, life safety, water usage, obscuration) has not been universally recognized.

8-2 General. For occupancies that present a high challenge to sprinkler systems, concern has been raised that the inclusion of automatic roof venting or curtain boards, or both, can be detrimental to the performance of automatic sprinklers. Although there is no universally accepted conclusion from fire experience [Miller 1980], studies on a model scale [Heskestad 1974] suggested the following:

(a) Venting delays loss of visibility.

(b) Venting results in increased fuel consumption.

(c) Depending on the location of the fire relative to the vents, the necessary water demand to achieve control is either increased or decreased over an unvented condition. With the fire directly under the vent, water demand is decreased. With the fire equidistant from the vents, water demand is increased.

8-3 Automatic Roof Vents. A series of tests was conducted to increase the understanding of the role of automatic roof vents simultaneously employed with automatic sprinklers [Waterman 1982]. The data submitted did not provide a consensus on whether sprinkler control was impaired or enhanced by the presence of automatic (roof) vents for the typical spacing and area.

8-4 Curtain Boards. Large-scale fire tests [Troup 1994] indicated that the presence of curtain boards can cause increases in sprinkler operation, smoke production, and fire damage (i.e., sprinklers opened well away from the fire).

8-5 Other Tests. Other large-scale fire tests were conducted [Hinkley et al. 1992] employing liquid fuels, small vent spacings (minimum of 4.7 m), and vents open at ignition. Hinkley reached the following conclusions:

(a) The prior opening of vents had little effect on the operation of the first sprinkler.

(b) Venting substantially reduced the total number of sprinkler operations.

In an independent analysis of these tests, Gustafsson noted that sprinklers near the fire source were often delayed or did not operate altogether [Gustafsson 1992].

8-6 Conclusions. While the use of automatic venting and curtain boards in sprinklered buildings is still under review, the designer is encouraged to use the available tools and data referenced in this document for solving problems peculiar to a particular type of hazard control [Miller 1980; Heskestad 1974; Waterman 1982; Troup 1994; Hinkley et al. 1992; Gustafsson 1992].

Chapter 9 Inspection and Maintenance

9-1 Importance. Smoke and heat vents, as in the case of other fire protection systems and equipment, are subject to mishandling, improper installation, and on-site impairments. Regular inspection and maintenance is essential for emergency equipment and systems that are not subjected to their intended use for many years.

9-2 General.

9-2.1 Various types of approved automatic thermal smoke and heat vents have been made available commercially. These vents fall into two general categories:

(a) *Mechanically Opened Vents.* Examples include spring-lift, pneumatic-lift, or electric motor-driven vents.

(b) *Gravity-Opened Vents.* Examples include PVC or acrylic drop-out panels.

9-2.2 Generally, mechanically opened vents are provided with manual release devices that allow direct activation; inspection, maintenance, or both; as well as replacement of actuation components (e.g., heat-responsive devices, thermal sensors, compressed gas cylinders, explosive squibs).

9-2.3 Gravity-opened vents do not allow nondestructive operation, but inspection of the installed unit is necessary to ensure that the units are installed in accordance with the manufacturer's instructions and accepted trade practices and that all components are in place, undamaged, and free of soiling, debris, and extraneous items that might interfere with the operation and function of the unit.

9-2.4 The inspection and maintenance of multiple-function vents should also ensure that other functions do not impair the intended fire protection operation.

9-3 Frequency of Inspection and Maintenance.

9-3.1 Inspection Schedules. A written inspection schedule and procedures for inspection and maintenance should be developed and enforced. Inspection programs need to provide for written notations of date and time of inspections and for discrepancies found. All deficiencies found should be corrected immediately.

9-3.2 Mechanically Opened Vents.

9-3.2.1 It is important that an acceptance performance test and inspection of all mechanically opened vents be conducted immediately following installation to establish that all operating mechanisms function properly and that installation is in accordance with the manufacturer's specifications and accepted trade practices.

9-3.2.2 It is necessary to follow the manufacturer's recommendations regarding the maintenance and inspection schedule of mechanically operated vents.

9-3.2.3 Inspection schedules should include provisions for all units to be tested at 12-month intervals or on a schedule based on a percentage of the total units to be tested every month or every two months. Such procedures improve reliability.

9-3.2.4 Recording and logging of all pertinent characteristics of performance will allow a comparison of results with those of previous inspections or acceptance tests and thus provide a basis for determining the need for maintenance or for modifying the frequency of the inspection schedule to fit the experience.

9-3.2.5 A change in occupancy, or in neighboring occupancies, and in materials being used could introduce a significant change in the nature or severity of corrosive atmosphere exposure, debris accumulation, or physical encumbrance and necessitate a change in the inspection schedule.

9-3.2.6 Special mechanisms such as gas cylinders, thermal sensors, or detectors should be checked regularly on a schedule provided by the manufacturer.

9-3.3 Gravity-Opened Vents.

9-3.3.1 The same general considerations for inspection that apply to mechanically opened vents *(see 9-3.1)* also pertain to gravity-opened vents. The thermoplastic panels of these vents are designed to soften and drop out from the vent opening in response to the heat of a fire. This makes an operational test after installation impracticable. Recognized fire protection testing laboratories have developed standards and procedures for evaluating gravity-opened vents, including factory and field inspection schedules.

9-3.3.2 An acceptance inspection of all gravity-opened vents should be conducted immediately after installation. Compliance with the manufacturer's drawings and recommendations should be verified by direct examination. A suitable installation should follow accepted trade practices.

9-3.3.3 Changes in appearance, damage to any components, fastening security, weather tightness, and the adjacent roof and flashing condition should be noted at the time of inspection.

9-3.3.4 Prompt and careful removal of any soiling, debris, or encumbrances that could impair the operation of the vent is essential.

9-3.4 Intake Air Sources. Where necessary for the operation of vent systems, intake air sources should be inspected at the same frequency as vents.

9-4 Conduct and Observation of Operational Tests.

9-4.1 Mechanically Opened Vents.

9-4.1.1 Where feasible, releasing the vent should simulate actual fire conditions. Disconnecting the restraining cable at the heat-responsive device (or other releasing device) and suddenly releasing the restraint allows the trigger or latching mechanism to operate normally.

9-4.1.2* The heat-responsive device restraining cable is usually under considerable tension. Observation should be made of its whip and travel path to determine any possibility that the vent, building construction feature, or service piping could obstruct complete release. Any possible interference should be corrected by removal of the obstruction, enclosure of cable in a suitable conduit, or other appropriate arrangement. Following any modification, the unit should be retested for evaluation of adequacy of corrective measures.

9-4.1.3 Latches should release smoothly. The vent should start to open immediately and move through its design travel to the fully opened position without any assistance and without any problems such as undue delay indicative of a sticking weather seal, corroded or unaligned bearings, and distortion binding.

9-4.1.4 Manual releases should be tested to determine whether the vents operate.

9-4.1.5 All operating levers, latches, hinges, and weather-sealed surfaces should be examined to determine conditions, such as any indication of deterioration and accumulation of foreign material, that might warrant corrective action or suggest the need for another inspection in advance of the normal schedule.

9-4.1.6 Following painting of the interior or exterior of vents, the units should be opened and inspected to check for paint that could "glue" surfaces together.

9-4.1.7 Painted heat-responsive devices should be replaced with devices having an equivalent temperature and load rating.

9-4.2 Gravity-Opened Vents.

9-4.2.1 All weather-sealed surfaces should be examined to determine conditions, such as any indication of deterioration and accumulation of foreign material, that might warrant corrective action or suggest the need for another inspection in advance of the normal schedule.

9-4.2.2 Following painting of the interior or exterior of the frame or flashing of the vents, the units should be inspected to check for paint that could "glue" surfaces together.

9-5 Air Intakes.

9-5.1 Air intakes necessary for operation of smoke and heat vents should be maintained clear and free of obstructions.

9-5.2 Operating air intake louvers, doors, dampers, and shutters should be examined to assure movement to fully open positions.

9-5.3 Operating equipment should be maintained and lubricated as necessary.

9-6 Ice and Snow Removal. Removal of ice and snow from vents is an essential part of a vent maintenance program.

Chapter 10 Referenced Publications

10-1 The following documents or portions thereof are referenced within this guide and should be considered as part of its recommendations. The edition indicated for each referenced document is the current edition as of the date of the NFPA issuance of this guide. Some of these documents might also be referenced in this guide for specific informational purposes and, therefore, are also listed in Appendix E.

10-1.1 NFPA Publications. National Fire Protection Association, 1 Batterymarch Park, P.O. Box 9101, Quincy, MA 02269-9101.

NFPA 68, *Guide for Venting of Deflagrations,* 1998 edition.

NFPA 72, *National Fire Alarm Code®,* 1996 edition.

NFPA 92B, *Guide for Smoke Management Systems in Malls, Atria, and Large Areas,* 1995 edition.

10-1.2 Other Publications.

10-1.2.1 ASTM Publications. American Society for Testing and Materials, 100 Barr Harbor Drive, West Conshohocken, PA 19428-2959.

ASTM E 1321, *Standard Test Method for Determining Material Ignition and Flame Spread Properties,* 1993.

ASTM E 1354, *Standard Test Method for Heat and Visible Smoke Release Rates for Materials and Products Using an Oxygen Consumption Calorimeter,* 1994.

10-1.2.2 ICBO Publication. International Conference of Building Officials, 5360 Workman Mill Road, Whittier, CA 90601.

UBC Standard 15-7, *Automatic Smoke and Heat Vents,* 1997.

10-1.2.3 UL Publication. Underwriters Laboratories Inc., 333 Pfingsten Road, Northbrook, IL 60062.

UL 793, *Automatically Operated Roof Vents for Smoke and Heat,* 1995.

Appendix A Explanatory Material

Appendix A is not a part of the requirements of this NFPA document but is included for informational purposes only. This appendix contains explanatory material, numbered to correspond with the applicable text paragraphs.

A-1-1.4 Large, undivided floor areas present extremely difficult fire-fighting problems, since the fire department might need to enter these areas in order to combat fires in central portions of the building. If the fire department is unable to enter because of the accumulation of heat and smoke, fire-fighting efforts might be reduced to an application of hose streams to perimeter areas while fire continues in the interior. Windowless buildings also present similar fire-fighting problems. One fire protection tool that can be a valuable asset for fire-fighting operations in such buildings is smoke and heat venting.

A-1-2.1 The provisions of this guide can be permitted to be applied to the top story of multiple-story buildings. Many features of these provisions would be difficult or impracticable to incorporate into the lower stories of such buildings.

A-6-1.4.6.1 *t*-Squared Fires. Over the past decade, those interested in developing generic descriptions of the rate of heat release of accidental open flaming fires have used a "*t*-squared" approximation for this purpose. A *t*-squared fire is one in which the burning rate varies proportionally to the square of time. Frequently, *t*-squared fires are classified by their speed of growth as fast, medium, or slow (and occasionally ultra-fast). Where these classes are used, they are determined by the time needed for the fire to grow to a rate of heat release of 1000 kW. The times for each of these classes are provided in Table A-6-1.4.6.1. For many fires involving storage arrays, the time to reach 1000 kW might be much shorter than the 75 seconds depicted for ultra-fast fires.

Table A-6-1.4.6.1 Classifications of *t*-Squared Fires

Class	Time to Reach 1000 kW
Ultra-fast	75 sec
Fast	150 sec
Medium	300 sec
Slow	600 sec

The general equation is as follows:

$$Q = \alpha_g t^2$$

where:

Q = rate of heat release (kW)
α_g = a constant describing the speed of growth (kW/sec^2)
t = time (sec)

Relevance of *t*-Squared Approximation to Real Fires.

A *t*-squared fire can be viewed as a fire in which the rate of heat release per unit area is constant over the entire ignited surface and the fire spreads in circular form with a steadily increasing radius. In such cases, the increase in the burning area is the square of the steadily increasing fire radius. Of course, other fires that do not have such a conveniently regular fuel array and consistent burning rate might or might not actually produce a *t*-squared curve. The tacit assumption is that the *t*-squared approximation is close enough for reasonable design decisions.

Figure A-6-1.4.6.1(a) demonstrates that most fires have an incubation period during which the fire does not conform to a *t*-squared approximation. In some cases, this incubation period might be a serious detriment to the use of the *t*-squared approximation. In most instances, this is not a serious concern in large spaces covered by this guide. It is expected that the rate of heat release during the incubation period would not usually be sufficient to cause activation of the smoke detection system. In any case, where such activation occurs or human observation results in earlier activation of the smoke-venting system, a fortuitous safeguard would result.

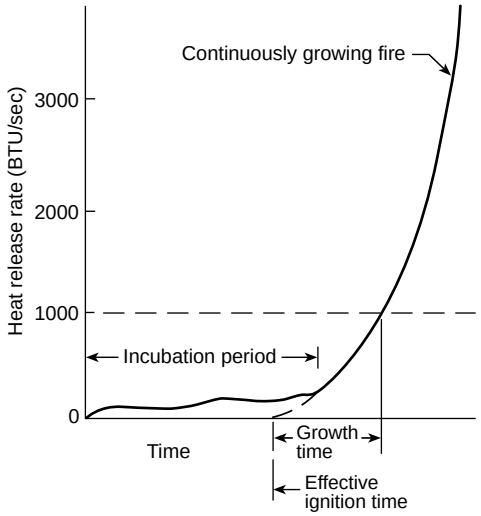

Figure A-6-1.4.6.1(a) Conceptual illustration of continuous fire growth.

Figure A-6-1.4.6.1(b), extracted from Harold E. Nelson, *An Engineering Analysis of the Early Stages of Fire Development—The Fire at the DuPont Plaza Hotel and Casino,* December 31, 1986, Report NBSIR 87-3560, National Institute of Standards and Technology, Gaithersburg, Maryland, 1987, compares rate of heat release curves developed by the aforementioned classes of *t*-squared fires and two test fires commonly used for test purposes. The test fires are shown as dashed lines labeled as furniture and 6-ft storage. The dashed curves farther from the fire origin show the actual rates of heat release of the test fires used in the development of the residential sprinkler and a standard 6-ft high array of test cartons containing foam plastic pails that also are frequently used as a standard test fire.

The other set of dashed lines in Figure A-6-1.4.6.1(b) shows these same fire curves relocated to the origin of the graph. This is a more appropriate comparison with the generic curves. It can be seen that the rate of growth in these fires is actually faster than that prescribed for an ultra-fast fire. This is appropriate for a test fire designed to challenge the fire suppression system being tested.

Figure A-6-1.4.6.1(c) relates the classes of *t*-squared fire growth curves to a selection of actual fuel arrays.

A-6-2.3.2(e) If ceiling vents are actuated by smoke detectors, the guidelines outlined in 6-1.4.7.2.2 should be followed. LAVENT can be made to simulate this function with a very sensitive fusible link (i.e., a link with a negligibly small RTI) and an appropriate fuse temperature.

As specified in B-4.1, LAVENT always assumes that the flow coefficient, *C,* for ceiling vents is $C = 0.68$; if the user has reason to believe that a different value, C_{user}, is more appropriate for a particular vent (such as the value 0.61 suggested in 6-1.4.3), then the input vent area for that vent should be scaled up proportionately (i.e., $A_{V,input} = A_V C_{user}/0.68$).

A-6-2.3.2(f) LAVENT calculates the time that the first sprinkler link fuses and the fire environment that develops in the curtained space prior to that time. Since the model does not simulate the interaction of sprinkler sprays and fire environments, any LAVENT simulation results subsequent to sprinkler waterflow should be ignored.

A-9-4.1.2 The whipping action of the cable on release presents a possibility of injury to anyone in the area. For this reason, the person conducting the test should ensure that all personnel are well clear of the area where whipping of the cable might occur.

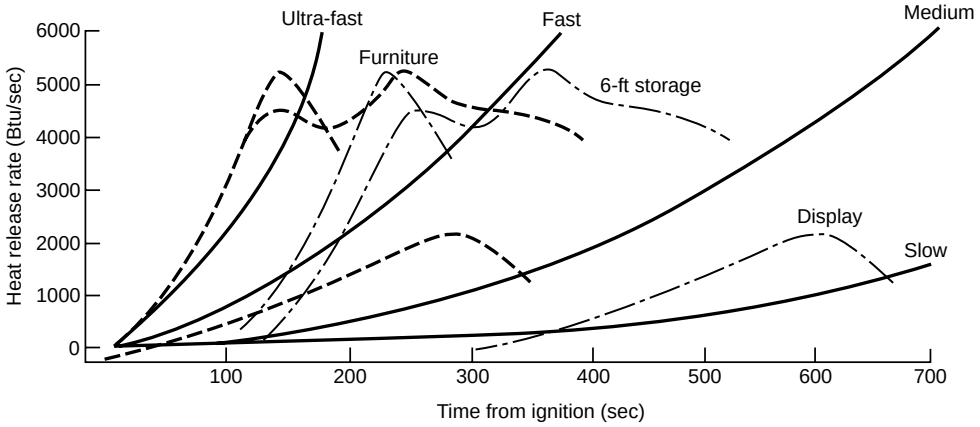

Figure A-6-1.4.6.1(b) Rates of energy release for *t*-squared fire.

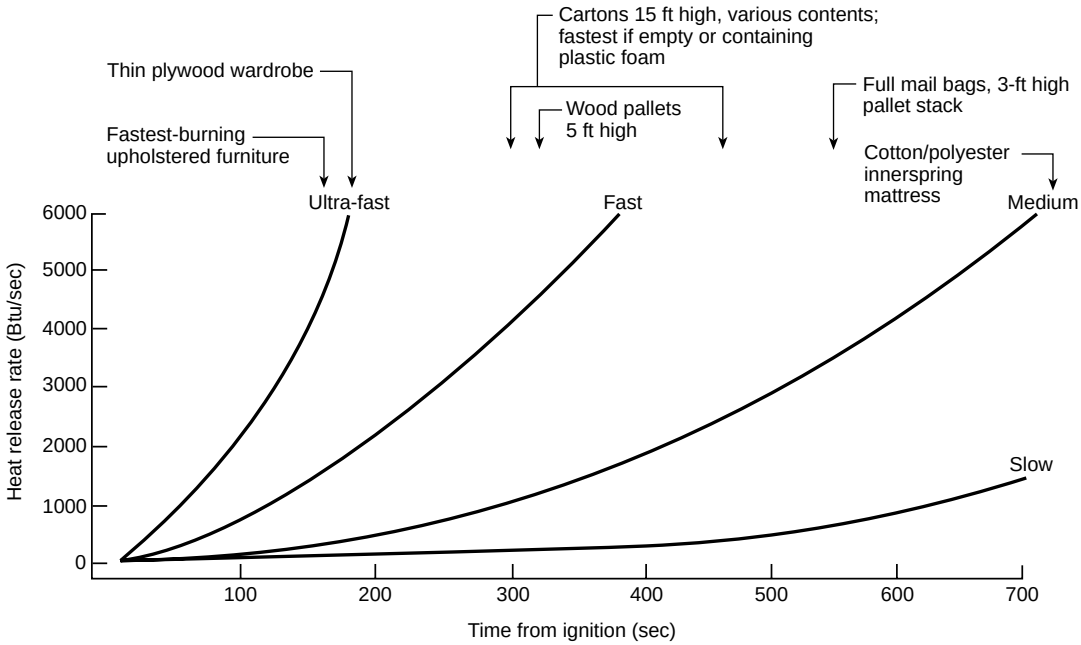

Figure A-6-1.4.6.1(c) Relation of *t*-squared fires to some fire tests.

Appendix B The Theoretical Basis of LAVENT

This appendix is not part of the recommendations of this NFPA document but is included for informational purposes only.

B-1 Overview. In this appendix, the physical basis and an associated mathematical model for estimating the fire-generated environment and the response of sprinkler links in well-ventilated compartment fires with curtain boards and ceiling vents actuated by heat-responsive elements such as fusible links or thermoplastic "drop-out" panels is developed. Complete equations and assumptions are presented. Phenomena taken into account include the following:

(a) Flow dynamics of the upward-driven, buoyant fire plume

(b) Growth of the elevated-temperature smoke layer in the curtained compartment

(c) Flow of smoke from the layer to the outside through open ceiling vents

(d) Flow of smoke below curtain partitions to building spaces adjacent to the curtained space of fire origin

(e) Continuation of the fire plume in the upper layer

(f) Heat transfer to the ceiling surface and the thermal response of the ceiling as a function of radial distance from the point of plume-ceiling impingement

(g) Velocity and temperature distribution of plume-driven near-ceiling flows and the response of near-ceiling–deployed fusible links as functions of distance below the ceiling

(h) Distance from plume-ceiling impingement

The theory presented here is the basis of the LAVENT computer program that is supported by a user guide, which is presented in Appendix C, and that can be used to study parametrically a wide range of relevant fire scenarios [1,2,3].

B-2 Introduction. The space under consideration is a space of a plan area, A, defined by ceiling-mounted curtain boards with a fire of time-dependent energy release rate, $Q(t)$, and with open ceiling vents of total time-dependent area, $A_V(t)$. The curtained area can be considered as one of several such spaces in a large building compartment. Also, by specifying that the curtains be deep enough, they can be thought of as simulating the walls of a single, uncurtained compartment. This appendix presents the physical basis and associated mathematical model for estimating the fire-generated environment and the response of sprinkler links in curtained compartment fires with ceiling vents actuated by heat-responsive elements such as fusible links or thermoplastic "drop-out" panels.

The overall building compartment is assumed to have near-floor wall vents that are large enough to maintain the inside environment, below any near-ceiling smoke layers that could form, at assumed initial outside-ambient conditions. Figure 6-2.2.1 depicts the generic fire scenario for the space under consideration. The assumption of large near-floor wall vents necessitates that the modeling be restricted to conditions where y, the elevation of the smoke layer interface, is above the floor elevation (i.e., $y > 0$). The assumption also has important implications with regard to the cross-ceiling vent pressure differential. This is the pressure differential that drives elevated-temperature upper-layer smoke through the ceiling vents to the outside. Therefore, below the smoke layer (i.e., from the floor of the facility to the elevation of the smoke layer interface), the inside-to-outside hydrostatic pressure differential exists at all elevations in the reduced-density smoke layer itself (higher pressure inside the curtained area, lower pressure in the outside environment), the maximum differential occurring at the ceiling and across the open ceiling vents.

B-3 The Basic Equations. A two-layer zone-type compartment fire model is used to describe the phenomena under investigation. As is typical in such models, the upper smoke layer of total mass, m_U, is assumed to be uniform in density, ρ_U, and absolute temperature, T_U.

The following time-dependent equations describe conservation of energy, mass, and the perfect gas law in the upper smoke layer.

Conservation of energy,

$$\frac{d[(y_{ceil}-y)\rho_U T_U A C_V]}{dt} = \dot{q}_U + \left(\rho A \frac{dy}{dt}\right) \tag{B-1}$$

Conservation of mass,

$$\frac{dm_U}{dt} = \dot{m}_U \tag{B-2}$$

$$m_U = (y_{ceil} - y)\rho_U A \tag{B-3}$$

Perfect gas law,

$$\frac{\rho_U}{R} \propto \frac{\rho}{R} = constant = \rho_U T_U = \rho_{amb} T_{amb} \tag{B-4}$$

That is,

$$T_U = \frac{T_{amb}\rho_{amb}}{\rho_U} \tag{B-5}$$

In the preceding equations, y_{ceil} is the elevation of the ceiling above the floor, $R = C_p - C_V$ is the gas constant, C_P and C_V are the specific heats at a constant pressure and volume, respectively, and ρ is a constant characteristic pressure (e.g., ρ_{atm}) at the floor elevation. In Eq. (B-1), $\dot{q}_U$ is the net rate of enthalpy flow plus heat transfer to the upper layer and is made up of flow components as follows: $\dot{q}_{curt}$, from below the curtain; $\dot{q}_{plume}$, from the plume; $\dot{q}_{vent}$, from the ceiling vent; and the component $\dot{q}_{HT}$, the total heat transfer rate.

$$\dot{q}_U = \dot{q}_{curt} + \dot{q}_{plume} + \dot{q}_{vent} + \dot{q}_{HT} \tag{B-6}$$

In Eq.(B-2), $\dot{m}_U$ is the net rate of mass flow to the upper layer with flow components; $\dot{m}_{curt}$, from below the curtain; $\dot{m}_{plume}$, from the plume; and $\dot{m}_{vent}$, from the ceiling vent.

$$\dot{m}_U = \dot{m}_{curt} + \dot{m}_{plume} + \dot{m}_{vent} \tag{B-7}$$

Using Eq. (B-3) in Eq. (B-1) leads to

$$\frac{dy}{dt} = \frac{\dot{q}_U}{AC_P\rho_{amb}T_{amb}} \tag{B-8}$$

if

$$y = y_{ceil} \quad \text{and} \quad \dot{q}_U \geq 0$$

or

$$0 < y > y_{ceil} \quad \text{and} \quad \text{arbitrary } \dot{q}_U$$

Since both of these conditions are satisfied, Eq. (B-8) is always applicable.

The basic problem of mathematically simulating the growth and properties of the upper layer for the generic Figure 6-2.2.1 scenario necessitates the solution of the system of Eq. (B-2) and Eq. (B-8) for m_U and y. Where $m_U > 0$, ρ_U can be computed from Eq. (B-3).

$$\rho_U = \frac{(y_{ceil} - y)A}{m_U}; \qquad \text{if } m_U > 0 \tag{B-9}$$

and T_U can be determined from Eq. (B-5).

B-4 Mass Flow and Enthalpy Flow Plus Heat Transfer.

B-4.1 Flow to the Upper Layer from the Vents. Conservation of momentum across all open ceiling vents as expressed by Bernoulli's equation leads to the following:

$$V = C\left(\frac{2\Delta\rho_{ceil}}{\rho_U}\right)^{1/2} \tag{B-10}$$

$$\dot{m}_{vent} = -\rho_U A_V V = -A_V C\,(2\rho_U \Delta\rho_{ceil})^{1/2} \tag{B-11}$$

where:
V = the average velocity through all open vents
C = the vent flow coefficient (0.68)
$\Delta\rho_{ceil}$ = the cross-vent pressure difference [4]

From hydrostatics,

$$\Delta\rho_{ceil} = \rho_U(y = y_{ceil}) - \rho_{amb}(y = y_{ceil}) = (\rho_{amb} - \rho_U)g(y_{ceil} - y) \tag{B-12}$$

where g = the acceleration of gravity.

Substituting Eq. (B-12) into Eq. (B-11) leads to the desired $\dot{m}_{vent}$ result as follows:

$$\dot{m}_{vent} = -A_V C[2\rho_U(\rho_{amb} - \rho_U)g(y_{ceil} - y)]^{1/2} \tag{B-13}$$

which is equivalent to the equations used to estimate ceiling vent flow rates, Eq. (6-8) and references [5 and 6]. Using Eq. (B-13), the desired $\dot{q}_{vent}$ result is as follows:

$$\dot{q}_{vent} = \dot{m}_{vent} C_P T_U \tag{B-14}$$

B-4.2 Flow to the Layer from the Plume and Radiation from the Fire. It is assumed that the mass generation rate of the fire is small compared to $\dot{m}_{ent}$, the rate of mass of air entrained into the plume between the fire elevation, y_{fire}, and the layer interface, or compared to other mass flow rate components of $\dot{m}_U$. It is also assumed that all of the $\dot{m}_{ent}$ penetrates the layer interface and enters the upper layer. Therefore,

$$\dot{m}_{plume} = \dot{m}_{ent} \tag{B-15}$$

$$\dot{q}_{plume} = \dot{m}_{ent} C_P T_{amb} + (1 - \lambda_r)\dot{Q} \tag{B-16}$$

The first term on the right side of Eq. (B-16) is the enthalpy associated with $\dot{m}_{ent}$, and λ_r, in the second term in Eq. (B-16), is the effective fraction of Q assumed to be radiated isotropically from the fire's combustion zone.

It is assumed that the smoke layer is relatively transparent and that it does not participate in any significant radiation heat transfer exchanges. In particular, all of the $\lambda_r Q$ radiation is assumed to be incident on the bounding surfaces of the compartment. Therefore, the last term of Eq. (B-16) is the net amount of enthalpy added to the upper layer from the combustion zone and its buoyancy-driven plume. Flaming fires exhibit values for λ_r of $0 < \lambda_r < 0.6$ (e.g., even smaller values for small methane and higher values for large polystyrene fires). However, for a hazardous fire involving a wide range of common groupings of combustibles, it is reasonable to approximate flame radiation by choosing $\lambda \propto 0.37$[7].

A specific plume entrainment model is necessary to complete Eqs. (B-14) and (B-15) for $\dot{m}_{plume}$ and q_{plume}. The following estimate for $\dot{m}_{ent}$ [8 and 9] is adopted as follows:

$$\dot{m}_{ent} = \begin{cases} 0; & \text{if } y - y_{fire} \le 0; \\ 0.0054\left[\left(1-\lambda_r\right)\dot{Q}\right]\dfrac{y - y_{fire}}{L_{flame}}; & \text{if } 0 < \dfrac{y - y_{fire}}{L_{flame}} < 1 \\ 0.071\left[\left(1-\lambda_r\right)\dot{Q}\right]^{1/3} \times \left\{(y - y_{fire} - L_{flame}) + 0.166\left[\left(1-\lambda_r\right)\dot{Q}\right]^{2/5}\right\}^{5/3} & \\ \times \left[1 + \in \left[\left(1-\lambda_r\right)\dot{Q}\right]^{2/3}\left\{\left(y - y_{fire} - L_{flame}\right) + 0.166\left[\left(1-\lambda_r\right)\dot{Q}\right]^{2/5}\right\}^{-5/3}\right]; & \\ \quad \text{if } \dfrac{y - y_{fire}}{L_{flame}} \ge 1 & \end{cases} \tag{B-17}$$

where $\dot{m}_{ent}$ is in kg/sec, $\dot{Q}$ is in kW, and y, y_{fire}, and L_{flame} are in m.

$$\frac{L_{flame}}{D_{fire}} = \begin{cases} 0; & \text{if } \dfrac{0.249\left[\left(1-\lambda_r\right)\dot{Q}\right]^{2/5}}{D_{fire}} - 1.02 < 0 \\ \dfrac{0.249\left[\left(1-\lambda_r\right)\dot{Q}\right]^{2/5}}{D_{fire}} - 1.02; & \text{if } \dfrac{0.249\left[\left(1-\lambda_r\right)\dot{Q}\right]^{2/5}}{D_{fire}} - 1.02 \geq 0 \end{cases} \tag{B-18}$$

where $\dot{Q}$ is in kW and D_{fire} is in m.

$$\in = \left(\frac{0.0054}{0.071}\right) - (0.166)^{5/3} = 0.02591682 \ldots \approx 0.026 \tag{B-19}$$

In Eqs. (B-17) through (B-19),

L_{flame} is the fire's flame length.

D_{fire} is the effective diameter of the fire source ($\pi D_{fire}^2/4$ = area of the fire source).

$\in$ is chosen so that, analytically, the value of $\dot{m}_{ent}$ is exactly continuous at the elevation $y = y_{fire} + L_{flame}$.

B-4.3 Flow to the Layer from Below the Curtains. If the upper layer interface, y, drops below the elevation of the bottom of the curtains, y_{curt}, mass and enthalpy flows occur from the upper layer of the curtained area where the file is located to adjacent curtained areas of the overall building compartment. The mass flow rate is the result of hydrostatic cross-curtain pressure differentials. Provided adjacent curtained areas are not yet filled with smoke, this pressure difference increases linearly from zero at the layer interface to $\Delta\rho_{curt}$ at $y = y_{curt}$.

From hydrostatics,

$$\begin{aligned} \Delta\rho_{curt} &\equiv \rho_U(y = y_{curt}) - \rho_{amb}(y = y_{curt}) \\ &= (\rho_{amb} - \rho_U) g (y_{curt} - y) \end{aligned} \tag{B-20}$$

Using Eq. (B-20) together with well-known vent flow relations (e.g., Eq. 32 of reference [4]), $\dot{m}_{curt}$ and $\dot{q}_{curt}$ can be estimated from the following:

$$\dot{m}_{curt} = \begin{cases} 0; & \text{if } y \geq y_{curt} \\ -\dfrac{L_{curt}}{3}\left[8\left(y_{curt} - y\right)^3 \rho_U \left(\rho_{amb} - \rho_U\right) g\right]^{1/2}; & \text{if } y \leq y_{curt} \end{cases} \tag{B-21}$$

$$\dot{q}_{curt} = \dot{m}_{curt} C_P T_U \tag{B-22}$$

where L_{curt} is that length of the perimeter of the curtained areas of the fire origin that is connected to other curtained areas of the overall building compartment. For example, if the curtained area is in one corner of the building compartment, then the length of its two sides coincident with the walls of the compartment are not included in L_{curt}.Since the generic vent flow configuration under consideration in this case is long and narrow, a flow coefficient for the vent flow incorporated into Eq. (B-21) is taken to be 1.

B-4.4 Heat Transfer to the Upper Layer. As discussed in B-4.3, where the fire is below the layer interface, the buoyant fire plume rises toward the ceiling and all of its mass and enthalpy flow, $\dot{m}_{plume}$ and $\dot{q}_{plume}$, is assumed to be deposited into the upper layer. Having penetrated the interface, the plume continues to rise toward the ceiling of the curtained compartment. As it impinges on the ceiling surface, the plume flow turns and forms a relatively high temperature, high velocity, turbulent ceiling jet that flows radially outward along the ceiling and transfers heat to the relatively cool ceiling surface. The ceiling jet is cooled by convection, and the ceiling material is heated by conduction. The convective heat transfer rate is a strong

function of the radial distance from the point of plume-ceiling impingement and reduces rapidly with increasing radius. It is dependent also on the characteristics of the plume immediately upstream of ceiling impingement.

The ceiling jet is blocked eventually by the curtains or wall surfaces or both. It then turns downward and forms vertical surface flows. In the case of wall surfaces and very deep curtains, the descent of these flows is stopped eventually by upward buoyant forces, and they finally mix with the upper layer. In this case, it is assumed that the plume-ceiling impingement point is relatively far from the closest curtain or wall surface (e.g., greater than a few fire-to-ceiling lengths). Under such circumstances, the ceiling jet-wall flow interactions are relatively weak, and compared to the net rate of heat transfer from the ceiling and near the plume-ceiling impingement point, the heat transfer to the upper layer from all vertical surfaces is relatively small.

The symbol λ_{conv} is defined as the fraction of $\dot{Q}$, which is transferred by convection from the upper-layer gas ceiling jet to the ceiling and wall-curtain surfaces, as follows:

$$\dot{q}_{HT} = -\lambda_{conv}\dot{Q} \tag{B-23}$$

Once the values of $\lambda_{conv}\dot{Q}$ and $\dot{q}_{HT}$ are determined from a time-dependent solution to the coupled, ceiling jet–ceiling material, convection-conduction problem, the task of determining an estimate for each component of $\dot{m}_U$ and $\dot{q}_U$ is complete.

B-4.4.1 Properties of the Plume in the Upper Layer Where $y_{fire} < y$. Times when the elevation of the fire is below the interface (i.e., when $y_{fire} < y$) should be considered.

As the plume flow moves to the center of the upper layer, the forces of buoyancy that act to drive the plume toward the ceiling (i.e., as a result of relatively high-temperature, low-density plume gases being submerged in a relatively cool, high-density ambient environment) are reduced immediately because of the temperature increase of the upper-layer environment over that of the lower ambient. As a result, the continued ascent of the plume gases is less vigorous (i.e., ascent is at reduced velocity) and of higher temperature than it would be in the absence of the layer. Indeed, some of the penetrating plume flow will be at a lower temperature than T_U.The upper-layer buoyant forces on this latter portion of the flow actually retard and can possibly stop its subsequent rise to the ceiling.

The simple point-source plume model [10] is used to simulate the plume flow, first immediately below or upstream of the interface and then throughout the depth of the upper layer itself.

The plume above a point-source of buoyancy [10], where the source is below the interface, is equivalent to the plume of the fire (in the sense of having identical mass and enthalpy flow rates at the interface) if the point-source strength is $(1-\lambda_r)\dot{Q}$ and the elevation of the equivalent source, y_{eq}, satisfies the following:

$$\dot{m}_{plume} = 0.21\rho_{amb}g^{1/2}\left(y-y_{eq}\right)^{5/2}\dot{Q}_{eq}^{*1/3} \tag{B-24}$$

In Eq. (B-24), $\dot{Q}_{eq}^{*}$, a dimensionless measure of the strength of the fire plume at the interface, is defined as follows:

$$\dot{Q}_{eq}^{*} = \frac{\left(1-\lambda_r\right)\dot{Q}}{\rho_{amb}C_P T_{amb} g^{1/2}\left(y-y_{eq}\right)^{5/2}} \tag{B-25}$$

It should be noted that at an arbitrary moment of time on the simulation of a fire scenario, $\dot{m}_{plume}$ in Eq. (B-24) is a known value that is determined previously from Eqs. (B-15) and (B-17).

Using (B-24) and (B-25) in order to solve for y_{eq} and $\dot{Q}_{eq}^{*}$,

$$y_{eq} = y - \left[\frac{\left(1 - \lambda_r\right)\dot{Q}}{\dot{Q}^*_{eq}\rho_{amb}C_P T_{amb} g^{1/2}} \right]^{2/5} \tag{B-26}$$

$$\dot{Q}^*_{eq} = \left[\frac{0.21(1 - \lambda_r)\dot{Q}}{C_P T_{amb}\dot{m}_{plume}} \right]^{3/2} \tag{B-27}$$

As the plume crosses the interface, the fraction, $\dot{m}^*$, of $\dot{m}_{plume}$, which is still buoyant relative to the upper-layer environment and presumably continues to rise to the ceiling, entraining upper-layer gases along the way, is predicted [11] to be as follows:

$$\dot{m}^* = \begin{cases} 0; & \text{if } -1 < \sigma \le 0 \\ \dfrac{1.04599\sigma + 0.360391\sigma^2}{1.0 + 1.37748\sigma + 0.360391\sigma^2}; & \text{if } \sigma > 0 \end{cases} \tag{B-28}$$

where the dimensionless parameter, σ, is defined as follows:

$$\sigma = \frac{1 - \alpha + C_T Q^{*2/3}_{eq}}{\alpha - 1} \tag{B-29}$$

$$\alpha = \frac{T_U}{T_{amb}} \tag{B-30}$$

where $C_T = 9.115$ and where $\dot{Q}^*_{eq}$ is the value computed in Eq. (B-27).

The parameters necessary to describe plume flow continuation in the upper layer (i.e., between y and y_{ceil}) are further identified *(see [11])* according to a point-source plume *(see [10])*. It has been determined that this plume can be modeled as being driven by a nonradiating buoyant source of strength, $\dot{Q}'$, located a distance

$$H = y_{ceil} - y'_{source} > y_{ceil} - y_{fire} \tag{B-31}$$

below the ceiling in a downward-extended upper-layer environment of temperature, T_U, and density, ρ_U. The relevant parameters predicted [11] are as follows:

$$\dot{Q}' = \frac{(1 - \lambda_r)\dot{Q}\sigma\dot{m}^*}{1 + \sigma} \tag{B-32}$$

$$y'_{source} = y - (y - y_{eq})\alpha^{3/5}\dot{m}^{*2/5}\left(\frac{1 + \sigma}{\sigma}\right)^{1/5} \tag{B-33}$$

The fire and the equivalent source in the lower layer and the continuation source in the upper layer are depicted in Figures B-4.4.1 (a) through (c). Times during a fire simulation when Eq. (B-29) predicts $\sigma >> 1$ are related to states of the fire environment in which the temperature distribution above T_{amb} of the plume flow, at the elevation of interface penetration, is predicted to be mostly much larger than $T_U - T_{amb}$. Under such circumstances, the penetrating plume flow is still very strongly buoyant as it enters the upper layer. The plume continues to rise to the ceiling and to drive ceiling jet convective heat transfer at rates that differ only slightly (due to the elevated temperature upper-layer environment) from the heat transfer rates that could occur in the absence of an upper layer.

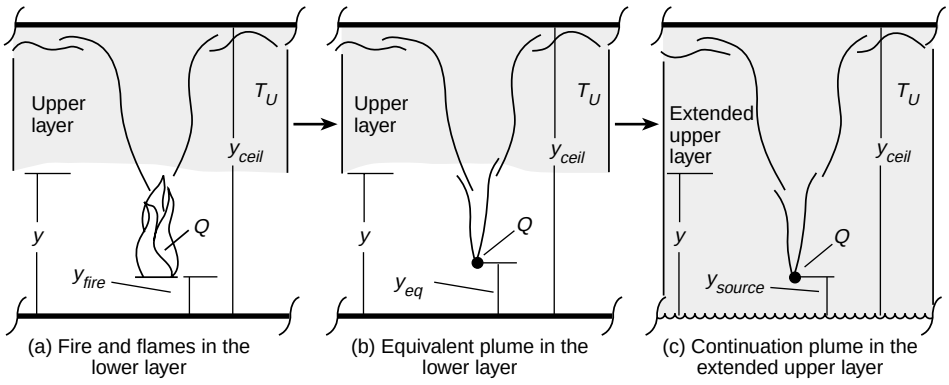

Figure B-4-4.1 Fire and equivalent source.

Conditions where Eq. (B-29) predicts $\sigma < 0$ are related to times during a fire scenario when the temperature of the plume at the elevation of interface penetration is predicted to be uniformly less than T_U. Under such circumstances, the penetration plume flow is not positively (i.e., upward) buoyant at any point as it enters the upper layer. Therefore, while all of this flow is assumed to enter and mix with the upper layer, it is predicted that none of it rises to the ceiling in a coherent plume (i.e., $Q' = 0$). For this reason, where $\sigma < 0$, the existence of any significant ceiling jet flow is precluded along with significant convective heat transfer to the ceiling surface or to near-ceiling–deployed fusible links.

The preceding analysis assumes that $y_{fire} < y$. However, at the onset of the fire scenario, $y_{fire} < y = y_{ceil}$ and α, σ, and $\dot{m}^*$ of Eqs. (B-28) through (B-31), which depend on the indeterminate initial value of T_U, are themselves undefined. The situation at $t = 0$ is properly taken into account if $Q' = (1 - \lambda_r) Q$ and

$$y'_{source} = y_{eq} \quad \text{at } t = 0$$

B-4.4.2 General Properties of the Plume in the Upper Layer. Where the fire is below the interface, the results of Eqs. (B-32) and (B-33) allow the fire-driven plume dynamics in the upper layer to be described according to the point-source plume model [10]. If the fire is at or above the interface (i.e., $y_{fire} \geq y$), then $\dot{m}_{plume} = 0$, $\dot{q}_{plume} = (1 - \lambda_r)\ Q$, and the point-source model is continued in use to simulate the upper-layer plume flow. All cases can be treated using the following final versions of original Eqs. (B-32) and (B-33) as follows:

$$\dot{Q}' = \begin{cases} \dfrac{(1-\lambda_r) Q \sigma \dot{m}^*}{(1+\sigma)}; & \text{if } y_{fire} < y < y_{ceil} \\ (1-\lambda_r)\dot{Q}; & \text{if } y_{fire} \geq y \quad \text{or} \quad \text{if } y = y_{ceil} \end{cases} \tag{B-34}$$

$$y'_{source} = \begin{cases} y_{fire}; & \text{if } y \leq y_{fire} < y_{ceil} \\ y - \left(y - y_{eq}\right) \alpha^{3/5} \dot{m}^{*2/5} \left(\dfrac{1+\sigma}{\sigma}\right)^{1/5}; & \text{if } y_{fire} < y < y_{ceil} \\ y_{eq}; & \text{if } y = y_{ceil} \end{cases} \tag{B-35}$$

where $\dot{m}^*$, σ, and α are calculated from Eqs. (B-26) through (B-30).

B-4.5 Computing $\dot{q}_{HT}$ and the Thermal Response of the Ceiling. Where the fire is below the interface and the interface is below the ceiling, the method for calculating the heat transfer from the plume-driven ceiling jet to the ceiling and the thermal response of the ceiling [12] is used. This method was developed to treat generic, confined ceiling, room fire scenarios. As outlined in this method [12], the confined ceiling problem is solved by applying the unconfined ceiling heat transfer solution [13, 14, 15] to the problem of an upper-layer source in an extended upper-layer environment equivalent to Eqs. (B-34) and (B-35). Where the fire is about the interface, the unconfined ceiling methodology applies directly.

To use these methods [12 through 15] an arbitrary moment of time during the course of the fire development is considered. It is assumed that the temperature distribution of the ceiling material, T, has been computed up to this moment and is known as a function of distance, Z, measured upward from the bottom surface of the ceiling, and radial distance, r, measured from the constant point of plume-ceiling impingement. The equivalent, extended upper-layer, unconfined ceiling flow and heat transfer problem is depicted in Figure B-4-4.1(c). It involves the equivalent $\dot{Q}'$ heat source from Eq. (B-34) located a distance, H, below the ceiling surface in an extended ambient environment of density, ρ_U, and absolute temperature, T_U, where H is determined from Eqs. (B-31) and (B-33).

The objective is to estimate the instantaneous convective heat transfer flux from the upper-layer gas to the lower-ceiling surface, $\dot{q}_{conv,L}(r,t)$, and the net heat transfer fluxes to the upper and lower ceiling surface of the ceiling, $\dot{q}''_u(r,t)$ and $\dot{q}''_L(r,t)$, respectively. With this information, the time-dependent solution for the in-depth thermal response of the ceiling material can be advanced to subsequent times. Also, $\dot{q}''_{conv,L}$ can be integrated over the lower-ceiling surface to obtain the desired instantaneous value for $\dot{q}_{HT}$.

In view of the assumptions of the relatively large distance of the fire from walls or curtains and on the relatively small contribution of heat transfer to these vertical surfaces, it is reasonable to carry out a somewhat simplified calculation for $\dot{q}_{HT}$. Therefore, $\dot{q}_{HT}$ is approximated by the integral of $\dot{q}''_{conv,L}$ over an effective circular ceiling area, A_{eff}, with a diameter, D_{eff}, centered at the point of impingement.

$$\dot{q}_{HT} = \lambda_{conv}\dot{Q}(t) \tag{B-36}$$

$$= -\int_A \dot{q}''_{conv,L}(r,t)\,dA$$

$$\approx -2\pi \int_0^{D_{eff}/2} \dot{q}''_{conv,L}(r,t)\,r\,dr$$

The value $A_{eff} = \pi D_{eff}^2/4$ is taken to be the actual area of the curtained space, A, plus the portion of the vertical curtain and wall surfaces estimated to be covered by ceiling jet-driven wall flows. An estimate for this extended, effective ceiling surface area is obtained [16] where it is concluded with some generality that ceiling jet-driven wall flows penetrate for a distance of approximately $0.8H$ from the ceiling in a downward direction. Therefore,

$$A_{eff} = \frac{\pi D^2_{eff}}{4} \tag{B-37}$$

$$= A + 0.8H(P - L_{curt}) + L_{curt}\,\min\left[0.8H, \left(y_{ceil} - y_{curt}\right)\right]$$

where P = the total length of the perimeter of the curtained area.

B-4.5.1 Net Heat Transfer Flux to the Ceiling's Lower Surface. The net heat transfer flux to the ceiling's lower surface, $\dot{q}''_L$, is made by means of up to three components: incident radiation, $\dot{q}''_{rad-fire}$; convection, $\dot{q}''_{conv,L}$; and reradiation, $\dot{q}''_{rerad,L}$ as follows:

$$\dot{q}''_L = \dot{q}''_{rad-fire} + \dot{q}''_{conv,L} + \dot{q}''_{rerad,L} \tag{B-38}$$

As discussed in B-4.4, the radiant energy from the fire, $\lambda_r\dot{Q}$, is assumed to be radiated isotropically from the fire with negligible radiation absorption and emission from the compartment gases.

$$\dot{q}''_{rad-fire} = \left[\frac{\lambda_r\dot{Q}}{4\pi(y_{ceil} - y_{fire})^2}\right]\left[1 + \left(\frac{r}{y_{ceil} - y_{fire}}\right)^2\right]^{-3/2} \tag{B-39}$$

The convective heat transfer flux from the upper-layer gas to the ceiling's lower surface can be calculated [13,14] as follows.

$$\dot{q}''_{conv,L} = h_L(T_{AD} - T_{S,L}) \tag{B-40}$$

where:

$T_{S,L}$ = the absolute temperature of the ceiling's lower surface
T_{AD} (a characteristic gas temperature) = the temperature that is measured adjacent to an adiabatic lower-ceiling surface
h_L = a heat transfer coefficient

Eqs. (B-41) and (B-42) determine h_L and T_{AD} as follows:

$$\frac{h_L}{\tilde{h}} = \begin{cases} 8.82 Re_H^{-1/2} Pr^{-2/3} \left[1 - (5.0 - 0.284 Re_H^{0.2})\left(\frac{r}{H}\right)\right]; & \text{if } 0 \le \frac{r}{H} < 0.2 \\ 0.283 Re_H^{-0.3} Pr^{-2/3} \left(\frac{r}{H}\right)^{-1/2} \left(\frac{\frac{r}{H} - 0.0771}{\frac{r}{H} + 0.279}\right); & \text{if } 0.2 \le \frac{r}{H} \end{cases} \tag{B-41}$$

$$\frac{T_{AD} - T_U}{T_U \dot{Q}_H^{*2/3}} = \begin{cases} 10.22 - \frac{14.9r}{H}; & \text{if } 0 \le \frac{r}{H} < 0.2 \\ 8.39 f\left(\frac{r}{H}\right); & \text{if } 0.2 \le \frac{r}{H} \end{cases} \tag{B-42}$$

where:

$$f\left(\frac{r}{H}\right) = \frac{1 - 1.10\left(\frac{r}{H}\right)^{0.8} + 0.808\left(\frac{r}{H}\right)^{1.6}}{1 - 1.10\left(\frac{r}{H}\right)^{0.8} + 2.20\left(\frac{r}{H}\right)^{1.6} + 0.690\left(\frac{r}{H}\right)^{2.4}} \tag{B-43}$$

$$\tilde{h} = \rho_U C_p g^{1/2} H^{1/2} \dot{Q}_H^{*1/3} \tag{B-44}$$

$$Re_H = \frac{g^{1/2} H^{3/2} \dot{Q}_H^{*1/3}}{\nu_U}$$

$$\dot{Q}_H^* = \frac{\dot{Q}'}{\rho_U C_P T_U (gH)^{1/2} H^2}$$

In Eq. (B-41), Pr is the Prandtl number (taken to be 0.7), and in Eq. (B-44), V_U is the kinematic viscosity of the upper-layer gas, which is assumed to have the properties of air. Also, $\dot{Q}_H^*$, a dimensionless number, is a measure of the strength of the plume, and Re_H is a characteristic Reynolds number of the plume at the elevation of the ceiling.

The following estimate for V_U [17] is used where computing Re_H from Eq. (B-44):

$$\nu_U = \frac{0.04128\left(10^{-7}\right) T_U^{5/2}}{T_U + 110.4} \tag{B-45}$$

where V_U is in m^2/s, and T_U is in K.

Eqs. (B-40) through (B-45) use a value for T_U. At $t = 0$, where it is undefined, T_U should be set equal to T_{amb}. This yields the correct limiting result for the convective heat transfer to the ceiling, specifically, convective heat transfer to the ceiling from an unconfined ceiling jet in an ambient environment.

As the fire simulation proceeds, the ceiling's lower surface temperature, $T_{S,L}$, initially at T_{amb}, begins to increase. At all times, the lower-ceiling surface is assumed to radiate diffusely to the initially ambient temperature floor surface and to exposed surfaces of the building contents. In response to this radiation and to the direct radiation from the fire's combustion zone, the temperature of these surfaces also increases with time. However, for specific times, it is assumed that the effective temperature increase of these floor-contents surfaces is relatively small compared to the characteristic increases of $T_{S,L}$. Accordingly at a given radial position of the ceiling's lower surface, the net radiation exchange between the ceiling and floor-contents surfaces can be approximated by the following:

$$\dot{q}''_{rerad,L} = \frac{\sigma\left(T_{amb}^4 - T_{S,L}^4\right)}{\frac{1}{\in_L} + \frac{1}{\in_{floor}} - 1} \tag{B-46}$$

where σ is the Stefan-Boltzmann constant and $\in_L$ and $\in_{floor}$ are the effective emittance-absorptance of the ceiling's upper surface and floor-contents surfaces (assumed to be grey), respectively, both of which are taken to be 1.

B-4.5.2 Net Heat Transfer Flux to Ceiling's Upper Surface. It is assumed that the ceiling's upper surface is exposed to a relatively constant-temperature far-field environment at T_{amb}. Therefore, the net heat transfer flux to this surface, $\dot{q}_U$, is made up of two components, convection, $\dot{q}''_{conv,U}$, and reradiation, $\dot{q}''_{rerad,U}$, as follows:

$$q''_U = \dot{q}''_{conv,U} + \dot{q}''_{rerad,U} \tag{B-47}$$

These can be estimated from the following:

$$\dot{q}''_{conv,U} = h_U(T_{amb} - T_{S,U}) \tag{B-48}$$

$$\dot{q}''_{rerad,U} = \frac{\sigma\left(T_{amb}^4 - T_{S,U}^4\right)}{\frac{1}{\in_U} + \frac{1}{\in_{far}} - 1} \tag{B-49}$$

where $T_{S,U}$ is the absolute temperature of the upper surface of the ceiling, h_U is a heat transfer coefficient, and $\in_{far}$ and $\in_U$ are the effective emittance-absorptance of the far-field and ceiling's upper surface (assumed to be grey), respectively, both of which are taken to be 1.

The value for h_U to be used [18] is as follows:

$$h_U = 1.65(T_{amb} - T_{S,U})^{1/3} \tag{B-50}$$

where h_U is in W/m^2, and T_{amb} and $T_{S,U}$ are in K.

B-4.5.3 Solving for the Thermal Response of the Ceiling for $\dot{q}_{HT}$. The temperature of the ceiling material is assumed to be governed by the Fourier heat conduction equation. By way of the lower-ceiling surface boundary condition, the boundary value problem is coupled to, and is to be solved together with, the system of Eqs. (B-2) and (B-8).

Initially the ceiling is taken to be of uniform temperature, T_{amb}. The upper- and lower-ceiling surfaces are then exposed to the radial- and time-dependent rates of heat transfer, $\dot{q}''_U$ and $\dot{q}''_L$, determined from Eqs. (B-47) and (B-48), respectively. For specific times in this case, radial gradients of $\dot{q}''_U$ and $\dot{q}''_L$ are assumed to be small enough so that conduction in the ceiling is quasi-one-dimensional in space [i.e., $T = T(Z, t; r)$]. Therefore, the two-dimensional thermal

response for the ceiling can be obtained from the solution to a set of one-dimensional conduction problems for

$$T_n(Z, t) = T(Z, t; r = r_n); \quad n = 1 \text{ to } N_{rad}$$

where N_{rad} is the number of discrete radial positions necessary to obtain a sufficiently smooth representation of the overall ceiling temperature distribution. The r_n radial positions are depicted in Figure B-4.5.3.

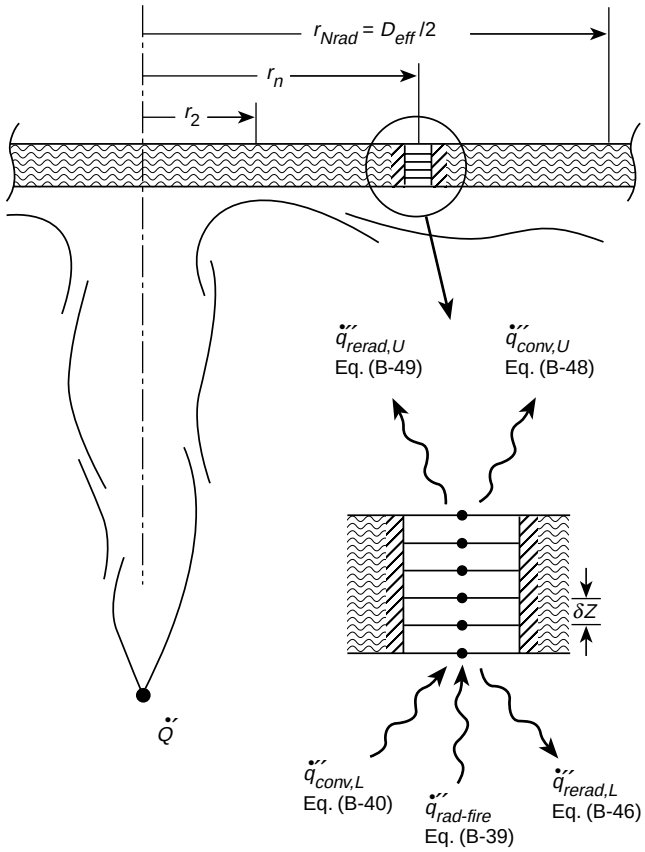

Figure B-4.5.3 Illustration of the geometry for the boundary value problems of the temperature distributions, T_n, through the ceiling at radial positions r_n.

T_{max} is assumed to be the maximum temperature of the ceiling (i.e., the temperature of the exposed surface at $r = 0$). The parametric study [15] for the thermal response of unconfined ceilings above constant and growing fires indicates generally that changes in T/T_{max} as a function of r/H are such that

$$\frac{d\left(T/T_{max}\right)}{d(r/H)} = 0(1)$$

Therefore, it is reasonable to expect accurate results for the Eq. (B-36) integral of $\dot{q}''_{conv,L}$ by interpolating between values of $\dot{q}''_{conv,L}$ calculated at radial positions separated by r/H intervals of 0.1 to 0.2.

Using the preceding ideas, the following procedure for finding the thermal response of the ceiling and solving for $\dot{q}''_{HT}$ is implemented:

(a) Since $y_{ceil} - y_{fire}$ is a measure of H in the current problem and $D_{eff} / 2$ is a measure of the maximum value of r, N_{rad} is chosen as several multiples of the following:

$$\frac{D_{eff}/2}{y_{ceil}-y_{fire}}$$

In this case, N_{rad} is chosen as the first integer equal to or greater than

$$\frac{5(D_{eff}/2)}{y_{ceil}-y_{fire}} + 2$$

(b) One temperature calculation point is placed at $r = 0$ and the remaining N_{rad} calculation points are distributed with uniform separation at and between $r = 0.2(y_{ceil} - y_{fire})$ and $r = D_{eff}/2$, the latter value being the upper limit of the integral of Eq. (B-36); that is:

$$r_1 = 0$$

$$r_2 = 0.2(y_{ceil}-y_{fire})$$

$$r_{N_{rad}} = \frac{D_{eff}}{2}$$

$$r_n = r_n + \Delta r \qquad \text{if } 1 < n < N_{rad}$$

where $\Delta r = \dfrac{r_{N_{rad}} - r_1}{N_{rad} - 2}$

(c) The boundary value problems are solved for the N_{rad} temperature distributions, T_n. At arbitrary radius, r_n, these are indicated in the inset portion of Figure B-4.5.3.

(d) For any moment of time during the calculation, the lower surface values of the T_n are used to compute the corresponding discrete values of $\dot{q}''_{conv,L,n}(t) = \dot{q}''_{conv,L}(r = r_n, t)$ from Eq. (B-40).

(e) The $\dot{q}''_{conv,L}$ distribution in r is approximated by interpolating linearly between the $\dot{q}''_{conv,L,n}$. The integration indicated in Eq. (B-36) is carried out.

The procedure for solving for the T_n is the same as that used in reference [15]. It requires the thickness, thermal conductivity, and thermal diffusivity of the ceiling material. The solution to the one-dimensional heat conduction equation involves an explicit finite difference scheme that uses an algorithm taken from references [19,20]. For a given set of calculations, $N \leq 20$ equal-spaced nodes are positioned at the surfaces and through the thickness of the ceiling at every radius position, r_n. The spacing, δZ *(see Figure B-4.5.3),* of these is selected to be large enough (based on a maximum time step) to ensure stability of the calculation.

B-5 Actuation of Vents and Sprinklers. It is an objective of this guide to simulate conditions in building spaces where ceiling vents and sprinkler links can be actuated by the responses of near-ceiling–deployed fusible links. The concept is that, during the course of a compartment fire, a deployed link is engulfed by the near-ceiling convective flow of the elevated-temperature products of combustion and entrained air of the fire-generated plume. As the fire continues, convective heating of the link leads to an increase in its temperature, If and when its fuse temperature is reached, any devices being operated by the link are actuated.

The near-ceiling flow engulfing the link is the plume-driven ceiling jet referred to previously, which transfers the flow to the lower-ceiling surface and is cooled as it traverses under the ceiling from the point of plume-ceiling impingement. In the case of relatively smooth ceiling configurations, assumed to be representative of the facilities studied in this guide, the ceiling jet flows outward radially from the point of impingement, and its gas velocity and temperature distributions, V_{CJ} and T_{CJ}, respectively, are a function of radius from the impingement point, r, distance below the ceiling, z, and time, t.

Vents actuated by alternate means such as thermoplastic “drop-out” panels with equivalent performance characteristics can also be modeled using LAVENT. Refer to 1-1.2.

B-5.1 Predicting the Thermal Response of the Fusible Links. The thermal response of deployed fusible links is calculated up to their fuse temperature, T_F, by the convective heating flow model [21]. It is assumed that the specific link is positioned at a specified radius from the impingement point, $r = r_L$, and the distance below the lower-ceiling surface, $z = z_L$. T_L has been defined as the link's assumed near-uniform temperature. Therefore, instantaneous changes in T_L are determined by the following:

$$\frac{dT_L}{dt} = \frac{(T_{CJ,L} - T_L)V_{CJ,L}^{1/2}}{RTI} \tag{B-51}$$

where $T_{CJ,L}$ and $V_{CJ,L}$ are the values of V_{CJ} and T_{CJ}, respectively, evaluated near the link position, and where RTI (response time index), a property of the link and relative flow orientation, can be measured in the "plunge test" [21,22]. The RTI for ordinary sprinkler links range from low values of 22 $(\text{m}\cdot\text{sec})^{1/2}$ for quick-operating residential sprinklers, to 375 $(\text{m}\cdot\text{sec})^{1/2}$ for slower standard sprinklers [23]. The utility of Eq. (B-51) is shown to be valid typically through the link-fusing processes [24], is discussed further [23], and actually is used to predict link response in a parametric study involving two-layer compartment fire scenarios. Also, the link response prediction methodology has been used [23] and demonstrates favorable comparisons between predicted and measured link responses in a full-scale, one-room, open-doorway compartment fire experiment.

To compute T_L from Eq. (B-51) for a different link location necessitates estimates of $V_{CJ,L}$ and $T_{CJ,L}$ for arbitrary link positions, r_L and z_L.

B-5.2 The Velocity Distributions of the Ceiling Jet. Outside of the plume-ceiling impingement stagnation zone, defined approximately by $r/H \le 0.2$, and at a given r, V_{CJ} rises rapidly from zero at the ceiling's lower surface, $z = 0$, to a maximum, V_{max}, at a distance $z = 0.23\delta$, $\delta(r)$ being the distance below the ceiling where $V/V_{max} = 1/2$ [16]. In this region outside the stagnation zone, V_{CJ} can be estimated [16] as follows:

if $\dfrac{r}{H} \ge 0.2$;

$$\frac{V_{CJ}}{V_{max}} = \begin{cases} \left(\dfrac{8}{7}\right)\left(\dfrac{z}{0.23\delta}\right)^{1/7}\left[1 - \dfrac{z/(0.23\delta)}{8}\right]; & \text{if } 0 \le \dfrac{z}{0.23\delta} \le 1 \\ \cosh^{-2}\left\{\left(\dfrac{0.23}{0.77}\right)\text{arccosh}(2^{1/2}) \times \left[\dfrac{z}{0.23\delta} - 1\right]\right\}; & \text{if } 1 \le \dfrac{z}{0.23\delta} \end{cases} \tag{B-52}$$

$$\frac{V_{max}}{V} = 0.85\left(\frac{r}{H}\right)^{-1.1} \tag{B-53}$$

$$\frac{\delta}{H} = 0.10\left(\frac{r}{H}\right)^{0.9}$$

$$V = g^{1/2}H^{1/2}\dot{Q}_H^{*1/3}$$

where $\dot{Q}_H^*$ is defined in Eq. (B-44). V_{CJ}/V_{max} per Eq. (B-52) is plotted in Figure B-5.2.

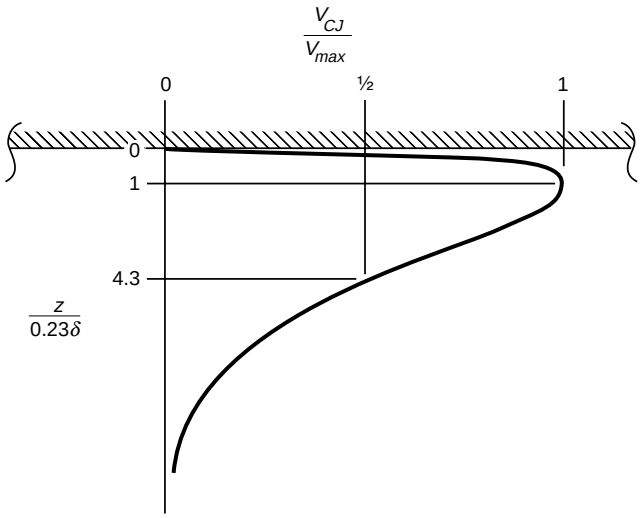

Figure B-5.2 A plot of dimensionless ceiling jet velocity distribution, V_{CJ}/V_{max}, as a function of $z/0.23\delta$ per Eq. (B-52).

In the vicinity of near-ceiling-deployed links located inside the stagnation zone, the fire-driven flow is changing directions from an upward-directed plume flow to an outward-directed ceiling jet-type flow. There the flow velocity local to the link, the velocity that drives the link's connective heat transfer, involves generally a significant vertical as well as radial component of velocity. Nevertheless, at such link locations, it is reasonable to continue to approximate the link response using Eq. (B-51) with V_{CJ} estimated using Eqs. (B-52) and (B-53) and with r/H set equal to 0.2. This approximation is shown as follows:

$$V_{CJ} = V_{CJ}\left(\frac{r}{H} = 0.2\right) \quad \text{if } 0 \le \frac{r}{H} < 0.2 \tag{B-54}$$

B-5.3 The Temperature Distribution of the Ceiling Jet. Outside of the plume-ceiling impingement stagnation zone (i.e., where $r/H \ge 0.2$) and at a given value of r, T_{CJ} rises very rapidly from the temperature of the ceiling's lower surface, $T_{S,L}$, at $z = 0$, to a maximum, T_{max}, somewhat below the ceiling surface. It is assumed that this maximum value T_{CJ} occurs at the identical distance below the ceiling as does the maximum of V_{CJ} (i.e., at $z = 0.23\delta$). Below this elevation, T_{CJ} drops with increasing distance from the ceiling until it reaches the upper-layer temperature, T_U. In this latter, outer region of the ceiling jet, the shape of the normalized T_{CJ} distribution, $(T_{CJ} - T_U)/(T_{max} - T_U)$, has the same characteristics as that of V_{CJ}/V_{max}. Also, since a turbulent boundary flow exists, it is reasonable to expect that the characteristic thicknesses of the outer region of both the velocity and temperature distributions is the same, dictated by the distribution of the turbulent eddies.

For these reasons the velocity and temperature distribution are approximated as to be identical in the outer region of the ceiling jet flow, $0.23\delta \le z$. In the inner region of the flow, between $z = 0$ and 0.23δ, the normalized temperature distribution is approximated by a quadratic function of $z/(0.23\delta)$, necessitating the use of $T_{CJ} = T_{S,L}$ at $z = 0$ and $T_{CJ} = T_{max}$, $dT_{CJ}/dz = 0$ at $z = 0.23\delta$. Therefore, where $r/H \ge 0.2$,

$$\Theta \equiv \frac{T_{CJ} - T_U}{T_{max} - T_U} = \begin{cases} \Theta_S + 2\left[(1-\Theta_S)\left(\frac{z}{0.23\delta}\right)\right] - \left[(1-\Theta_S)\left(\frac{z}{0.23\delta}\right)^2\right] \\ \qquad \text{if } 0 \le \frac{z}{0.23\delta} \le 1 \\ \frac{V_{CJ}}{V_{max}}; \qquad \text{if } 1 \le \frac{z}{0.23\delta} \end{cases} \tag{B-55}$$

$$\Theta_S = \Theta(T_{CJ} = T_{S,L}) = \frac{T_{S,L} - T_U}{T_{max} - T_U} \tag{B-56}$$

It should be noted that Θ_S is the negative when the ceiling surface temperature is less than the upper-layer temperature (e.g., relatively early in a fire, when the original ambient-temperature ceiling surface has not yet reached the average temperature of the growing upper layer). Also, Θ_S is greater than 1 when the ceiling surface temperature is greater than T_{max}. This is possible, for example, during times of reduced fire size when the fire's near-ceiling plume temperature is reduced significantly, perhaps temporarily, from previous values, but the ceiling surface, heated previously to relatively high temperatures, has not cooled substantially. Plots of Θ per Eq. (B-55) are shown in Figure B-5-3 for cases where Θ is < 0, between 0 and 1, and > 0.

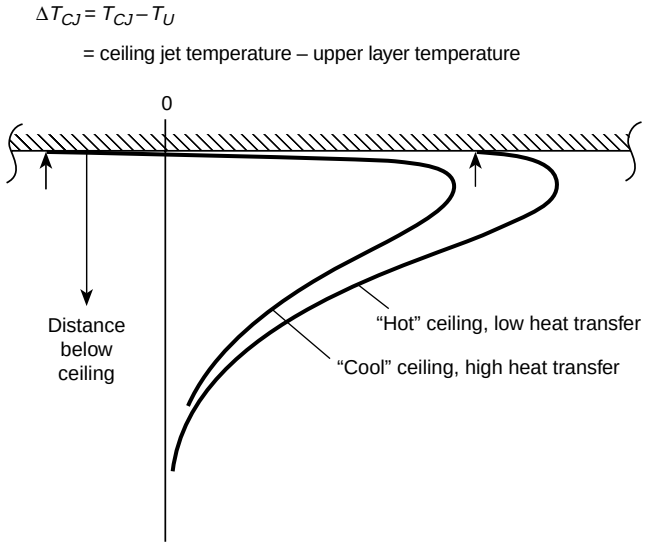

Figure B-5.3 Plots of dimensionless ceiling jet temperature distribution, Θ, as a function of $z/0.23\delta$ per Eq. (B-55) for cases where Θ_S is < 0, between 0 and 1, and > 0.

In a manner similar to the treatment of V_{CJ}/V_{max}, for the purpose of calculating T_L, from Eq.(B-51), Θ_S is approximated inside the stagnation zone by the description of Eqs. (B-55) and (B-56), with r/H set equal to 0.2 as follows:

$$\Theta_S = \Theta_S\left(\frac{r}{H} = 0.2\right); \qquad \text{if } 0 \le \frac{r}{H} \le 0.2 \tag{B-57}$$

With the radial distribution for $T_{S,L}$ and T_U already calculated up to a specific time, only T_{max} is needed to complete the Eqs. (B-55) through (B-57) estimate for the ceiling jet temperature distribution. This is obtained by invoking conservation of energy. Therefore, at an arbitrary r outside the stagnation zone, the total rate of radial outflow of enthalpy (relative to the upper-layer temperature) of the ceiling jet is equal to the uniform rate of enthalpy flow in the upper-layer portion of the plume, $\dot{Q}'$, less the integral (from the plume-ceiling impingement prior to r) of the flux of convective heat transfer from the ceiling jet to the ceiling surface as follows:

$$2\pi \int_0^\infty \rho_U C_P (T_{CJ} - T_U) V_{CJ} z \, dz = \dot{Q}' - 2\pi \int_0^r \dot{q}''_{conv,L}(r,t) r \, dr \tag{B-58}$$

$$\equiv (1 - \lambda'_{conv})\dot{Q}'; \quad \text{if } 0.2 \le \frac{r}{H}$$

λ'_{conv} is the fraction of $\dot{Q}'$ transferred by convection to the ceiling from the point of ceiling impingement to r as follows:

$$\lambda'_{conv}(r) = \frac{2\pi \int_0^r \dot{q}''_{conv,L}(r,t) r \, dr}{\dot{Q}'} \tag{B-59}$$

In Eqs. (B-58) and (B-59), $\dot{Q}'$ has been calculated previously in Eq. (B-34). Also, the integral on the right-hand sides of Eqs. (B-58) and (B-59) can be calculated by approximating $\dot{q}_{conv,L}(r,t)$, as shown in Eq. (B-59), as a linear function of r between previously calculated values of $\dot{q}_{conv,L}(r = r_n, t)$.

The integral on the left-hand side of Eq. (B-58) is calculated using V_{CJ} of Eqs. (B-52) and (B-53) and T_{CJ} of Eqs. (B-55) and (B-56). From this, the desired distribution for T_{max} is determined as follows:

$$(T_{max} - T_U) = 2.6(1 - \lambda'_{conv})\left(\frac{r}{H}\right)^{-0.8} \dot{Q}_H^{*2/3} T_U - 0.090(T_{S,L} - T_U); \qquad \text{if } 0.2 \le \frac{r}{H} \tag{B-60}$$

The result of Eq. (B-60), together with Eqs. (B-55) and (B-56), represents the desired estimate for T_{CJ}. This and the Eqs. (B-52) through (B-54) estimate for T_{CJ} are used to calculate T_L from Eq. (B-51).

B-5.4 Dependence of Open Vent Area on Fusible-Link–Actuated Vents. As discussed, the influence of ceiling vent action on the fire-generated equipment is dependent on the active area of the open ceiling vents, A_V. A variety of basic vent opening design strategies is possible, and a major application of the current model equations is to evaluate these strategies within the context of the developing fire environment. For example, one of the simplest strategies [9] assumes that all vents deployed in the specified curtained area are opened by whatever means at the onset of the fire. In general, A_V will be time-dependent. To the extent that a strategy of vent opening is dependent directly on the fusing of any one or several deployed fusible links, the location of these links and their characteristics (i.e., likely spacings from plume-ceiling impingement, distance below the ceiling, and the *RTI*) and the functional relationship between link fusing and A_V need to specified. These matters can be examined in the context of different solutions to the overall problem by exercising parametrically the LAVENT computer program [2], which implements all the model equations provided in this appendix.

B-5.5 Concluding Remarks — A Summary of Guidelines, Assumptions, and Limitations. The theory presented here is the basis of LAVENT, a user-friendly computer program [2] that is supported by a user guide [3] and that can be used to study parametrically a wide range of relevant fire scenarios.

The assumptions made in the development of the set of model equations limit fire scenarios or aspects of fire scenarios that can be simulated and studied with confidence. A summary of guidelines and assumptions that characterize what are perhaps the most critical of these limitations follows. These are the result of explicit or implicit assumptions necessary for valid application of the variety of submodels introduced throughout this work.

L and W are the length and width, respectively, of the plan area of the curtained space. Simulated configurations should be limited to those with aspect ratios, L/W, that are not much different than 1 (e.g., $0.5 \le L/W < 2$). Also, in such configurations, the fire should not be too close to or too far from the walls [e.g., the fire should be no closer to a wall than $(y_{ceil} - y_{fire})/2$ and no farther than $3(y_{ceil} - y_{fire})$].

The curtain boards should be deep enough to satisfy $(y_{ceil} - y_{curt}) \ge 0.2(y_{ceil} - y_{fire})$, unless the equations and the code are used to simulate an unconfined ceiling scenario where $(y_{ceil} - y_{curt}) = 0$.

The ceiling of the curtained space should be relatively smooth, with protuberances having depths significantly less than $0.1W$. Except at the locations of the curtain boards, below-ceiling–mounted barriers to flow, such as solid beams, should be avoided. Ceiling surface protuberances near to and upstream of fusible links (i.e., between the links and the fire) should be significantly smaller than link-to-ceiling distances.

W_V is the width, that is, the smaller dimension of a single ceiling vent (or vent cluster). Therefore, the prediction of smoke layer thickness, $y_{ceil} - y$, is reliable only after the time that

$(y_{ceil} - y)/W_V$ is greater than 1. Note that this places an additional limitation on the minimum depth of the curtain boards [i.e., $(y_{ceil} - y_{curt})/W_V$ should exceed 1].

At all times during a simulated fire scenario, the overall building space should be vented to the outside (e.g., through open doorways).

In this regard, compared to the open ceiling vents in the curtained compartment, the area of the outside vents must be large enough so that the pressure drop across the outside vents is small compared to the pressure drop across ceiling vents. For example, under near-steady-state conditions, when the rate of mass flow into the outside vents is approximately equal to the rate of mass outflow from the ceiling vents, the outside vent area must satisfy $(A_{Vout}/A_V)^2(T_U/T_{amb})^2 >> 1$, or, more conservatively and independent of T_U, $(A_{Vout}/A_V)^2 >> 1$. The latter criterion will always be reasonably satisfied if $A_{Vout}/A_V > 2$. Under flashover-level conditions, say, when $T_U/T_{amb} = 3$, the former criterion will be satisfied if $(3A_{Vout}/A_V)^2 >> 1$, say, if $A_{Vout} = A_V$, or even if A_{Vout} is somewhat smaller than A_V.

The simulation assumes a relatively quiescent outside environment (i.e., without any wind) and a relatively quiescent inside environment (i.e., remote from vent flows, under-curtain flows, ceiling jets, and the fire plume). In real fire scenarios, such an assumption should be valid where the characteristic velocities of actual flows in these quiescent environments are much less than the velocity of the fire plume near its ceiling impingement point [i.e., where the characteristic velocities are much less than V_{max} of Eq. (B-53)]. It should be noted that, for a given fire strength, Q, this latter assumption places a restriction on the maximum size of $(y_{ceil} - y_{fire})$, which is a measure of H, since V_{max} is approximately proportional to $(y_{ceil} - y_{fire})^{-1/3}$.

In configurations where smoke flows below curtain partitions to adjacent curtained spaces, the simulation is valid only up to the time that it takes for any one of the adjacent spaces to fill with smoke to the level of the bottom of the curtain. While it is beyond the scope of this guide to provide any general guidelines for this limiting time, the following rule can be useful where all curtained spaces of a building are similar and where the fire is not growing too rapidly: The time to fill an adjacent space is of the order of the time to fill the original space.

The reliability of the simulation begins to degrade subsequent to the time that the top of the flame penetrates the layer elevation and especially if Eq. (B-20) predicts a flame height that reaches the ceiling.

It is assumed that the smoke is relatively transparent and that the rate of radiation absorbed by or emitted from the smoke layer is small compared to the rate of radiation transfer from the fire's combustion zone. The assumption is typically true and a simulation is valid at least up to those times that the physical features of the ceiling can be discerned visually from the floor elevation.

It should be emphasized that the above limitations are intended only as guidelines. Therefore, even when the characteristics of a particular fire scenario satisfy these limitations, the results should be regarded with caution until solutions to the overall model equations have been validated by a substantial body of experimental data. Also, where a fire scenario does not satisfy the above limitations but is close to doing so, it is possible that the model equations can still provide useful quantitative descriptions of the simulated phenomena.

B-6 References for Appendix B.

1. Cooper, L.Y., "Estimating the Environment and the Response of Sprinkler Links in Compartment Fires with Draft Curtains and Fusible Link-Actuated Ceiling Vents," *Fire Safety Journal*, 16, pp. 137–163,1990.
2. LAVENT software, available from National Institute of Standards and Technology, Gaithersburg, MD.
3. Davis, W.D., and Cooper, L.Y., "Estimating the Environment and the Response of Sprinkler Links in Compartment Fires with Draft Curtains and Fusible Link-Actuated Ceiling Vents—Part II: User Guide for the Computer Code LAVENT," NISTIR 89-4122, National Institute of Standards and Technology, Gaithersburg, MD, August 1989.
4. Emmons, H.W., "The Flow of Gases Through Vents," Harvard University Home Fire Project Technical Report No. 75, Cambridge, MA, 1987.
5. Thomas, P.H., et al., "Investigations into the Flow of Hot Gases in Roof Venting," Fire Research Technical Paper No. 7, HMSO, London, 1963.
6. Heskestad, G., "Smoke Movement and Venting," *Fire Safety Journal*, 11, pp. 77–83, 1986, and Appendix A, *Guide for Smoke and Heat Venting*, NFPA 204M, National Fire Protection Association, Quincy, MA, 1982.
7. Cooper, L.Y., "A Mathematical Model for Estimating Available Safe Egress Time in Fires," *Fire and Materials*, 6, 3/4, pp. 135–144, 1982.

8. Heskestad, G., "Engineering Relations for Fire Plumes," *Fire Safety Journal*, 7, pp. 25–32, 1984.
9. Hinkley, P.L., "Rates of 'Production' of Hot Gases in Roof Venting Experiments," *Fire Safety Journal*, 10, pp. 57–64, 1986.
10. Zukoski, E.E., Kubota, T., and Cetegen, B., *Fire Safety Journal*, 3, p. 107, 1981.
11. Cooper, L.Y., "A Buoyant Source in the Lower of Two, Homogeneous, Stably Stratified Layers," 20th International Symposium on Combustion, Combustion Institute, Michigan Univ., Ann Arbor, MI, pp. 1567–1573, 1984.
12. Cooper, L.Y., "Convective Heat Transfer to Ceilings Above Enclosure Fires," 19th Symposium (International) on Combustion, Combustion Institute, Haifa, Israel, pp. 933–939, 1982.
13. Cooper, L.Y., "Heat Transfer from a Buoyant Plume to an Unconfined Ceiling," *Journal of Heat Transfer*, 104, pp. 446–451, August 1982.
14. Cooper, L.Y., and Woodhouse, A., "The Buoyant Plume-Driven Adiabatic Ceiling Temperature Revisited," *Journal of Heat Transfer*, 108, pp. 822–826, November 1986.
15. Cooper, L.Y., and Stroup, D.W., "Thermal Response of Unconfined Ceilings Above Growing Fires and the Importance of Convective Heat Transfer," *Journal of Heat Transfer*, 109, pp. 172–178, February 1987.
16. Cooper, L.Y., "Ceiling Jet-Driven Wall Flows in Compartment Fires," *Combustion Science and Technology*, 62, pp. 285–296, 1988.
17. Hilsenrath, J., "Tables of Thermal Properties of Gases," Circular 564, National Bureau of Standards, Gaithersburg, MD, November, 1955.
18. Yousef, W.W., Tarasuk, J.D., and McKeen, W.J., "Free Convection Heat Transfer from Upward-Facing, Isothermal, Horizontal Surfaces," *Journal of Heat Transfer*, 104, pp. 493–499, August 1982.
19. Emmons, H.W., "The Prediction of Fire in Buildings," 17th Symposium (International) in Combustion, Combustion Institute, Leeds, England, pp. 1101–1111, 1979.
20. Mitler, H.E., and Emmons, H.W., "Documentation for the Fifth Harvard Computer Fire Code," Harvard University, Home Fire Project Technical Report 45, Cambridge, MA, 1981.
21. Heskestad, G., and Smith, H.F., "Investigation of a New Sprinkler Sensitivity Approval Test: The Plunge Test," Technical Report Serial No. 22485, RC 76-T-50, Factory Mutual Research Corporation, Norwood, MA, 1976.
22. Heskestad, G., "The Sprinkler Response Time Index (RTI)," Paper RC-81-Tp-3 presented at the Technical Conference on Residential Sprinkler Systems, Factory Mutual Research Corporation, Norwood, MA, April 28–29, 1981.
23. Evans, D.D., "Calculating Sprinkler Actuation Times in Compartments," *Fire Safety Journal*, 9, pp. 147–155, 1985.
24. Evans, D.D, "Characterizing the Thermal Response of Fusible Link Sprinklers," NBSIR 81-2329, National Bureau of Standards, Gaithersburg, MD, 1981.
25. Cooper, L.Y., and Stroup, D.W., "Test Results and Predictions for the Response of Near-Ceiling Sprinkler Links in Full-Scale Compartment Fires," *Fire Safety Science—Proceedings of the Second International Symposium*, Tokyo, June 13–17, 1988, pp. 623–632, T. Wakumatsu et al. eds., International Association of Fire Safety Science, Hemisphere Publishing Co., New York, 1989.

B-7 Nomenclature for Appendix B.

A = plan area of single curtain space

A_{eff} = effective area for heat transfer to the extended lower-ceiling surface, $\pi D_{eff}^2/4$

A_V = total area of open ceiling vents in curtained space

A_{Vout} = total area of open vents to outside exclusive of A_V

C = vent flow coefficient (0.68)

C_P = specific heat at constant pressure

C_T = 9.115, dimensionless constant in plume model

C_V = specific heat at constant volume

D_{eff} = effective diameter of A_{eff}

D_{fire} = effective diameter of fire source ($\pi D_{fire}^2/4$ = area of fire source)

g = acceleration of gravity

H = distance below ceiling of equivalent source

$\tilde{h}$ = characteristic heat transfer coefficient

h_L, h_U = lower-, upper-ceiling surface heat transfer coefficient

L = characteristic length of the plan area of curtained space

L_{curt} = length of the perimeter of A connected to other curtained areas of the building

L_{flame} = flame length

$\dot{m}_{curt}$ = mass flow rate from below curtain to upper layer

$\dot{m}_{ent}$ = rate of plume mass entrainment between the fire and the layer interface

$\dot{m}_{plume}$ = mass flow rate of plume at interface

m_U = total mass of the upper layer

$\dot{m}_U$ = net mass flow rate to upper layer

$\dot{m}_{vent}$ = mass flow rate through ceiling vents to upper layer

N = number of equal-spaced nodes through the ceiling

N_{rad} = number of values of r_n

P = length of perimeter of single curtained area

Pr = Prandtl number, taken to be 0.7

$p = p_{amb}$ at floor elevation

p_U, p_{amb} = pressure in upper-layer, outside ambient

$\dot{Q}$ = energy release rate of fire

$\dot{Q}'$ = strength of continuation source in extended upper layer

$\dot{Q}_H^*$ = dimensionless strength of plume at ceiling

$\dot{Q}_{eq}^*$ = dimensionless strength of plume at interface

$\dot{q}''_{conv,L}$, $\dot{q}''_{conv,U}$ = convective heat transfer flux to lower-, upper-ceiling surface

$\dot{q}''_{conv,L,n} = \dot{q}''_{conv,L}(r = r_n, t)$

$\dot{q}_{curt}$ = enthalpy flow rate from below curtain to upper layer

$\dot{q}_{HT}$ = heat transfer rate to upper layer

$\dot{q}_{plume}$ = enthalpy flow rate of plume at interface

$\dot{q}_{rad-fire}$ = radiation flux incident on lower surface of ceiling

$\dot{q}''_{rerad,L}$, $\dot{q}''_{rerad,U}$ = reradiation flux to lower, upper surface of ceiling

$\dot{q}_U$ = net enthalpy flow rate plus heat transfer rate to upper layer

$\dot{q}''_L$, $\dot{q}''_U$ = net heat transfer fluxes to upper-, lower-ceiling surface

$\dot{q}_{vent}$ = enthalpy flow rate through ceiling vent to upper layer

R = gas constant, $\dfrac{(\tau - 1)C_P}{\tau = C_P - C_V}$

Re_H = Reynolds number of plume at ceiling elevation

RTI = response time index

r = radial distance from plume-ceiling impingement

$r_L = r$ at link

r_n = discrete values of r

T = absolute temperature of ceiling material

T_{AD} = adiabatic lower-ceiling surface temperature

T_{CJ} = temperature distribution of ceiling jet gas

$T_{CJ,L} = T_{CJ}$ at link

$T_{max}(t) = T_{S,L}(r = 0, t) = T(Z = 0, t\ r = 0)$

$T_{S,L}$, $T_{S,U}$ = absolute temperature of lower-, upper-ceiling surface

$T_{S,L,n}(t) = T_{S,L}(r = r_n, t) = T_n(Z = 0, t\ r = r_n)$

T_U, T_{amb} = absolute temperature of upper-layer, outside ambient

$T_n = T\,(Z,\ t\ r = r_n)$

t = time

V = average flow velocity through all open vents

V_{CJ} = velocity distribution of ceiling jet gas

$V_{CJ,L} = V_{CJ}$ at link

V_{max} = maximum value of V_{CJ} at a given r

W = characteristic width of plan area of curtained space

W_V = width of a single ceiling vent (or vent cluster)

y, y_{ceil}, y_{curt}, y_{eq}, y_{fire} = elevation of smoke layer interface, ceiling, bottom of curtain, equivalent source fire above floor

y'_{source} = elevation of plume continuation point source in extended upper-layer above floor

Z = distance into the ceiling, measured from bottom surface

z, z_L = distance below lower-ceiling surface, z, at link

$$\alpha = \frac{T_U}{T_{amb}}$$

τ = ratio of specific heat, $\frac{C_P}{C_V}$

$\Delta\rho_{ceil}$ = cross-vent pressure difference

$\Delta\rho_{curt}$ = cross-curtain pressure difference

δ = value of z where $V_{CJ} = \frac{V_{max}}{2}$

δZ = distance between nodes through the ceiling thickness

$\in$ = constant, Eq. (B-18)

$\in_L$, $\in_U$, $\in_{floor}$, $\in_{far}$ = emittance-absorptance of lower, upper, floor, and far-field gray surfaces, all taken to be 1

Θ = normalized, dimensionless ceiling jet temperature distribution,

$$\frac{T_{CJ} - T_U}{T_{max} - T_U}$$

$\Theta_S = \Theta$ at lower-ceiling surface, $\frac{T_{S,L} - T_U}{T_{max} - T_U}$

λ_r = fraction of $\dot{Q}$ radiated from combustion zone

λ_{conv} = fraction of $\dot{Q}$ transferred by convection from upper layer

λ'_{conv} = fraction of $\dot{Q}'$ transferred to the ceiling in a circle of radius, r, and centered at r = 0, Eq. (B-56).

V_U = kinematic viscosity of upper-layer gas

ρ_U, ρ_{amb} = density of upper-layer, outside ambient

σ = dimensionless variable, Eq. (B-28)

Appendix C User Guide for the LAVENT Computer Code

This appendix is not a part of the recommendations of this NFPA document but is included for informational purposes only.

C-1 Overview. This appendix is a user guide for the LAVENT computer code (Link-Actuated VENTs), Version 1.1, and an associated graphics code called GRAPH. As discussed in Section 6-2 and Appendix B, LAVENT has been developed to simulate the environment and the response of sprinkler links in compartment fires with curtain boards and fusible-link–actuated ceiling vents. Vents actuated by alternate means such as thermoplastic "drop-out" panels with equivalent performance characteristics can also be modeled using LAVENT. Refer to 1-1.2.

A fire scenario simulated by LAVENT is defined by the following input parameters:

(a) Area and height of the curtained space

(b) Separation distance from the floor to the bottom of the curtain

(c) Length of the curtain (A portion of the perimeter of the curtained space can include floor-to-ceiling walls.)

(d) Thickness and properties of the ceiling material (density, thermal conductivity, and heat capacity)

(e) Constants that define a specified time-dependent energy release rate of the fire

(f) Fire elevation

(g) Area or characteristic energy release rate per unit area of the fire

(h) Total area of ceiling vents whose openings are actuated by a single fusible link (Multiple vent area/link system combinations may be permitted in any particular simulation.)

(i) Identifying numbers of fusible links used to actuate single sprinkler heads or groups of sprinkler heads (Multiple sprinkler links are permitted in any particular simulation.)

The characteristics of the simulated fusible links are defined by the following input parameters:

(a) Radial distance of the link from the fire–ceiling impingement point

(b) Ceiling–link separation distance

(c) Link fuse temperature

(d) The response time index (RTI) of the link

For any particular run of LAVENT, the code outputs a summary of the input information and simulation results of the calculation, in tabular form, at uniform simulation time intervals requested by the user. The output results include the following:

(a) Temperature of the upper smoke layer

(b) Height of the smoke layer interface

(c) Total mass in the layer

(d) Fire energy release rate

(e) Radial distributions of the lower-ceiling surface temperature

(f) Radial distribution of heat transfer rates to the lower- and upper-ceiling surfaces

(g) The temperature for each link and the local velocity and temperature of the ceiling jet

This appendix explains LAVENT using a series of exercises in which the reader reviews and modifies a default input data file that describes vent and sprinkler actuation during fire growth in an array of wood pallets located in a warehouse-type occupancy. Results of the default simulation are discussed.

LAVENT is written in Fortran 77. The executable code operates on IBM PC-compatible computers and needs a minimum of 300 kilobytes of memory.

C-2 Introduction — The Phenomena Simulated by LAVENT. Figure C-2 depicts the generic fire scenario simulated by LAVENT. This scenario involves a fire in a building space with ceiling-mounted curtain boards and near-ceiling, fusible-link–actuated ceiling vents and sprinklers. The curtained area can be considered as one of several such spaces in a single large building compartment. By specifying that the curtains be deep enough, they can be thought of as simulating the walls of a single uncurtained compartment that is well-ventilated near the floor.

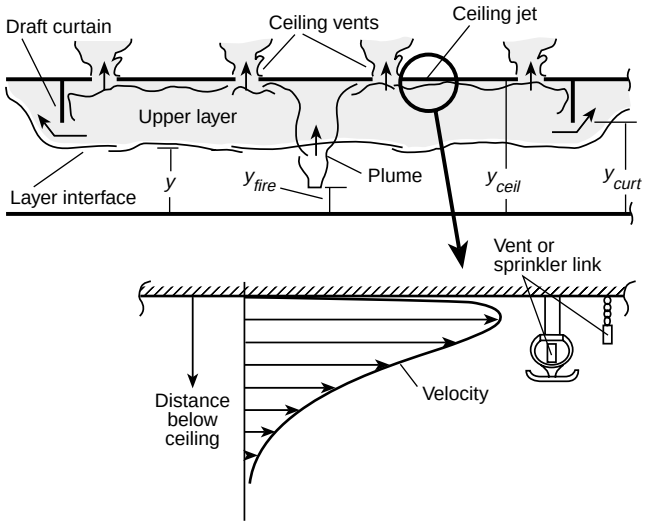

Figure C-2 Fire in a building space with curtain boards, ceiling vents, and fusible links.

The fire generates a mixture of gaseous and solid-soot combustion products. Because of high temperature, buoyancy forces drive the products upward toward the ceiling, forming a plume of upward-moving hot gases and particulates. Cool gases are laterally entrained and mixed with the plume flow, reducing its temperature as it continues its ascent to the ceiling.

When the hot plume flow impinges on the ceiling, it spreads under it, forming a relatively thin, high-temperature ceiling jet. Near-ceiling–deployed fusible links engulfed by the ceiling jet are depicted in Figure C-2. There is reciprocal convective cooling and heating of the ceiling jet and of the cooler lower-ceiling surface, respectively. The lower-ceiling surface is also heated due to radiative transfer from the combustion zone and cooled due to reradiation to the floor of the compartment. The compartment floor is assumed to be at ambient temperature. The upper-ceiling surface is cooled as a result of convection and radiation to a far-field, ambient temperature environment.

When the ceiling jet reaches a bounding vertical curtain board or wall surface, its flow is redistributed across the entire curtained area and begins to form a relatively quiescent smoke layer (now somewhat reduced in temperature) that submerges the continuing ceiling jet flow activity. The upper smoke layer grows in thickness. Away from bounding surfaces, the time-dependent layer temperature is assumed to be relatively uniform throughout its thickness. It should be noted that the thickness and temperature of the smoke layer affect the upper-plume characteristics, the ceiling jet characteristics, and the heat-transfer exchanges to the ceiling.

If the height of the bottom of the smoke layer drops to the bottom of the curtain board and continues downward, the smoke begins to flow below the curtain into the adjacent curtained spaces. The growth of the upper layer is retarded.

Fusible links that are designed to actuate the opening of ceiling vents and the onset of waterflow through sprinklers are deployed at specified distances below the ceiling and at specified radial distances from the plume–ceiling impingement point. These links are submerged within the relatively high-temperature, high-velocity ceiling jet flow. Since the velocity and temperature of the ceiling jet varies with location and time, the heat transfer to and time of fusing of any particular link design also vary.

The fusing of a ceiling vent link leads to the opening of all vents "ganged" to that link. Once a ceiling vent is open, smoke flows out of the curtained space. Again, as when smoke flows below the curtains, growth of the upper-layer thickness is retarded.

The fusing of a sprinkler link initiates the flow of water through the sprinkler.

All of the described phenomena, up to the time that waterflow through a sprinkler is initiated, are simulated by LAVENT. Results cannot be used after water begins to flow through a sprinkler.

C-3 The Default Simulation. The use of LAVENT is discussed and is illustrated in the following paragraphs where exercises in reviewing and modifying the LAVENT default-simulation input file are provided. To appreciate the process more fully, a brief description of the default simulation is presented at the outset.

NOTE: As explained in Section C-4, Getting Started, the user can choose to run LAVENT using either English or metric units. The default simulation uses English units. The example in Appendix D uses metric units.

The default scenario involves an 84 ft × 84 ft curtained compartment (7056 ft^2 in area) with the ceiling located 30 ft above the floor. A curtain board 15 ft in depth completely surrounds and defines the compartment, which is one of several such compartments in a larger building space. The ceiling is constructed of a relatively thin sheet-steel lower surface that is well insulated from above. *[See Figure C-3(a).]*

The curtained compartment has four, uniformly spaced, 48 ft^2 ceiling vents with a total area of 192 ft^2, or 2.7 percent of the compartment area. Opening of the ceiling vents is actuated by quick-response fusible links with RTIs of 50 (ft·sec)$^{1/2}$ and fuse temperatures of 165°F. The links are located at the centers of the vents and 0.3 ft below the ceiling surface.

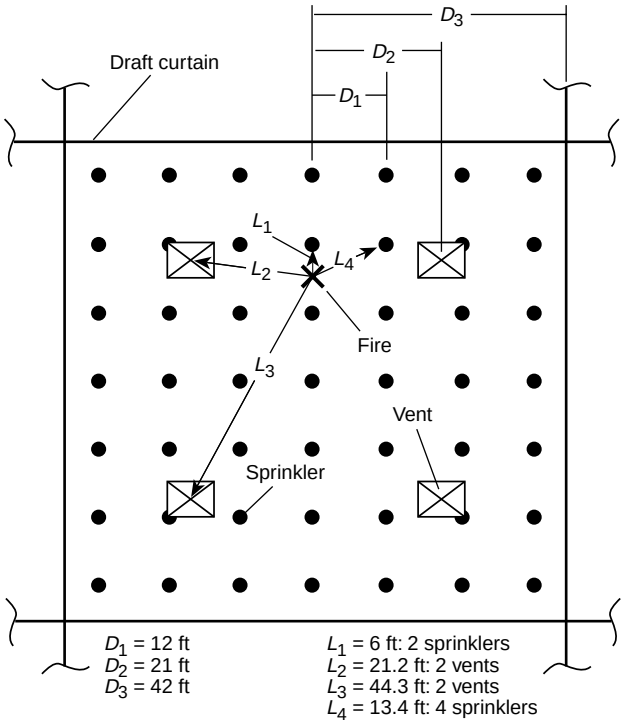

Figure C-3(a) Vent and sprinkler spacing and fire location for the default simulation.

Fusible-link–actuated sprinklers are deployed on a square grid with 12-ft spacing between sprinklers. The links have RTIs of 400 (ft·sec)$^{1/2}$ and fuse temperatures of 165°F. The sprinklers and links are mounted 1 ft below the ceiling surface.

The simulation fire involves four abutting 5-ft high stacks of 5 ft × 5 ft wood pallets. The combined grouping of pallets makes up a combustible array 10 ft × 10 ft (100 ft^2 in area) on the floor and 5 ft in height. It is assumed that other combustibles in the curtained compartment are far enough away from this array that they cannot be ignited in the time interval to be simulated.

The total energy release rate of the simulation fire, $\dot{Q}$, assumed to grow from ignition, at time $t = 0$, in proportion to t^2. According to the guidance in Table 4.2, in the growth phase of the fire, Q is taken specifically as follows:

$$\dot{Q} = 1000\left(\frac{t}{130\ \text{sec}}\right)^2 \text{Btu/sec}$$

The fire grows according to the preceding estimate until the combustibles are fully involved. It is then assumed that Q levels off to a relatively constant value. Following the guidance of Table 4.1 of [1] and Table 5-5.2(b), it is estimated that, at the fully developed stage of the fire, the total energy release rate for the 5-ft high stack of wood pallets will be 330 Btu/sec · ft^2, or 33,000 Btu/sec for the entire 100-ft^2 array. The above equation leads to the result that the fully developed stage of the fire will be initiated at t_{fd} = 747 seconds.

A plot of the fire growth according to the preceding description is shown in Figure C-3(b). In the actual calculation, the fire's instantaneous energy release rate is estimated by interpolating linearly between a series of N input data points at times t_n, $n = 1$ to N, on the fire-growth curve. These points are defined by user-specified values of $[t_n, Q(t_n)]$. For times larger than t_N, the fire's energy release rate is assumed to stay constant at $Q(t_N)$. The calculation fire-growth curve involves six input data points (i.e., $N = 6$). These points are plotted in Figure C-3(b).

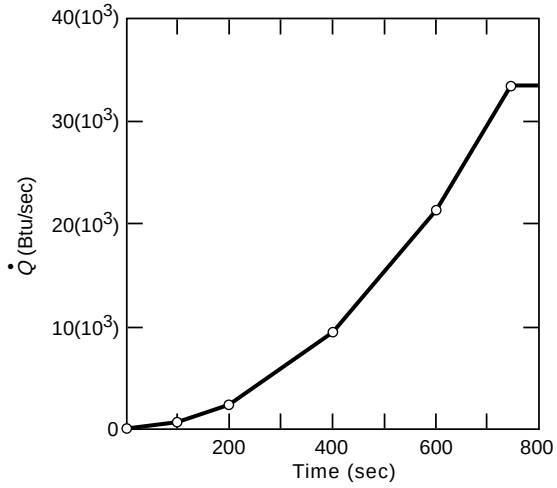

Figure C-3(b) Energy release rate versus time for the fire of the default simulation.

The position of the fire's center is identified in Figure C-3(a). In terms of this plan view, the fire is assumed to be located at the midpoint of a 12-ft line between two sprinkler links, at a distance of 21.2 ft from each of the two closest equidistant vents (a total area of 96 ft^2) and at a distance of 44.3 ft from the remaining two equidistant vents (a total area of 96 ft^2). Of the sprinklers and associated links, two are closest and equidistant to the fire–plume axis at radial distances of 6 ft. Figure C-3(a) shows that the second and third closest groups of sprinklers and links are at radial distances of 13.4 ft (four sprinklers and links) and 18 ft (two sprinklers and links). In the default calculation, the opening of each of the four vents occurs, and the flow out of the vents is initiated at the simulated time of fusing of their associated links. Also simulated in the default calculation is the thermal response, including time of fusing, of the pair of sprinkler links closest to the fire.

As a final specification of the fire, it is assumed that the characteristic elevation of the fire remains at a fixed value, 2.5 ft above the floor, at the initial mid-elevation of the array of combustibles.

For the purpose of the default calculation, the simulation is carried out to $t = 400$ seconds, with data output every 30 seconds.

Having described the default simulation, the procedure for getting started and using LAVENT follows.

C-4 Getting Started. The executable code, LAVENT.EXE, is found on the floppy disk. Before using it, backup copies should be made. If the user has a hard drive, a separate directory should be created and the executable code should be copied into that directory. The code operates on an IBM PC or compatible computer containing a math coprocessor. It is written in Fortran 77 and needs a minimum of 300 kilobytes of memory.

To execute LAVENT, change to the proper directory or insert a floppy disk containing a copy of the executable code and enter LAVENT <ret>. In this case, <ret> refers to the ENTER or RETURN key. The first prompt provides an option for english or metric units:

```
1 FOR ENGLISH UNITS

2 FOR METRIC UNITS
```

The program has a unit conversion function and transforms files that are in one set of units to another set. The code executes in SI units and so conversion is done only on input and output in order to avoid rounding errors.

For the purposes of getting started, choose Option 1, ENGLISH UNITS. Enter 1 <ret>. The following menu will be displayed on the screen:

```
1 READ AND RUN A DATA FILE
2 READ AND MODIFY A DATA FILE
3 MODIFY THE DEFAULT CASE TO CREATE A NEW FILE
4 RUN THE DEFAULT CASE
```

If Option 1 or 2 is chosen, the program will ask for the name of the data file to be used. If the chosen file resides on the hard disk, this question should be answered by typing the path of the file name, for example, C:\subdirectory\filename. If the file is on a floppy disk, type A:filename or B:filename, depending on whether the A or B drive is being used. It is recommended that all data files use a common extender such as ".dat" in order to facilitate identification of these files.

A first-time user should select Option 4, RUN THE DEFAULT CASE, by entering 4 <ret>. This selection will ensure that the code has been transferred intact. The default-case output is provided in Computer Printout C-1 and is discussed in Section C-8. As a point of information, the times needed to carry out the default simulation on IBM PC-compatible 486/33 MHZ and Pentium/90 MHZ computers were 40 seconds and 8 seconds, respectively.

Now restart the code and, at this point, choose Option 3, MODIFY THE DEFAULT CASE, to review and modify the default input data. Enter 3 <ret>.

C-5 The Base Menu.

C-5.1 Modifying the Default Case — General. When Option 3, MODIFY THE DEFAULT CASE, is chosen, the following menu is displayed:

```
1 ROOM PROPERTIES
2 PHYSICAL PROPERTIES
3 OUTPUT PARAMETERS
4 FUSIBLE LINK PROPERTIES
5 FIRE PROPERTIES
6 SOLVER PARAMETERS
0 NO CHANGES
```

This menu will be referred to as the *base menu*.

Entering the appropriate option number of the base menu and then <ret> will always transfer the user to the indicated item on the menu. Entering a zero will transfer the user to the file status portion of the input section discussed in Section C-6.

The next sub-sections discuss data entry under Options 1 through 6 of the base menu.

Now choose Option 1, ROOM PROPERTIES, of the base menu to review and modify the default room-property input data. Enter 1 <ret>.

C-5.2 Room Properties. When Option 1, ROOM PROPERTIES, of the base menu is chosen, the following room properties menu is displayed:

```
1      30.00000      CEILING HEIGHT (FT)
2      84.00000      ROOM LENGTH (FT)
3      84.00000      ROOM WIDTH (FT)
4      2             NUMBER OF VENTS, ETC.
5      336.00000     CURTAIN LENGTH (FT)
6      15.00000      HEIGHT TO BOTTOM OF CURTAIN (FT)
0                    TO CHANGE NOTHING
```

All input values are expressed in either S.I. or U.S. customary units, and the units are prompted on the input menus.

Note that the default number of vents is 2, not 4, since the symmetry of the default scenario, as indicated in Figure C-3(a), leads to "ganged" operation of each of two pairs of the four vents involved.

To change an input value in the preceding above room properties menu (e.g., to change the ceiling height from 30 ft to 20 ft), the user would enter 1 <ret> and 20. <ret>. The screen would show revisions using the new value of 20 ft for the ceiling height. This value or other values on this screen can be changed by repeating the process.

Warning

The user is warned that it is critical to end each entry number with a decimal point when a noninteger number is indicated (i.e., when the screen display shows a decimal point for that entry). The user is warned further that the code will attempt to run with any specified input file and that it will not distinguish between realistic and unrealistic input values.

Computer Printout C-1 The default-case output

```
CEILING HEIGHT =           30.0 FT
ROOM LENGTH =              84.0 FT
ROOM WIDTH =               84.0 FT
CURTAIN LENGTH =           336.0 FT
CURTAIN HEIGHT =           15.0 FT
MATERIAL =                 INSULATED DECK (SOLID POLYSTYRENE)
CEILING CONDUCTIVITY =     .240E-04 BTU/FT F S
CEILING DENSITY =          .655E+02 LB/FT3
CEILING HEAT CAPACITY =    .277E+00 BTU/LB F
CEILING THICKNESS =        .500E+00 FT
FIRE HEIGHT =              2.5 FT
FIRE POWER/AREA =          0.3300E+03 BTU/S FT2

LINK NO =  1 RADIUS =     6.0 FT    DIST CEILING =    1.00 FT
         RTI=  400.00 SQRT FUSION TEMPERATURE FOR LINK =   165.00 K
LINK NO =  2 RADIUS =    21.2 FT    DIST CEILING =    0.30 FT
         RTI=   50.00 SQRT FUSION TEMPERATURE FOR LINK =   165.00 K
LINK NO =  3 RADIUS =    44.3 FT    DIST CEILING =    0.30 FT
         RTI=   50.00 SQRT FUSION TEMPERATURE FOR LINK =   165.00 K
VENT =   1   VENT AREA =     96.0 FT2           LINK CONTROLLING VENT =   2
VENT =   2   VENT AREA =     96.0 FT2           LINK CONTROLLING VENT =   3

TIME (S)=    0.000 LYR TEMP (F)=    80.0 LYR HT (FT)=   30.00 LYR MASS (LB)= 0.000E+00
FIRE OUTPUT (BTU/S)=  0.0000E+00 VENT AREA (FT2)=      0.00
LINK =  1 LINK TEMP (F)=   80.00 JET VELOCITY (FT/S)=     0.000 JET TEMP (F) =     80.0
LINK =  2 LINK TEMP (F)=   80.00 JET VELOCITY (FT/S)=     0.000 JET TEMP (F) =     80.0
LINK =  3 LINK TEMP (F)=   80.00 JET VELOCITY (FT/S)=     0.000 JET TEMP (F) =     80.0
R (FT)=    0.00 TSL (F)=    80.0 QB (BTU/FT2 S)= 0.000E+00 QT (BTU/FT2 S)= 0.000E+00
R (FT)=   12.41 TSL (F)=    80.0 QB (BTU/FT2 S)= 0.000E+00 QT (BTU/FT2 S)= 0.000E+00
R (FT)=   24.82 TSL (F)=    80.0 QB (BTU/FT2 S)= 0.000E+00 QT (BTU/FT2 S)= 0.000E+00
R (FT)=   37.23 TSL (F)=    80.0 QB (BTU/FT2 S)= 0.000E+00 QT (BTU/FT2 S)= 0.000E+00
R (FT)=   49.64 TSL (F)=    80.0 QB (BTU/FT2 S)= 0.000E+00 QT (BTU/FT2 S)= 0.000E+00
R (FT)=   62.05 TSL (F)=    80.0 QB (BTU/FT2 S)= 0.000E+00 QT (BTU/FT2 S)= 0.000E+00

TIME (S)=   30.000 LYR TEMP (F)=    89.6 LYR HT (FT)=   28.90 LYR MASS (LB)= 0.562E+03
FIRE OUTPUT (BTU/S)=  0.1776E+03 VENT AREA (FT2)=      0.00
LINK =  1 LINK TEMP (F)=   80.78 JET VELOCITY (FT/S)=     1.866 JET TEMP (F) =     94.9
LINK =  2 LINK TEMP (F)=   85.37 JET VELOCITY (FT/S)=     2.077 JET TEMP (F) =     95.3
LINK =  3 LINK TEMP (F)=   81.83 JET VELOCITY (FT/S)=     0.873 JET TEMP (F) =     87.4
R (FT)=    0.00 TSL (F)=    84.5 QB (BTU/FT2 S)= 0.312E-01 QT (BTU/FT2 S)= 0.847E-18
R (FT)=   12.41 TSL (F)=    81.7 QB (BTU/FT2 S)= 0.122E-01 QT (BTU/FT2 S)= 0.847E-18
R (FT)=   24.82 TSL (F)=    80.8 QB (BTU/FT2 S)= 0.570E-02 QT (BTU/FT2 S)= 0.847E-18
R (FT)=   37.23 TSL (F)=    80.4 QB (BTU/FT2 S)= 0.325E-02 QT (BTU/FT2 S)= 0.847E-18
R (FT)=   49.64 TSL (F)=    80.3 QB (BTU/FT2 S)= 0.212E-02 QT (BTU/FT2 S)= 0.847E-18
R (FT)=   62.05 TSL (F)=    80.2 QB (BTU/FT2 S)= 0.152E-02 QT (BTU/FT2 S)= 0.847E-18

TIME (S)=   60.000 LYR TEMP (F)=    96.5 LYR HT (FT)=   27.34 LYR MASS (LB)= 0.134E+04
FIRE OUTPUT (BTU/S)=  0.3552E+03 VENT AREA (FT2)=      0.00
LINK =  1 LINK TEMP (F)=   82.80 JET VELOCITY (FT/S)=     2.395 JET TEMP (F) =    105.0
LINK =  2 LINK TEMP (F)=   95.13 JET VELOCITY (FT/S)=     2.657 JET TEMP (F) =    105.8
LINK =  3 LINK TEMP (F)=   85.76 JET VELOCITY (FT/S)=     1.117 JET TEMP (F) =     92.9
R (FT)=    0.00 TSL (F)=    92.7 QB (BTU/FT2 S)= 0.517E-01 QT (BTU/FT2 S)= 0.847E-18
R (FT)=   12.41 TSL (F)=    85.2 QB (BTU/FT2 S)= 0.223E-01 QT (BTU/FT2 S)= 0.847E-18
R (FT)=   24.82 TSL (F)=    82.5 QB (BTU/FT2 S)= 0.107E-01 QT (BTU/FT2 S)= 0.847E-18
R (FT)=   37.23 TSL (F)=    81.4 QB (BTU/FT2 S)= 0.619E-02 QT (BTU/FT2 S)= 0.847E-18
R (FT)=   49.64 TSL (F)=    80.9 QB (BTU/FT2 S)= 0.405E-02 QT (BTU/FT2 S)= 0.847E-18
R (FT)=   62.05 TSL (F)=    80.6 QB (BTU/FT2 S)= 0.292E-02 QT (BTU/FT2 S)= 0.847E-18

TIME (S)=   90.000 LYR TEMP (F)=   103.2 LYR HT (FT)=   25.65 LYR MASS (LB)= 0.216E+04
FIRE OUTPUT (BTU/S)=  0.5328E+03 VENT AREA (FT2)=      0.00
LINK =  1 LINK TEMP (F)=   85.90 JET VELOCITY (FT/S)=     2.809 JET TEMP (F) =    114.5
LINK =  2 LINK TEMP (F)=  105.74 JET VELOCITY (FT/S)=     3.104 JET TEMP (F) =    115.8
LINK =  3 LINK TEMP (F)=   90.66 JET VELOCITY (FT/S)=     1.305 JET TEMP (F) =     98.2
```

Computer Printout C-1 The default-case output ***(continued)***

```
R (FT)=    0.00 TSL (F)=   102.4 QB (BTU/FT2 S)= 0.687E-01 QT (BTU/FT2 S)= 0.847E-18
R (FT)=   12.41 TSL (F)=    89.7 QB (BTU/FT2 S)= 0.317E-01 QT (BTU/FT2 S)= 0.847E-18
R (FT)=   24.82 TSL (F)=    84.7 QB (BTU/FT2 S)= 0.156E-01 QT (BTU/FT2 S)= 0.847E-18
R (FT)=   37.23 TSL (F)=    82.7 QB (BTU/FT2 S)= 0.908E-02 QT (BTU/FT2 S)= 0.847E-18
R (FT)=   49.64 TSL (F)=    81.8 QB (BTU/FT2 S)= 0.598E-02 QT (BTU/FT2 S)= 0.847E-18
R (FT)=   62.05 TSL (F)=    81.1 QB (BTU/FT2 S)= 0.987E-03 QT (BTU/FT2 S)= 0.847E-18

TIME (S)=  120.000 LYR TEMP (F)=   111.5 LYR HT (FT)=   23.85 LYR MASS (LB)= 0.301E+04
FIRE OUTPUT (BTU/S)=  0.9470E+03 VENT AREA (FT2)=      0.00
LINK =  1 LINK TEMP (F)=   90.30 JET VELOCITY (FT/S)=     3.614 JET TEMP (F) =    129.3
LINK =  2 LINK TEMP (F)=  118.43 JET VELOCITY (FT/S)=     3.966 JET TEMP (F) =    132.1
LINK =  3 LINK TEMP (F)=   96.66 JET VELOCITY (FT/S)=     1.667 JET TEMP (F) =    106.2
R (FT)=    0.00 TSL (F)=   115.6 QB (BTU/FT2 S)= 0.113E+00 QT (BTU/FT2 S)= 0.847E-18
R (FT)=   12.41 TSL (F)=    96.2 QB (BTU/FT2 S)= 0.543E-01 QT (BTU/FT2 S)= 0.847E-18
R (FT)=   24.82 TSL (F)=    87.9 QB (BTU/FT2 S)= 0.266E-01 QT (BTU/FT2 S)= 0.847E-18
R (FT)=   37.23 TSL (F)=    84.6 QB (BTU/FT2 S)= 0.154E-01 QT (BTU/FT2 S)= 0.847E-18
R (FT)=   49.64 TSL (F)=    83.0 QB (BTU/FT2 S)= 0.101E-01 QT (BTU/FT2 S)= 0.847E-18
R (FT)=   62.05 TSL (F)=    82.0 QB (BTU/FT2 S)= 0.728E-02 QT (BTU/FT2 S)= 0.847E-18

TIME (S)=  150.000 LYR TEMP (F)=   124.4 LYR HT (FT)=   21.85 LYR MASS (LB)= 0.390E+04
FIRE OUTPUT (BTU/S)=  0.1479E+04 VENT AREA (FT2)=      0.00
LINK =  1 LINK TEMP (F)=   97.16 JET VELOCITY (FT/S)=     4.364 JET TEMP (F) =    149.2
LINK =  2 LINK TEMP (F)=  137.37 JET VELOCITY (FT/S)=     4.754 JET TEMP (F) =    153.4
LINK =  3 LINK TEMP (F)=  105.49 JET VELOCITY (FT/S)=     1.998 JET TEMP (F) =    117.4
R (FT)=    0.00 TSL (F)=   136.5 QB (BTU/FT2 S)= 0.158E+00 QT (BTU/FT2 S)= 0.847E-18
R (FT)=   12.41 TSL (F)=   107.0 QB (BTU/FT2 S)= 0.810E-01 QT (BTU/FT2 S)= 0.847E-18
R (FT)=   24.82 TSL (F)=    93.3 QB (BTU/FT2 S)= 0.405E-01 QT (BTU/FT2 S)= 0.847E-18
R (FT)=   37.23 TSL (F)=    87.7 QB (BTU/FT2 S)= 0.236E-01 QT (BTU/FT2 S)= 0.847E-18
R (FT)=   49.64 TSL (F)=    85.1 QB (BTU/FT2 S)= 0.155E-01 QT (BTU/FT2 S)= 0.847E-18
R (FT)=   62.05 TSL (F)=    83.5 QB (BTU/FT2 S)= 0.112E-01 QT (BTU/FT2 S)= 0.847E-18

TIME (S)=  180.000 LYR TEMP (F)=   140.2 LYR HT (FT)=   19.77 LYR MASS (LB)= 0.477E+04
FIRE OUTPUT (BTU/S)=  0.2012E+04 VENT AREA (FT2)=      0.00
LINK =  1 LINK TEMP (F)=  106.66 JET VELOCITY (FT/S)=     5.008 JET TEMP (F) =    171.4
LINK =  2 LINK TEMP (F)=  159.68 JET VELOCITY (FT/S)=     5.414 JET TEMP (F) =    176.5
LINK =  3 LINK TEMP (F)=  116.69 JET VELOCITY (FT/S)=     2.275 JET TEMP (F) =    130.2
R (FT)=    0.00 TSL (F)=   160.3 QB (BTU/FT2 S)= 0.195E+00 QT (BTU/FT2 S)= 0.847E-18
R (FT)=   12.41 TSL (F)=   120.4 QB (BTU/FT2 S)= 0.106E+00 QT (BTU/FT2 S)= 0.847E-18
R (FT)=   24.82 TSL (F)=   100.2 QB (BTU/FT2 S)= 0.545E-01 QT (BTU/FT2 S)= 0.847E-18
R (FT)=   37.23 TSL (F)=    91.8 QB (BTU/FT2 S)= 0.322E-01 QT (BTU/FT2 S)= 0.847E-18
R (FT)=   49.64 TSL (F)=    87.8 QB (BTU/FT2 S)= 0.213E-01 QT (BTU/FT2 S)= 0.847E-18
R (FT)=   62.05 TSL (F)=    85.3 QB (BTU/FT2 S)= 0.332E-02 QT (BTU/FT2 S)= 0.847E-18

TIME (S)=  210.000 LYR TEMP (F)=   158.7 LYR HT (FT)=   19.59 LYR MASS (LB)= 0.471E+04
FIRE OUTPUT (BTU/S)=  0.2722E+04 VENT AREA (FT2)=     96.00
LINK =  1 LINK TEMP (F)=  118.85 JET VELOCITY (FT/S)=     5.605 JET TEMP (F) =    196.8
LINK =  2 LINK TEMP (F)=  184.03 JET VELOCITY (FT/S)=     6.021 JET TEMP (F) =    202.7
LINK =  3 LINK TEMP (F)=  129.71 JET VELOCITY (FT/S)=     2.530 JET TEMP (F) =    144.9
TIME LINK    2  OPENS EQUALS     186.7478 (S)
R (FT)=    0.00 TSL (F)=   185.7 QB (BTU/FT2 S)= 0.239E+00 QT (BTU/FT2 S)= 0.847E-18
R (FT)=   12.41 TSL (F)=   135.8 QB (BTU/FT2 S)= 0.137E+00 QT (BTU/FT2 S)= 0.847E-18
R (FT)=   24.82 TSL (F)=   108.5 QB (BTU/FT2 S)= 0.718E-01 QT (BTU/FT2 S)= 0.847E-18

R (FT)=   37.23 TSL (F)=    96.8 QB (BTU/FT2 S)= 0.427E-01 QT (BTU/FT2 S)= 0.847E-18
R (FT)=   49.64 TSL (F)=    91.1 QB (BTU/FT2 S)= 0.285E-01 QT (BTU/FT2 S)= 0.847E-18
R (FT)=   62.05 TSL (F)=    87.2 QB (BTU/FT2 S)= 0.210E-01 QT (BTU/FT2 S)= 0.847E-18

 TIME (S)=  240.000 LYR TEMP (F)=   184.9 LYR HT (FT)=   19.77 LYR MASS (LB)= 0.444E+04
FIRE OUTPUT (BTU/S)=  0.3787E+04 VENT AREA (FT2)=     96.00
LINK =  1 LINK TEMP (F)=  134.89 JET VELOCITY (FT/S)=     6.327 JET TEMP (F) =    231.8
LINK =  2 LINK TEMP (F)=  215.69 JET VELOCITY (FT/S)=     6.741 JET TEMP (F) =    238.2
LINK =  3 LINK TEMP (F)=  146.44 JET VELOCITY (FT/S)=     2.832 JET TEMP (F) =    165.1
TIME LINK    2  OPENS EQUALS     186.7478 (S)
```

Computer Printout C-1 The default-case output ***(continued)***

```
R (FT)=    0.00 TSL (F)=   218.6 QB (BTU/FT2 S)= 0.299E+00 QT (BTU/FT2 S)= 0.847E-18
R (FT)=   12.41 TSL (F)=   156.6 QB (BTU/FT2 S)= 0.180E+00 QT (BTU/FT2 S)= 0.847E-18
R (FT)=   24.82 TSL (F)=   119.9 QB (BTU/FT2 S)= 0.971E-01 QT (BTU/FT2 S)= 0.847E-18
R (FT)=   37.23 TSL (F)=   103.7 QB (BTU/FT2 S)= 0.582E-01 QT (BTU/FT2 S)= 0.847E-18
R (FT)=   49.64 TSL (F)=    95.7 QB (BTU/FT2 S)= 0.389E-01 QT (BTU/FT2 S)= 0.847E-18
R (FT)=   62.05 TSL (F)=    90.3 QB (BTU/FT2 S)= 0.288E-01 QT (BTU/FT2 S)= 0.847E-18

TIME (S)=  270.000 LYR TEMP (F)=   217.5 LYR HT (FT)=   20.17 LYR MASS (LB)= 0.407E+04
FIRE OUTPUT (BTU/S)=  0.4852E+04 VENT AREA (FT2)=    192.00
LINK =  1 LINK TEMP (F)=  155.49 JET VELOCITY (FT/S)=     6.854 JET TEMP (F) =    271.3
LINK =  2 LINK TEMP (F)=  253.19 JET VELOCITY (FT/S)=     7.244 JET TEMP (F) =    277.0
LINK =  3 LINK TEMP (F)=  167.24 JET VELOCITY (FT/S)=     3.043 JET TEMP (F) =    188.5
TIME LINK    2  OPENS EQUALS     186.7478 (S)
TIME LINK    3  OPENS EQUALS     266.9820 (S)
R (FT)=    0.00 TSL (F)=   254.4 QB (BTU/FT2 S)= 0.339E+00 QT (BTU/FT2 S)= 0.847E-18
R (FT)=   12.41 TSL (F)=   181.1 QB (BTU/FT2 S)= 0.217E+00 QT (BTU/FT2 S)= 0.847E-18
R (FT)=   24.82 TSL (F)=   133.9 QB (BTU/FT2 S)= 0.121E+00 QT (BTU/FT2 S)= 0.847E-18
R (FT)=   37.23 TSL (F)=   112.2 QB (BTU/FT2 S)= 0.735E-01 QT (BTU/FT2 S)= 0.847E-18
R (FT)=   49.64 TSL (F)=   101.5 QB (BTU/FT2 S)= 0.494E-01 QT (BTU/FT2 S)= 0.847E-18
R (FT)=   62.05 TSL (F)=    93.7 QB (BTU/FT2 S)= 0.371E-01 QT (BTU/FT2 S)= 0.847E-18

TIME (S)=  300.000 LYR TEMP (F)=   253.4 LYR HT (FT)=   22.84 LYR MASS (LB)= 0.281E+04
FIRE OUTPUT (BTU/S)=  0.5918E+04 VENT AREA (FT2)=    192.00
LINK =  1 LINK TEMP (F)=  179.59 JET VELOCITY (FT/S)=     6.901 JET TEMP (F) =    308.7
LINK =  2 LINK TEMP (F)=  289.67 JET VELOCITY (FT/S)=     7.195 JET TEMP (F) =    311.3
LINK =  3 LINK TEMP (F)=  189.77 JET VELOCITY (FT/S)=     3.023 JET TEMP (F) =    211.4
TIME LINK    1  OPENS EQUALS     282.8710 (S)
TIME LINK    2  OPENS EQUALS     186.7478 (S)
TIME LINK    3  OPENS EQUALS     266.9820 (S)
R (FT)=    0.00 TSL (F)=   287.1 QB (BTU/FT2 S)= 0.352E+00 QT (BTU/FT2 S)= 0.847E-18
R (FT)=   12.41 TSL (F)=   205.5 QB (BTU/FT2 S)= 0.238E+00 QT (BTU/FT2 S)= 0.847E-18
R (FT)=   24.82 TSL (F)=   148.7 QB (BTU/FT2 S)= 0.138E+00 QT (BTU/FT2 S)= 0.847E-18
R (FT)=   37.23 TSL (F)=   121.5 QB (BTU/FT2 S)= 0.851E-01 QT (BTU/FT2 S)= 0.847E-18
R (FT)=   49.64 TSL (F)=   107.8 QB (BTU/FT2 S)= 0.574E-01 QT (BTU/FT2 S)= 0.847E-18
R (FT)=   62.05 TSL (F)=    98.8 QB (BTU/FT2 S)= 0.428E-01 QT (BTU/FT2 S)= 0.847E-18

TIME (S)=  330.000 LYR TEMP (F)=   284.4 LYR HT (FT)=   24.25 LYR MASS (LB)= 0.216E+04
FIRE OUTPUT (BTU/S)=  0.6983E+04 VENT AREA (FT2)=    192.00
LINK =  1 LINK TEMP (F)=  206.05 JET VELOCITY (FT/S)=     7.109 JET TEMP (F) =    342.3
LINK =  2 LINK TEMP (F)=  322.58 JET VELOCITY (FT/S)=     7.227 JET TEMP (F) =    341.6
LINK =  3 LINK TEMP (F)=  211.77 JET VELOCITY (FT/S)=     3.036 JET TEMP (F) =    231.8
TIME LINK    1  OPENS EQUALS     282.8710 (S)
TIME LINK    2  OPENS EQUALS     186.7478 (S)
TIME LINK    3  OPENS EQUALS     266.9820 (S)
R (FT)=    0.00 TSL (F)=   316.3 QB (BTU/FT2 S)= 0.366E+00 QT (BTU/FT2 S)= 0.847E-18
R (FT)=   12.41 TSL (F)=   229.1 QB (BTU/FT2 S)= 0.257E+00 QT (BTU/FT2 S)= 0.847E-18
R (FT)=   24.82 TSL (F)=   163.7 QB (BTU/FT2 S)= 0.153E+00 QT (BTU/FT2 S)= 0.847E-18

R (FT)=   37.23 TSL (F)=   130.9 QB (BTU/FT2 S)= 0.952E-01 QT (BTU/FT2 S)= 0.847E-18
R (FT)=   49.64 TSL (F)=   114.2 QB (BTU/FT2 S)= 0.644E-01 QT (BTU/FT2 S)= 0.847E-18
R (FT)=   62.05 TSL (F)=   103.0 QB (BTU/FT2 S)= 0.481E-01 QT (BTU/FT2 S)= 0.847E-18

 TIME (S)=  360.000 LYR TEMP (F)=   307.3 LYR HT (FT)=   24.77 LYR MASS (LB)= 0.191E+04
FIRE OUTPUT (BTU/S)=  0.8048E+04 VENT AREA (FT2)=    192.00
LINK =  1 LINK TEMP (F)=  233.80 JET VELOCITY (FT/S)=     7.559 JET TEMP (F) =    370.4
LINK =  2 LINK TEMP (F)=  351.11 JET VELOCITY (FT/S)=     7.461 JET TEMP (F) =    367.4
LINK =  3 LINK TEMP (F)=  231.51 JET VELOCITY (FT/S)=     3.134 JET TEMP (F) =    248.9
TIME LINK    1  OPENS EQUALS     282.8710 (S)
TIME LINK    2  OPENS EQUALS     186.7478 (S)
TIME LINK    3  OPENS EQUALS     266.9820 (S)
R (FT)=    0.00 TSL (F)=   344.3 QB (BTU/FT2 S)= 0.380E+00 QT (BTU/FT2 S)= 0.847E-18
R (FT)=   12.41 TSL (F)=   252.3 QB (BTU/FT2 S)= 0.275E+00 QT (BTU/FT2 S)= 0.847E-18
R (FT)=   24.82 TSL (F)=   178.8 QB (BTU/FT2 S)= 0.167E+00 QT (BTU/FT2 S)= 0.847E-18
```

Computer Printout C-1. The default-case output *(continued)*.

```
R (FT)=   37.23 TSL (F)=   140.5 QB (BTU/FT2 S)= 0.105E+00 QT (BTU/FT2 S)= 0.847E-18
R (FT)=   49.64 TSL (F)=   120.8 QB (BTU/FT2 S)= 0.709E-01 QT (BTU/FT2 S)= 0.847E-18
R (FT)=   62.05 TSL (F)=   107.5 QB (BTU/FT2 S)= 0.530E-01 QT (BTU/FT2 S)= 0.847E-18

TIME (S)=  390.000 LYR TEMP (F)=   327.0 LYR HT (FT)=   24.81 LYR MASS (LB)= 0.185E+04
FIRE OUTPUT (BTU/S)=  0.9113E+04 VENT AREA (FT2)=    192.00
LINK =  1 LINK TEMP (F)=  262.32 JET VELOCITY (FT/S)=     8.168 JET TEMP (F) =    397.0
LINK =  2 LINK TEMP (F)=  376.92 JET VELOCITY (FT/S)=     7.811 JET TEMP (F) =    392.0
LINK =  3 LINK TEMP (F)=  249.19 JET VELOCITY (FT/S)=     3.281 JET TEMP (F) =    264.9
TIME LINK    1  OPENS EQUALS     282.8710 (S)
TIME LINK    2  OPENS EQUALS     186.7478 (S)
TIME LINK    3  OPENS EQUALS     266.9820 (S)
R (FT)=    0.00 TSL (F)=   372.0 QB (BTU/FT2 S)= 0.398E+00 QT (BTU/FT2 S)= 0.847E-18
R (FT)=   12.41 TSL (F)=   275.6 QB (BTU/FT2 S)= 0.294E+00 QT (BTU/FT2 S)= 0.847E-18
R (FT)=   24.82 TSL (F)=   194.1 QB (BTU/FT2 S)= 0.181E+00 QT (BTU/FT2 S)= 0.847E-18
R (FT)=   37.23 TSL (F)=   150.3 QB (BTU/FT2 S)= 0.114E+00 QT (BTU/FT2 S)= 0.847E-18
R (FT)=   49.64 TSL (F)=   127.5 QB (BTU/FT2 S)= 0.773E-01 QT (BTU/FT2 S)= 0.847E-18
R (FT)=   62.05 TSL (F)=   113.2 QB (BTU/FT2 S)= 0.574E-01 QT (BTU/FT2 S)= 0.847E-18

TIME (S)=  400.000 LYR TEMP (F)=   333.5 LYR HT (FT)=   24.77 LYR MASS (LB)= 0.185E+04
FIRE OUTPUT (BTU/S)=  0.9468E+04 VENT AREA (FT2)=    192.00
LINK =  1 LINK TEMP (F)=  271.98 JET VELOCITY (FT/S)=     8.387 JET TEMP (F) =    406.0
LINK =  2 LINK TEMP (F)=  385.32 JET VELOCITY (FT/S)=     7.936 JET TEMP (F) =    400.2
LINK =  3 LINK TEMP (F)=  254.85 JET VELOCITY (FT/S)=     3.333 JET TEMP (F) =    270.2
TIME LINK    1  OPENS EQUALS     282.8710 (S)
TIME LINK    2  OPENS EQUALS     186.7478 (S)
TIME LINK    3  OPENS EQUALS     266.9820 (S)
R (FT)=    0.00 TSL (F)=   381.3 QB (BTU/FT2 S)= 0.403E+00 QT (BTU/FT2 S)= 0.847E-18
R (FT)=   12.41 TSL (F)=   283.5 QB (BTU/FT2 S)= 0.300E+00 QT (BTU/FT2 S)= 0.847E-18
R (FT)=   24.82 TSL (F)=   199.2 QB (BTU/FT2 S)= 0.186E+00 QT (BTU/FT2 S)= 0.847E-18
R (FT)=   37.23 TSL (F)=   153.6 QB (BTU/FT2 S)= 0.117E+00 QT (BTU/FT2 S)= 0.847E-18
R (FT)=   49.64 TSL (F)=   129.7 QB (BTU/FT2 S)= 0.794E-01 QT (BTU/FT2 S)= 0.847E-18
R (FT)=   62.05 TSL (F)=   115.0 QB (BTU/FT2 S)= 0.589E-01 QT (BTU/FT2 S)= 0.847E-18
```

Option 6, HEIGHT TO BOTTOM OF CURTAIN, of the room properties menu is used to define the height above the floor of the bottom of the curtain. As can be seen, in the default data, this is 15 ft. Where this height is chosen to be identical to the ceiling height, the user should always define the very special idealized simulation associated with an extensive, unconfined ceiling fire scenario (i.e., by whatever means, it is assumed that the flow of the ceiling jet is extracted from the compartment at the extremities of the ceiling). Under such a simulation, an upper layer never develops in the compartment. The lower-ceiling surface and fusible links are submerged in and respond to an unconfined ceiling jet environment, which is unaffected by layer growth. This idealized fire scenario, involving the unconfined ceiling, is used, for example, in [1] to simulate ceiling response and in [2] and [3] to simulate sprinkler response.

The choice of some options on a menu, such as Option 4, NUMBER OF VENTS, ETC., of the room properties menu, will lead to a subsequent display/requirement of additional associated input data. Menu options that necessitate multiple entries are indicated by the use of "ETC." In the case of Option 4, NUMBER OF VENTS, ETC., three values are involved for each vent or group of vents actuated by a fusible link. As indicated under Option 4, NUMBER OF VENTS, ETC., the default data describe a scenario with two vents or groups of vents.

Now choose Option 4, NUMBER OF VENTS, ETC., to review and modify the default input data associated with these two vents or groups of vents. Enter 4 <ret>. The following is displayed on the screen:

```
VENT NO. = 1 FUSIBLE LINK = 2   VENT AREA = 96.00000 FT2
VENT NO. = 2 FUSIBLE LINK = 3   VENT AREA = 96.00000 FT2
ENTER 6 TO REMOVE A VENT
ENTER VENT NO., LINK NO., AND VENT AREA (FT2) TO ADD OR MODIFY A VENT
MAXIMUM NO. OF VENTS IS 5
ENTER 0 TO RETURN TO THE MENU
```

This display indicates that the two simulated vents or groups of vents are numbered 1 (VENT NO. = 1) and 2 (VENT NO. = 2), that they are actuated by fusible links numbered 2 (FUSIBLE LINK = 2) and 3 (FUSIBLE LINK = 3), respectively, and that each of the two vents or groups of vents have a total area of 96 ft^2 (VENT AREA = 96.00000 FT2).

In the default fire scenario it would be of interest to study the effect of "ganging" the operation of all four vents (total area of 192 ft^2) to fusing of the closest vent link. To do so, it would be necessary to first remove vent number 2, as identified in the preceding menu, and then to modify the area of vent number 1.

To remove vent number 2, enter 6 <ret>. The following is now displayed on the screen:

```
ENTER NUMBER OF VENT TO BE ELIMINATED

ENTER 0 TO RETURN TO MENU
```

Now enter 2 <ret>. This completes removal of vent 2, with the following revision displayed on the screen:

```
VENT NO. = 1   FUSIBLE LINK = 2   VENT AREA = 96.00000 FT2

ENTER 6 TO REMOVE A VENT

ENTER VENT NO., LINK NO., AND VENT AREA (FT2) TO ADD OR MODIFY A VENT

MAXIMUM NO. OF VENTS IS 5

ENTER 0 TO RETURN TO THE MENU
```

Now modify the characteristics of vent number 1. To do so, enter 1 <ret>, 2 <ret>, 192. <ret>. The screen will now display the following:

```
VENT NO. = 1   FUSIBLE LINK = 2   VENT AREA = 192.00000 FT2

ENTER 6 TO REMOVE A VENT

ENTER VENT NO., LINK NO., AND VENT AREA (FT2) TO ADD OR MODIFY A VENT

MAXIMUM NO. OF VENTS IS 5

ENTER 0 TO RETURN TO THE MENU
```

To add or reimplement vent number 2, actuated by link number 3 and of area 96 ft^2, enter 2 <ret>, 3 <ret>, 96. <ret>. Now return to the original default scenario by bringing the area of vent number 1 back to its original 96 ft^2 value; enter 1<ret>, 2 <ret>, and 96. <ret>.

The user may now continue to modify or add additional ceiling vents or return to the room properties menu by entering 0 <ret>. If the user tries to associate a vent with a link not yet entered in the program, the code will warn the user, give the maximum number of links available in the present data set, and request a new link value. If the user deletes a link that is assigned to a vent, the code will assign the link with the next smallest number to that vent. The best method for assigning vents to links is to first use Option 4, FUSIBLE LINK PROPERTIES, of the base menu (to be discussed in C-5.5) to assign the link parameters and then to use Option 1, ROOM PROPERTIES, followed by the NUMBER OF VENTS, ETC. option to assign vent properties.

Now return to the room properties menu by entering 0 <ret>, then to the base menu by entering 0 <ret> again.

With the base menu back on the screen, choose Option 2, PHYSICAL PROPERTIES, to review and/or modify the default room property input data. Enter 2 <ret>.

C-5.3 Physical Properties. When Option 2, PHYSICAL PROPERTIES, of the base menu is chosen, the following physical properties menu is displayed:

```
MATERIAL = INSULATED   DECK   (SOLID   POLYSTYRENE)
HEAT CONDUCTIVITY = 2.400E-05 (BTU/S LB F)
HEAT CAPACITY = 2.770E-01 (BTU/LB F)
DENSITY = 6.550E+01 (LB/FT3)

1      80.00000          AMBIENT TEMPERATURE (F)
2      0.50000           MATERIAL THICKNESS (FT)
3      MATERIAL =        INSULATED  DECK  (SOLID POLYSTYRENE)
0                        CHANGE NOTHING
```

The values in Options 1 and 2 are modified by entering the option number and then the new value.

Now choose Option 3 by coding 3 <ret>. The following menu is displayed:

```
1 CONCRETE

2 BARE METAL DECK

3 INSULATED DECK (SOLID POLYSTYRENE)

4 WOOD

5 OTHER
```

By choosing one of Options 1 through 4 of this menu, the user specifies the material properties of the ceiling according to the table of standard material properties in [4]. When the option number of one of these materials is chosen, the material name, thermal conductivity, heat capacity, and density are displayed on the screen as part of an updated physical properties menu.

Now choose Option 5, OTHER, by entering 5 <ret>. The following screen is displayed:

```
ENTER MATERIAL NAME

THERMAL CONDUCTIVITY (BTU/S FT F)

HEAT CAPACITY (BTU/LB F)

DENSITY (LB/FT3)
```

The four indicated inputs are required. After they are entered, the screen returns to an updated physical properties menu.

Now return to the default material, INSULATED DECK (SOLID POLYSTYRENE). To do so, enter any arbitrary material name with any three property values (enter MATERIAL <ret>, 1. <ret>, 1. <ret>, 1. <ret>); then choose Option 3, MATERIAL, from the menu displayed (enter 3 <ret>); and, from the final menu displayed, choose Option 3, INSULATED DECK (SOLID POLYSTYRENE) by entering 3 <ret>.

Now return to the base menu. Enter 0 <ret>. Choose Option 3, OUTPUT PARAMETERS, of the base menu to review or modify the default output-parameter data. Enter 3 <ret>.

C-5.4 Output Parameters. When Option 3, OUTPUT PARAMETERS, of the base menu is chosen, the following output-parameters menu is displayed:

```
1      400.000000       FINAL TIME (S)
2      30.000000        OUTPUT INTERVAL (S)
0                       CHANGE NOTHING
```

FINAL TIME represents the ending time of the calculation. OUTPUT INTERVAL controls the time interval between successive outputs of the calculation results. All times are in seconds. For example, assume that it is desired to run a fire scenario for 500 seconds with an output of results each 10 seconds. First choose Option 1 with a value of 500 (enter 1 <ret>, 500. <ret>), then Option 2 with a value of 10 (enter 2 <ret>, 10. <ret>). The following revised output-parameters menu is displayed:

```
1      500.000000       FINAL TIME (S)
2      10.000000        OUTPUT INTERVAL (S)
0                       CHANGE NOTHING
```

Return to the original default output parameters menu by entering 1 <ret>, 400. <ret>, followed by 2 <ret>, 30. <ret>.

Now return to the base menu from the output parameters menu by entering 0 <ret>.

With the base menu back on the screen, choose Option 4, FUSIBLE LINK PROPERTIES, to review or modify the default fusible link properties data. Enter 4 <ret>.

C-5.5 Fusible Link Properties. When Option 4, FUSIBLE LINK PROPERTIES, of the base menu is chosen, the following fusible link properties menu is displayed:

```
TO ADD OR CHANGE A LINK, ENTER LINK NO., RADIUS (FT), DISTANCE BELOW
CEILING (FT), RTI (SQRT[FT S]), AND FUSE TEMPERATURE (F).

MAXIMUM NUMBER OF LINKS EQUALS 10.

ENTER 11 TO REMOVE A LINK.

ENTER 0 TO RETURN TO THE MENU.
```

LINK #	RADIUS (FT)	DISTANCE (FT) BELOW CEILING	RTI SQRT (FT S)	FUSE TEMP (F)
1	6.000	1.000	400.000	165.000
2	21.200	0.300	50.000	165.000
3	44.300	0.300	50.000	165.000

Each fusible link must be assigned a link number (e.g., LINK # = 1), radial position from the plume–ceiling impingement point (e.g., RADIUS = 6.00 FT), ceiling-to-link separation distance (e.g., DISTANCE BELOW CEILING = 1.00 FT), response time index (e.g., RTI = 400.00 SQRT[FT S]), and fuse temperature (e.g., FUSE TEMPERATURE = 165.00 F).

Suppose that in the default fire scenario it was desired to simulate the thermal response of the group of (four) sprinkler links second closest to the fire. According to the description of C-3 and Figure C-3(a), this would be done by adding a fourth link, link number 4, at a radial distance of 13.4 ft, 1 ft below the ceiling, with an RTI of 400 $(\text{ft/sec})^{1/2}$ and a fusion temperature of 165°F. To do this, enter 4 <ret>, 13.4 <ret>, 1. <ret>, 400. <ret>, 165. <ret>. Then the following screen is displayed:

```
TO ADD OR CHANGE A LINK, ENTER LINK NO., RADIUS (FT), DISTANCE BELOW
CEILING (FT), RTI (SQRT[FT S]), AND FUSE TEMPERATURE (F).

MAXIMUM NUMBER OF LINKS EQUALS 10.

ENTER 11 TO REMOVE A LINK.

ENTER 0 TO RETURN TO THE MENU.
```

LINK #	RADIUS (FT)	DISTANCE (FT) BELOW CEILING	RTI SQRT (FT S)	FUSE TEMP (F)
1	6.000	1.000	400.000	165.000
2	13.400	1.000	400.000	165.000
3	21.200	0.300	50.000	165.000
4	44.300	0.300	50.000	165.000

Note that the new link, which was entered as link number 4, was sorted automatically into the list of the original three links and that all four links were renumbered according to radial distance from the fire. The original link-vent assignments are preserved in this operation. Hence, the user need not return to Option 4, NUMBER OF VENTS, ETC., unless it is desired to reassign link-vent combinations.

A maximum of 10 link responses can be simulated in any one simulation.

Now remove link number 2 to return to the original default array of links. To do so, enter 11 <ret>. The following screen is displayed:

```
ENTER THE NUMBER OF THE LINK TO BE REMOVED
```

Enter 2 <ret> to remove link 2.

Now return to the base menu from the fusible link properties menu by entering 0 <ret>.

With the base menu back on the screen, choose Option 5, FIRE PROPERTIES, to review or modify the default fire properties data. Enter 5 <ret>.

C-5.6 Fire Properties. When Option 5, FIRE PROPERTIES, from the base menu is chosen, the following fire properties menu is displayed:

```
1       2.5         FIRE HEIGHT (FT)
2       330.0       FIRE POWER/AREA (BTU/S FT2), ETC.
3                   FIRE OUTPUT AS A FUNCTION OF TIME
0                   CHANGE NOTHING
```

The value associated with Option 1 is the height of the base of the fire above the floor. Change this to 3 ft, for example, by entering 1 <ret> and 3. <ret>. Then return to the default data by entering 1 <ret> and 2.5 <ret>.

The value associated with Option 2 is the fire energy release rate per fire area. It is also possible to consider simulations where the fire area is fixed by specifying a fixed fire diameter. The fire energy release rate per fire area can be changed, or the fixed fire area type of specification can be made by choosing Option 2 by entering 2 <ret>. This leads to a display of the following menu:

```
1 WOOD PALLETS, STACK, 5 FT HIGH                 330 (BTU/S FT2)
2 CARTONS, COMPARTMENTED, STACKED 15 FT HIGH     200 (BTU/S FT2)
3 PE BOTTLES IN COMPARTMENTED CARTONS 15 FT HIGH 540 (BTU/S FT2)
4 PS JARS IN COMPARTMENTED CARTONS 15 FT HIGH    1300 (BTU/S FT2)
5 GASOLINE                                       200 (BTU/S FT2)
6 INPUT YOUR OWN VALUE IN (BTU/S FT2)
7 SPECIFY A CONSTANT DIAMETER FIRE IN FT
0 CHANGE NOTHING
```

Options 1 through 5 of the preceding menu are for variable area fires. The Option 1 to 5 constants displayed on the right are the fire energy release rate per unit fire area. They are taken from Table 4.1 of [1]. If one of these options is chosen, an appropriately updated fire properties menu is then displayed on the screen. Option 0 would lead to the return of the original fire properties menu.

Option 6 allows any other fire energy release rate per unit fire area of the user's choice. Option 7 allows the user to specify the diameter of a constant area fire instead of an energy release rate per unit area fire. Choice of Option 6 or 7 must be followed by entry of the appropriate value. Then an appropriately updated fire properties menu appears on the screen.

To try Option 7, SPECIFY A CONSTANT DIAMETER FIRE IN FEET, enter 7 <ret>. The following screen is displayed:

```
ENTER YOUR VALUE FOR FIRE DIAMETER IN FT
```

Assume the fire diameter is fixed at 5 ft. Enter 5. <ret>. Then the following screen is displayed:

```
1      2.50000      FIRE HEIGHT (FT)
2      5.00000      FIRE DIAMETER (FT), ETC.
3                   FIRE OUTPUT AS A FUNCTION OF TIME
0                   CHANGE NOTHING
```

Now return to the original default fire properties menu by entering 2 <ret>. The previous menu will be displayed. In this, choose Option 1, WOOD PALLETS, STACK, 5 ft high, by entering 1 <ret>.

Option 3, FIRE OUTPUT AS A FUNCTION OF TIME, of the fire properties menu allows the user to prescribe the fire as a function of time. The prescription involves (1) linear interpolation between adjacent pairs of user-specified points with coordinates (time in seconds, fire energy release rate in BTU/sec) and (2) continuation of the fire to an arbitrarily large time at the fire energy release rate of the last data point.

Now choose Option 3 by entering 3 <ret>. The following screen associated with the default fire output data is displayed:

```
1  TIME(s) =   0.00000            POWER(BTU/S)   = 0.00000E+0
2  TIME(s) =   100.0000           POWER(BTU/S) = 0.59200E+03
3  TIME(s) =   200.0000           POWER(BTU/S) = 0.23670E+04
4  TIME(s) =   400.0000           POWER(BTU/S) = 0.94680E+04
5  TIME(s) =   600.0000           POWER(BTU/S) = 0.21302E+05
6  TIME(s) =   747.0000           POWER(BTU/S) = 0.33000E+05

ENTER DATA POINT NO., TIME (S), AND POWER (BTU/S)

ENTER 11 TO REMOVE A POINT

ENTER 0 TO RETURN TO MENU
```

As discussed in Section C-3, with use of the six preceding data points, the default simulation will estimate the fire's energy release rate according to the plot of Figure C-3(b).

Additional data points can be added to the fire growth simulation by entering the new data point number, <ret>, the time in seconds, <ret>, the energy release rate in BTU/sec, and <ret>.

The maximum number of data points permitted is 10. The points can be entered in any order. A sorting routine will order the points by time. One point must correspond to zero time.

As an example of adding an additional data point to the preceding six, assume that a closer match to the "*t*-squared" default fire growth curve was desired between 200 seconds and 400 seconds. From Section C-3 it can be verified that the fire energy release rate will be 5325 BTU/sec at $t = 300$. To add this point to the data, thereby forcing the fire growth curve to pass exactly through the "*t*-squared" curve at 300 seconds, enter 7 <ret>, 300. <ret>, and 5325. <ret>. The following revised screen will be displayed:

```
1  TIME(s) =   0.0000         POWER(BTU/S) = 0.00000E+00
2  TIME(s) =   100.0000       POWER(BTU/S) = 0.59200E+03
3  TIME(s) =   200.0000       POWER(BTU/S) = 0.23670E+04
4  TIME(s) =   300.0000       POWER(BTU/S) = 0.53250E+04
5  TIME(s) =   400.0000       POWER(BTU/S) = 0.94680E+04
6  TIME(s) =   600.0000       POWER(BTU/S) = 0.21302E+05
7  TIME(s) =   747.0000       POWER(BTU/S) = 0.33000E+05

ENTER DATA PT. NO., TIME (S), AND POWER (BTU/S)
ENTER 11 TO REMOVE A POINT
ENTER 0 TO RETURN TO MENU
```

Note that the revised point, which was entered as point number 7, has been resorted into the original array of data points and that all points have been renumbered appropriately.

Now remove the point just added (which is now point number 4). First enter 11 <ret>. Then the following screen is displayed:

```
ENTER THE NUMBER OF THE DATA POINT TO BE REMOVED
```

Now enter 4 <ret>. This brings the fire growth simulation data back to the original default set of values.

Now return to the fire properties menu. Enter 0 <ret>. Then return to the base menu by entering again 0 <ret>.

With the base menu back on the screen, it is assumed that inputing of all data required to define the desired fire simulation is complete. Now choose Option 0, NO CHANGES, to proceed to the file status menu. Enter 0 <ret>.

C-5.7 Solver Parameters. Users of the code will generally have no need to refer to this section (i.e., especially when learning to use the LAVENT code, a user should now skip to Section C-6), since they are rarely, if ever, expected to run into a situation where the code is not able to obtain a solution for a particular application or is taking an inordinate amount of time to produce the solution. However, if this does happen, there are a number of variations of the default solver parameter inputs that may resolve the problem.

Start the input part of the program to get to the base menu. Then choose Option 6, SOLVER PARAMETERS, by entering 6 <ret>. The following input options menu will be displayed:

```
1   0.6500E+00      GAUSS-SEIDEL RELAXATION
2   0.1000E-04      DIFF EQ SOLVER TOLERANCE
3   0.1000E-04      GAUSS-SEIDEL TOLERANCE
4   2.000000        FLUX UPDATE INTERVAL (S)
5   6               NUMBER OF CEILING GRID POINTS, MIN=2, MAX=50
6   0.1000E-07      SMALLEST   MEANINGFUL VALUE
7                   CHANGE NOTHING
```

The solvers used in this code consist of a differential equation solver DDRIVE2, used to solve the set of differential equations associated with the layer and the fusible links, and a Gauss–Seidel/tridiagonal solver using the Crank–Nicolson formalism to solve the set of partial differential equations associated with the heat conduction calculation for the ceiling. Since two different solvers are being used in the code, there is potential for the solvers to become incompatible with each other, particularly if the upper layer has nearly reached a steady-state temperature but the ceiling is still increasing its temperature. When this occurs, the differential equation solver will try to take time steps that are too large for the Gauss–Seidel solver to handle, and a growing oscillation in the ceiling temperature variable might occur. By reducing the FLUX UPDATE INTERVAL, the growing oscillation can be suppressed. The smaller the FLUX UPDATE INTERVAL, the slower the code will run.

The GAUSS–SEIDEL RELAXATION coefficient may be changed to produce a faster running code or to handle a case that will not run with a different coefficient. Typical values of this coefficient should range between 0.2 and 1.0.

The DIFF EQ SOLVER TOLERANCE and the GAUSS–SEIDEL TOLERANCE may also be changed. Decreasing or increasing these values can provide a faster running code for a given case, and by decreasing the value of the tolerances, the accuracy of the calculations can be increased. If the tolerance values are made too small, the code will either run very slowly or not run at all. Suggested tolerances would be in the range of 0.00001 to 0.000001.

Consistent with the model assumptions, accuracy in the radial ceiling temperature distribution around the plume–ceiling impingement point is dependent on the NUMBER OF CEILING GRID POINTS. Relatively greater or lesser accuracy is achieved by using relatively more or fewer grid points. This leads, in turn, to a relatively slower or faster computer run.

C-6 File Status — Running the Code. When Option 0, NO CHANGES, of the base menu is chosen, the following file status menu is displayed:

```
1   SAVE THE FILE AND RUN THE CODE
2   SAVE THE FILE BUT DON'T RUN THE CODE
3   DON'T SAVE THE FILE BUT RUN THE CODE
4   ABORT THE CALCULATION
```

If one of the save options is selected, the user will be asked to supply a file name to designate the file where the newly generated input data are to be saved. The program will automatically create the new file. File names may be as long as 8 characters and should have a common extender such as .DAT (for example MYFILE.DAT). The maximum length that may be used for the total length of input or output files is 25 characters. For example, C:\SUBDIRECT\FILENAME.DAT would allow a file named FILENAME.DAT to be read from the subdirectory SUBDIRECT on the C drive. To read a file from a floppy disk in the A drive, use A:FILENAME.DAT. If Option 4 is chosen, the program will end without any file being saved.

A request for an output file name can appear on the screen. File names may be as long as 8 characters and should have an extender such as ".OUT" so that the output files can easily be recognized. To output a file to a floppy disk in the A drive, name the file A:FILENAME.OUT. To output a file to a subdirectory other than the one that is resident to the program, use C:\SUBDIRECT\FILENAME.OUT for the subdirectory SUBDIRECT.

Once the output file has been designated, the program will begin to execute. The statement PROGRAM RUNNING will appear on the screen. Each time the program writes to the output file, a statement such as T = 3.0000E01 S will appear on the screen to provide the user with the present output time.

C-7 The Output Variables and the Output Options. The program generates two separate output files. An example of the first output file is appended at the end of this document. This file is named by the user and consists of a listing of the input data plus all the relevant output variables in a format where the output units are specified and the meanings of all but three of the output variables are clearly specified. These latter variables are *TSL, QB,* and *QT*, the temperature of the ceiling inside the enclosure, the net heat transfer flux to the bottom surface of the ceiling, and the net heat transfer flux to the top surface of the ceiling, respectively. The variables are output as a function of radius with $R = 0$ being the center of the fire plume projected on the ceiling. Other abbreviations include LYR TEMP, LYR HT, LYR MASS, JET VELOCITY, and JET TEMP — the upper-layer (layer adjacent to the ceiling) temperature, height of the upper-layer interface above the floor, mass of gas in the layer, ceiling jet velocity, and ceiling jet temperature at the position of each fusible link, respectively. The VENT AREA is the total area of roof vents open at the time of output.

The second output file, GRAPH.OUT, is used by the graphics program GRAPH. GRAPH is a Fortran program that makes use of a graphics software package to produce graphical output of selected output variables[5,6]. To use the graphics program, the file GRAPH.OUT must be in the same directory as the program GRAPH. GRAPH is a menu-driven program that provides the user with the ability to plot two sets of variables on the PC screen. An option exists that permits the user to print the plots from the screen to a printer. If using an attached EPSON-compatible printer, enter <ret> to produce a plot using the printer. To generate a PostScript file for use on a laser printer, enter <ret> and provide a file name when the file name prompt appears in the upper left hand corner of the graph. To exit to screen mode from the graphics mode, enter <ret>. The file GRAPH.OUT will be destroyed each time the code LAVENT is run. If the user wishes to save the graphics file, it must be copied using the DOS copy command into another file with a different file name.

To demonstrate the use of GRAPH, start the program by entering graph <ret>. GRAPH will read in the graphics output file GRAPH.OUT, and the following screen will be displayed:

```
ENTER 0 TO PLOT POINTS, ENTER 1 TO PLOT AND CONNECT POINTS
```

The graphics presented in Figures C-7(a) through C-7(e) were done with GRAPH using option 0. Enter 0 <ret> and the following graphics menu is displayed:

```
  ENTER THE X AND Y VARIABLES FOR THE DESIRED TWO GRAPHS

1                    TIME
2                    LAYER TEMPERATURE
3                    LAYER HEIGHT
4                    LAYER MASS
5                    FIRE OUTPUT
6                    CEILING VENT AREA
7                    PLUME FLOW
8                    LINK TEMPERATURE
9                    JET VELOCITY AT LINK
10                   JET TEMPERATURE AT LINK
```

Two plots can be studied on a single screen. For example, from the default simulation, assume that displays of the plots of Figure C-7(a) and C-7(b), LAYER HEIGHT vs. TIME and LAYER TEMPERATURE vs. TIME, respectively, are desired. Then enter 1 <ret>, 3 <ret>, 1 <ret>, and 2 <ret>. The program will respond with the following prompt:

```
ENTER THE TITLES FOR THE TWO GRAPHS, 16 CHARACTERS MAX.
```

The user might choose titles that would identify particular cases such as LY HT RUN 100 <ret> and LY TEMP RUN 100 <ret>. If a title longer than 16 characters is chosen, it will be truncated to 16 characters. After the titles have been entered, the program will respond with the following prompt:

```
ENTER 1 FOR DEFAULT SCALING, 2 FOR USER SCALING.
```

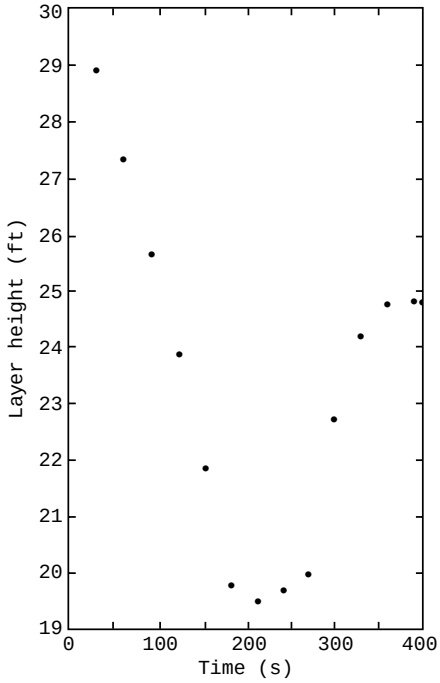

Figure C-7(a) Plot of the height of the smoke layer interface vs. time for the default simulation.

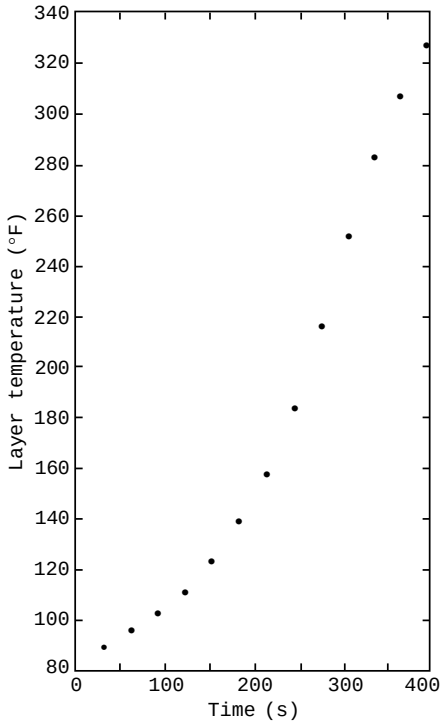

Figure C-7(b) Plot of the temperature of the smoke layer vs. time for the default simulation.